REVIEWS OF GEOPHYSICS, VOL. 23, NO. 3, PAGES 217–275, AUGUST 1985

The Auroral Luminosity Structure in the High-Latitude Upper Atmosphere: Its Dynamics and Relationship to the Large-Scale Structure of the Earth's Magnetosphere

Y. I. FELDSTEIN

Institute of Terrestrial Magnetism, Ionosphere, and Radio Wave Propagation of the Academy of Sciences of the USSR, Moscow

YU. I. GALPERIN

Institute of Space Research of the Academy of Sciences of the USSR, Moscow

The concept of the auroral oval was proposed independently by Feldstein and by Khorosheva in the early 1960's, and it has since been widely used as a reference frame for the organization of high-latitude optical, particle, and ionospheric data. More recently, different structural regions associated with the oval have been distinguished, and these have been identified with different magnetospheric regions by different workers. The net result is an inconsistent set of nomenclature and relationships. The literature of this development is reviewed in detail, and an interpretation and terminology that is consistent, in the opinion of the authors at least, are proposed. It is hoped that this proposal will serve as a useful basis for further discussion on the ordering of auroral phenomena in relation to the magnetosphere.

CONTENTS

Introduction 217
Energy fluxes in the auroral oval 218
Boundaries of the auroral oval and their dynamics 221
The diffuse luminosity region and its dynamics equatorward of the auroral oval 227
The diffuse luminescence region poleward from the auroral oval 236
Polar cap auroras 239
Relevance of the auroral luminescence regions to the large-scale magnetospheric structure 242
Conclusion 267

1. INTRODUCTION

The concept of the auroral oval was proposed independently by *Feldstein* [1960, 1963*a*, *b*], *Feldstein and Solomatina* [1961], and *Khorosheva* [1961*a*, *b*, 1962, 1963] in connection with the analysis of International Geophysical Year (IGY) data and, since then, has been extensively used to describe the diverse geophysical events at high latitudes [*Akasofu*, 1968]. The concept accounted for previously recognized statistical regularities in the occurrence of discrete auroras at an observer's zenith and in the orientation of extended auroral forms (arcs and bands). Later studies have shown that the auroral oval is closely associated with the large-scale magnetospheric structure of the earth's magnetic field, namely, with the compression of the dayside field and the formation of a magnetospheric tail on the nightside [*Feldstein*, 1966; *Akasofu and Chapman*, 1972]. This feature of the global auroral distribution has facilitated the extensive use of the oval concept to interpret the occurrence of various geophysical events at high latitudes. The auroral oval concept involves a particular auroral system of polar coordinates which was used by *Whalen* [1981, 1983] to obtain an ordered space-time distribution of the charged-particle fluxes penetrating the upper atmosphere and by *Lyatsky* [1978] and *Galperin et al.* [1980] to get the simplest description of the large-scale plasma convection in the earth's magnetosphere and ionosphere. The center of the auroral oval taken as the pole of the auroral coordinate system is shifted by $\sim 5°$ along the midnight meridian from the corrected (or invariant) geomagnetic pole.

Until the 1970's the principal information on the structure and dynamics of the auroral oval was inferred from thorough analysis of millions of all-sky camera films. A network of all-sky cameras was in operation in the high Arctic and the Antarctic during the IGY period, and the observations were carried out in the framework of a coordinated international program (*Annals of the International Geophysical Year*, 1962). However, the photographs of auroras covering simultaneously large areas at high latitudes could be obtained only for a few time intervals [*Akasofu and Kimball*, 1965; *Akasofu et al.*, 1969]. This is why the instantaneous locations of auroras in high latitudes were difficult to obtain.

The situation changed significantly after the first phototelevision imagings of auroras on board various satellites in individual emissions [*Shepherd et al.*, 1973; *Anger et al.*, 1973; *Lui and Anger*, 1973] or in integral light [*Pike and Whalen*, 1974; *Snyder and Akasofu*, 1974; *Akasofu*, 1974*a*]. In polar orbits the ISIS 2 and DMSP satellites traverse the high-latitude region within 15–20 min providing a single snapshot of the global auroral distribution per pass.

The ISIS 2 scanning photometers recorded the 3914-, 5577-, and 6300-Å emissions. The combination of electronic scanning with the satellite spin and orbital motion makes it possible to obtain a global pattern of auroras in the dark high-latitude region with the intensity of auroral luminosity above tens of rayleighs (R). DMSP detected the integral emission from the upper atmosphere in the 4000 to 11,000-Å interval with the intensity above about 1 kR. The auroral images were obtained with a scanning system using the satellite movement along its trajectory and an oscillating mirror to scan across the trajectory. As a result, a ~ 2500-km-wide band across the satellite trajectory was photographed. Although a low-altitude satellite can take sequential images of the northern or southern polar cap only once in about 100 min, the large-scale photographs taken from them yield extensive material to reveal new regu-

Paper number 5R0285.
8755-1209/85/005R-0285$15.00

larities in the global auroral pattern. Besides that, such photographs are widely used in scientific research to compare auroral patterns with local observations of other geophysical phenomena. Some of the results obtained when studying auroral patterns from satellites may be found in previous reviews [*Akasofu*, 1974*a*, 1976; *Hultqvist*, 1974*b*; *Feldstein*, 1978; *Meng*, 1979*a*; *Burch*, 1979; *Anger*, 1979]. The structure and dynamics of auroras in high-latitudes will be examined below on the basis of the data of all-sky cameras and the photographs taken from satellites.

More recently, global auroral imaging has been carried out at much higher altitudes [*Kaneda*, 1979; *Frank et al.*, 1981*a*]. The KYOKKO satellite, with its apogee at ~4000 km, imaged high-latitude auroras in vacuum UV optical emissions in the band λ1150–1650 Å. The imaging and readout cycle lasted for 128 s, so that, within a ~40-min interval during which the satellite traversed the region of geomagnetic latitudes higher than 45°, about 20 complete UV images of the high-latitude region were obtained. The KYOKKO orbiting period is 137 min. The apogee of the polar-orbiting Dynamics Explorer 1 (DE 1) satellite reached an altitude of 3.65 R_E, and, therefore, continuous television imaging of the global distribution of auroras was possible for up to 5 hours. Two photometers yielded images in the visible light in λ3914-Å, λ5577-Å, and λ6300-Å emissions, and the third, in one of the vacuum UV wavelengths (the Lyman-Birge-Hopfield (LBH) N_2 bands at λ = 1400–1700 Å, Lyman α, 1300 Å O I). The time to obtain one image may vary from ~3 to 12 min, with the data of three photometers being transmitted simultaneously. Such a schedule makes it possible to obtain a series of the images of the entire auroral oval during a long period at a high time resolution. The data of this type are very important when studying auroral substorms and have already been used to obtain new scientific results [*Frank et al.*, 1982*a*; *Craven et al.*, 1982; *Craven and Frank*, 1983].

The equipment designed for ground-based detection of the emissions from the upper atmosphere has also been recently improved. *Sears* [1982] has described the results of spectrographic observations carried out using detectors and TV equipment designed on the basis of the latest technological achievements in manufacturing narrow band spectral filters, digital electronics for image processing of counted photons, and sensitive TV detectors for recording images. The combination of the most novel detectors with the modern techniques of image processing makes it possible to carry out very high sensitive measurements with a high resolution. Even very weak subvisual emissions from the upper atmosphere and inhomogeneous structures in the airglow are accurately detected and displayed on a TV screen in real time.

Auroras are the end result of a long chain of events covering the space between the sun and the earth. They are the immediate consequence of the penetration of high-energy charged particles, electrons and protons and (to a small extent) heavier ions, into the upper atmosphere. It is expedient, therefore, that the present review should also include recent data on the distribution of the particles penetrating the upper atmosphere and their relevance to the major magnetospheric plasma regions. Naturally, the "auroral radiation," i.e., the electron fluxes with energies from several tens of eV to several tens of keV, will be examined. Detailed reviews devoted to this problem have been published by *Eather* [1975], *Frank* [1975], *Akasofu* [1977*a*, *b*], *Meng* [1978], *Swift* [1978, 1979], *Shepherd* [1979*a*], *Sergeev and Tsyganenko* [1980], and *Feldstein* [1978]. At the same time the accumulation of new data, especially in connection with satellite measurements of the auroral particles with a $\lesssim 10^{-3}$ erg cm^{-2} s^{-1} sr^{-1} energy flux threshold [*Meng*, 1978; *Cambou and Galperin*, 1982], has made it possible to construct a classification of precipitating electron characteristics in accordance with the observed auroral types and to obtain more accurate schemes of the relationships of various auroral regions to the earth's magnetic field structure and to the location of the major plasma domains in the magnetosphere. These problems and schemes will be discussed in the concluding part of this review.

2. Energy Fluxes in the Auroral Oval

The discrete auroras which encircle the geomagnetic poles and constitute the auroral oval arise from electron acceleration toward the earth's ionosphere under the effect of a field-aligned potential difference in the magnetosphere. The location of the discrete auroral region at different levels of magnetic disturbance estimated by the index Q in the nightside sector for $\varphi \sim 65°$ (where φ denotes corrected geomagnetic latitude) is shown in Figure 1 according to *Feldstein and Starkov* [1967]. (The corrected geomagnetic latitude is determined making allowance for the first four harmonics of the internal geomagnetic field expansion and may differ from the "geomagnetic latitude" by up to 5°. Allowance for higher harmonics makes it possible to find the so-called invariant latitude Λ (Λ = arccos $L^{-1/2}$, where L is the McIlwain parameter computed from the internal geomagnetic field expansion) which is usually used when analyzing satellite measurements. The difference between φ and Λ does not exceed 1° and will be neglected here.) The discrete auroral forms are superimposed on the diffuse auroras observed along the oval [*Westerlund*, 1969; *Eather and Mende*, 1972; *Whalen*, 1981; *Sharber*, 1981; *Whalen et al.*, 1977]. According to *Whalen* [1981, 1983], the major portion of the global energy flux transferred from the precipitating plasma sheet electrons is deposited in the diffuse auroras all along the oval. It should be noted that as long ago as 1959, *Jorjio* [1959] used photoelectric measurements to show that the major part of the integral luminosity emitted in such auroras is emitted in the spatially extended diffuse background rather than in the discrete bright forms, even during an auroral display. The oval-aligned diffuse auroras are due to electron precipitation from the plasma sheet where the energy spectrum in the 0.2- to 10-keV range is characterized by a Maxwellian distribution which is practically invariant along a force tube [*Rearwin and Hones*, 1974], as also in the diffuse aurora [*Lui et al.*, 1977; *Meng*, 1978; *Meng et al.*, 1979].

The results of specially designed multipoint expeditionary measurements of auroral brightness taken with wide-angle spectrophotometers were used by *Ponomarev* [1981] to show that the energy contribution from the diffuse precipitation of auroral electrons dominates the contribution of discrete auroras in all phases of a substorm. The rise of diffuse precipitation intensity over the entire night sector of the auroral oval follows the increase of pressure near the inner edge of the plasma sheet. The same conclusion can be drawn from the concepts of plasma pressure increase and the large-scale electric field in the magnetospheric tail.

The pattern proposed by *Ponomarev* [1981] may be used to qualitatively describe the behavior of mean auroral brightness, ionization, and heating of the thermosphere in the auroral oval disregarding the role of discrete auroras and field-aligned potential differences, in a satisfactory agreement with experimental data obtained during disturbed periods in the night sector. Discrete auroras are also due to plasma sheet electrons,

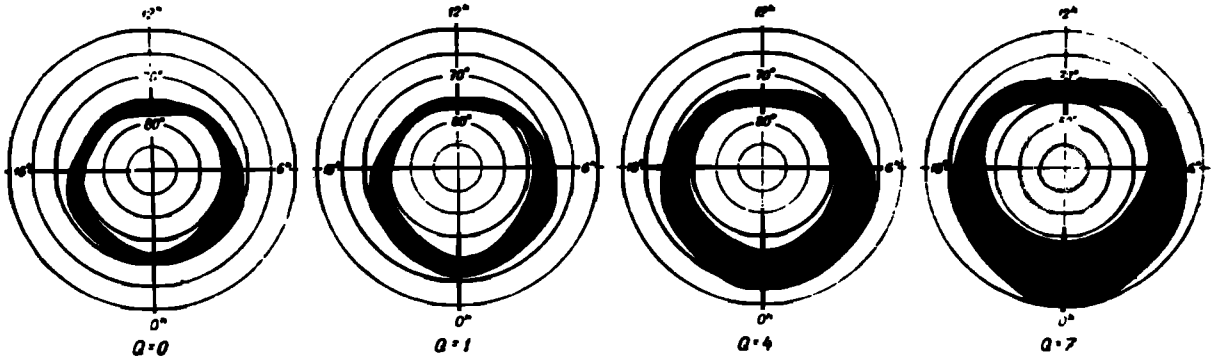

Fig. 1. The auroral oval at various geomagnetic activity levels [*Feldstein and Starkov*, 1967].

but the charged particles in these force tubes suffer an additional field-aligned acceleration as they move from the magnetosphere to the upper atmosphere [*Evans*, 1976; *Torbert and Mozer*, 1978; *Mozer et al.*, 1980; *Mizera and Funnell*, 1977; *Chiu et al.*, 1983]. Upward fluxes of high-energy ions of predominantly ionospheric origin are also observed in the same latitudes [*Ghielmetti et al.*, 1978] together with precipitations of such ions into the atmosphere. Thus the auroral ionosphere and the plasma sheet exchange particles with each other and are immersed in a complicated system of large- and small-scale currents, so that they constitute a unified physical object whose dynamics is most clearly visualized in the auroral luminosity pattern. In the present review we shall examine the large-scale auroral luminosity pattern but refrain from discussing the very interesting studies of the small-scale structures in individual discrete auroras and luminosity pulsations.

The character of the oval-aligned auroras in the dusk sector is closely related to the interplanetary medium conditions [*Murphree et al.*, 1981*b*]. Diffuse auroras are predominant for interplanetary magnetic field (IMF) components $B_z > 0$ and $B_y > 0$. For $B_z > 0$ and $B_y < 0$ the diffuse auroras have superimposed isolated auroral forms. Under such conditions the geomagnetic activity is usually low. The extended oval-aligned auroral arcs are characteristic of disturbed conditions of $B_z < 0$ for an IMF B_y component of both signs.

According to *Whalen* [1981, 1983] the latitude variation of energy flux E in a diffuse aurora can approximately be described by the Gaussoid

$$E = E_{\max} \exp\left[-\tfrac{1}{2}\left(\frac{\varphi - \varphi_{\max}}{\sigma}\right)^2\right]$$

where changes in maximum energy flux, $E_{\max}$, are confined between 0.3 and 30 ergs/cm^2 s; $\sigma \sim 1.4$ and may vary within a factor of 3; $\varphi_{\max}$ is the latitude of maximum flux which may shift by up to 5°. The equatorward boundary of the auroral oval for discrete forms at all longitudes is located along an isoline of constant energy flux. The latitude $\varphi_{\max}$ is located near this boundary during magnetically quiet periods and within the auroral oval during disturbed periods. The auroral coordinate system fixed to the instantaneous oval position makes the observed energy fluxes ordered. In this system, E is described by a Gaussoid characterized solely by the parameters $E_{\max}$ and $\varphi_{\max}$. During substorms, however, the Gaussian form of the latitude distribution of E is distorted.

The energy flux supplied from the magnetosphere to the auroral oval was determined by *Feldstein and Starkov* [1971] on the basis of ascafilm photometry in the sectors of a frame with zenith angles below 60°. This means that the mean luminosity intensity was determined over a ~90,000-km^2 area; i.e., the oval-aligned diffuse auroras made a major contribution. Figure 2 shows the observed energy fluxes in the various sectors of the auroral oval with increasing magnetic activity level. The surface brightness of the auroral forms is known to be variable by 3–4 orders of magnitude, and the local electron flux, by up to 5 orders of magnitude. In Figure 2 the mean energy flux changes by less than an order of magnitude with increasing activity, the difference being due to the fact that the mean brightness of a significant part of the sky, rather than the brightness of individual forms, was included in determining E.

The value of E increases with magnetic activity from 1.4 to 7 ergs/cm^2 s at night and from 0.45 to 1.4 ergs/cm^2 s in the daytime. Thus the energy flux density supplied to the auroral oval altitudes (1) is 3–5 times higher at nighttime compared with the daytime, (2) increases by a factor of 3–5 with rising activity from $Q = 0$ to $Q = 7$, and (3) increases at nighttime more steeply with increasing Q than in the daytime.

The absolute values of E are in good agreement with the data [*Eather and Mende*, 1972] inferred from the experimental determinations of E by various methods, namely, $E \sim 0.1$ erg cm^{-2} s^{-1} sr^{-1} in the dayside sector and ~1–8 ergs cm^{-2} s^{-1} sr^{-1} in the nightside sector of the oval.

Knowing the location of the poleward and equatorward boundaries of the auroral oval, *Feldstein and Starkov* [1971] obtained the following relation for the total power W supplied to the oval:

$$W(\text{erg s}^{-1}) = 5.5 \times 10^{16} (\delta H)^{1/2}$$

where δH is the amplitude of the magnetic disturbance in nanoteslas in the nightside sector centered on $\varphi = 65°$. The relation gives $W = 9 \times 10^{16}$ ergs/s at $Q = 0$ and 1.3×10^{18} ergs/s at $Q = 7$. The order of magnitude of such powers proved to be comparable with the powers measured by *Sharp and Johnson* [1968] for >80-eV electron fluxes (3×10^{16} ergs s^{-1} at $Kp = 1$ and 6×10^{17} ergs s^{-1} at $4 < Kp < 5$). According to *Ahn et al.* [1983*a*] the empirical relation between E and δH in the form $E \sim (\delta H)^{0.677}$ at $\delta H < 0$ is sufficiently close, in the functional dependence of E on δH, to the relation presented above.

McDiarmid et al. [1975] have presented the results of measuring the mean intensities and energies of auroral electrons as functions of magnetic local time (MLT) and invariant latitude on board ISIS 2. Their results were supplemented with new data obtained by *Wallis and Budzinski* [1981], who determined the electron fluxes with energies of 0.15, 1.3, 9.7, and 22

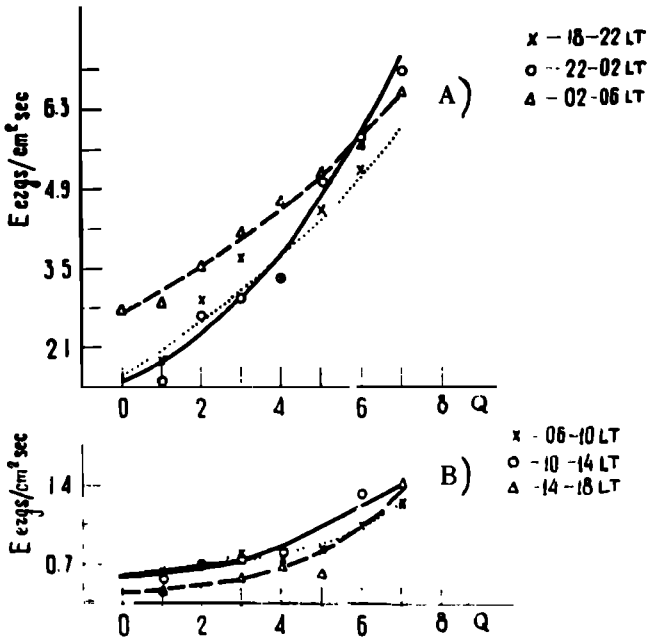

Fig. 2. The mean energy fluxes E (erg cm^{-2} s^{-1}) supplied to the various sectors of the auroral oval depending on the magnetic disturbance level [*Feldstein and Starkov*, 1971]. (*a*) Night sector. (*b*) Day sector.

keV for each hour of MLT in the invariant latitude band $60° \leq \varphi \leq 84°$ at two disturbance levels, $0 < Kp < 3$ and $3 < Kp < 9$. The values of W were found to be $\sim 2.7 \times 10^{17}$ ergs s^{-1} at $1 < Kp < 2$ and $\sim 5.5 \times 10^{17}$ ergs s^{-1} at $Kp = 4$.

The information on energy fluxes supplied to the upper atmosphere by auroral electrons presented in the work of *Spiro et al.* [1982] is the most detailed published so far. The Atmosphere Explorer D and C (AE-D and AE-C) satellites measured 0.2 to 27-keV electron fluxes. Following *Spiro et al.* [1982], Figure 3 presents a model for the energy flux of precipitating electrons, E (erg cm^{-2} s^{-1}). The model was obtained by statistical processing of the data obtained in many thousands of satellite orbits. The isoline representing the outward contour corresponds to $E = 0.25$ erg cm^{-2} s^{-1}; each of the next isolines corresponds to a doubled value of E. The coordinates used are invariant latitude–geomagnetic local time.

From the present data these points immediately follow:

1. The region where intense fluxes of precipitating auroral electrons are observed (and the maximum energy flux is supplied to the upper atmosphere) is a closed band encircling the geomagnetic pole. The band is located at lower latitudes on the nightside compared with the dayside.

2. The most intense energy fluxes exist at near-midnight hours.

3. As the magnetic disturbance rises, E increases rapidly in the nightside sector (by 8 times) and more slowly in the dayside sector (by 2 times).

4. The band is located within the latitude region which in general coincides with, but is somewhat broader than, the auroral oval. Such a location is due to the fact that the outward contour in Figure 3 corresponds to a somewhat lower energy flux compared with the auroral arcs the location of which was used to find the boundaries of the auroral oval shown in Figure 1.

5. The main morphological regularities characterizing the band of maximum E and the auroral oval are the same, namely: (1) during magnetically quiet periods the band in the dayside sector is located at higher latitudes compared with the nightside sector; such diurnal variations are characteristic of the equatorward and poleward boundaries of the band; (2) as magnetic activity rises, the region of maximum E shifts equatorward on the dayside and expands rapidly poleward and equatorward on the nightside; (3) the band is broader in the nightside sector compared with the dayside sector; (4) during intense magnetic disturbances the equatorward boundary of the band is located asymmetrically with respect to the geomagnetic pole ($\sim 60°$ at nighttime and $\sim 71°$ in the daytime), and its poleward boundary is at approximately the same latitude ($\sim 77°$); (5) the band is broader in the dawn sector compared with the dusk sector.

Comparison of the statistical model results with the data for individual orbits and the averaged data of the DMSP, TIROS, and P78-1 satellites [*Simons et al.*, 1983] has shown that the model is generally consistent with the large-scale features but disagrees in details.

Thus the auroral oval is precisely the region of the globe

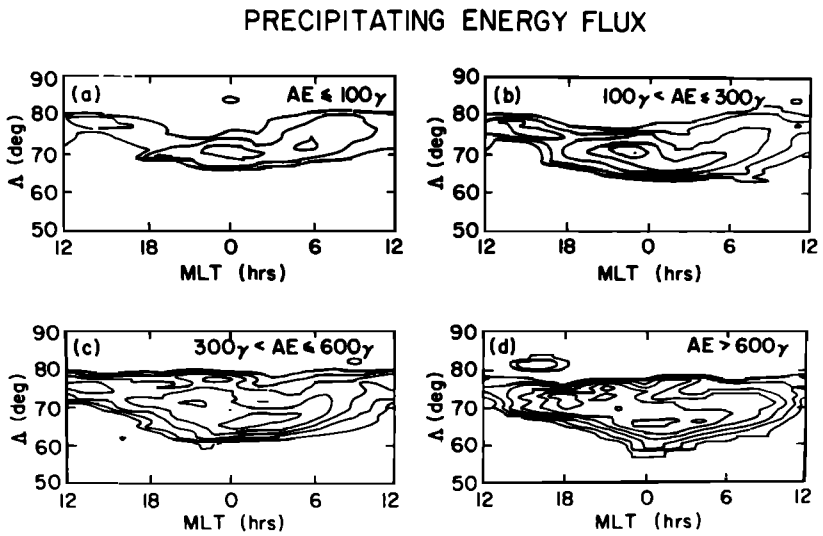

Fig. 3. The isolines of electron energy flux at various values of the magnetic activity index AE [*Spiro et al.*, 1982]. The outer isoline is for the energy flux $E = 0.25$ erg cm^{-2} s^{-1}, each of the next contours corresponds to a doubled energy flux.

where the maximum energy fluxes from corpuscular precipitations are supplied to the upper atmosphere from the magnetosphere. This fact accounts to a great extent for the relevance of the auroral oval to some geophysical phenomena at ionospheric altitudes.

Spiro et al. [1982] present the following relation for the total mean power supplied to the band:

$$W(\text{erg s}^{-1}) = \left[1.75 \frac{AE}{100} + 1.6\right] \times 10^{17}$$

where AE is expressed in nanoteslas.

Considering that $AE \sim AL \sim \delta H$ in winter, this relation is in sufficiently good agreement with the above relation inferred from photometric determinations. It should be noted that according to *Spiro et al.* [1982] and *Feldstein and Starkov* [1971], the resultant values of W are somewhat higher than what follows from the empirical relations obtained by *Ahn et al.* [1983*b*]:

$$W(\text{erg s}^{-1}) = 0.6 \times 10^{15}\, AE$$

$$W(\text{erg s}^{-1}) = 0.8 \times 10^{15}\, AL$$

where AE and AL are indices expressed in nanoteslas.

The energy fluxes of the 0.3- to 20-keV particles precipitating in the atmosphere were also inferred from observations on board TIROS-N, NOAA 6, and NOAA 7 [*Hill et al.*, 1982; D. S. Evans, private communication, 1982]. The dynamic parameters of the instruments flown on these satellites permitted the measurement of E in the $0.01 < E < 400$ ergs cm^{-2} s^{-1} range. During the period from 1978 the data obtained from more than 50,000 orbits were used to find the location of the band where the maximum fluxes of precipitating particles are supplied at the disturbance levels $0 < Kp < 1$, $1 < Kp < 3-$, $3o < Kp < 4-$, and $Kp > 4o$. The conclusions concerning the location of the band and its relevance to the auroral oval are in general agreement with the results obtained by *Spiro et al.* [1982], namely:

1. In quiescent periods ($0 < Kp < 1$) the $\sim 2°$ wide band is located at $\varphi \sim 78°$ in the daytime and at $\varphi \sim 70°$ at nighttime. The two boundaries are asymmetric with respect to the geomagnetic pole. The values of E are ~ 1 erg cm^{-2} s^{-1} at nighttime and ~ 0.4 erg cm^{-2} s^{-1} in the daytime.

2. As the disturbance level rises, (1) in the nightside sector the equatorward boundary of the band shifts toward the equator (to $\varphi \sim 60°$ at $3o < Kp < 4-$), and the poleward boundary shifts toward the pole; (2) in the dayside sector the two boundaries shift somewhat toward the equator, thereby resulting in a pronounced asymmetry of the width of the band in the dayside and nightside sectors; (3) the position of the equatorward boundary of the band remains asymmetric with respect to the geomagnetic pole, whereas the poleward boundary is extended approximately along the geomagnetic parallel $\varphi \sim 75°$; (4) the values of E at $4 < Kp < 7$ rise up to ~ 7 ergs cm^{-2} s^{-1} in the nightside sector and remain at a rather low level (< 1 erg cm^{-2} s^{-1}) in the daytime at all levels of disturbances.

3. An additional region of weak fluxes of $E \sim 0.2$ erg cm^{-2} s^{-1} is observed equatorward of the oval in the dayside sector.

Thus from ~ 1300 through midnight to ~ 1100 MLT, the band along which the maximum energy fluxes of the precipitating auroral particles are supplied to the upper atmosphere is located at the latitudes of the auroral oval and shows numerous peculiarities characteristic of the oval.

3. Boundaries of the Auroral Oval and Their Dynamics

According to *Khorosheva* [1962] the auroral oval may be considered, to a first approximation, to be a circle, and therefore the radius and the position of the center of the circle should be known for describing the oval quantitatively. Such an approximation was used by *Starkov and Feldstein* [1967, 1968] to find the parameters of the external and internal boundaries of the auroral oval at different intensities of geomagnetic disturbances.

Figure 4*a* shows the changes of radii of the circular equatorward (1) and poleward (2) boundaries of the auroral oval and the changes in radius of the circle drawn through the middle of the oval (the dashed line) as functions of the Q index of magnetic activity. It is seen that the radius of the equatorward boundary increases monotonically from 17° at $Q = 0$ to 24° at $Q = 7$. The radius of the poleward boundary changes much less and is on the average $\sim 16°$. The centers of all the circles at $Q = 0$ (Figure 4*b*) are at a $\sim 3°$ distance from the pole on the midnight meridian. As the disturbances increase, the equatorward boundary center shifts up to a 5° distance from the pole, and the poleward boundary center shifts down to a $< 1°$ distance from the pole. Thus during disturbed periods the asymmetry of position of the equatorward boundary between the daytime and the nighttime is $\sim 10°$ of latitude, whereas the asymmetry of the poleward boundary practically disappears and the boundary is located along the corrected geomagnetic parallel of $\sim 75°$.

In the near-midnight sector the equatorward boundary of the oval shifts from $\varphi = 70°$ under magnetically quiet conditions ($Q = 0$) to $\varphi = 61°$ under magnetic field disturbances of intensity $Q = 7$ (see also Figure 1). Such a significant equatorward expansion of the region of high-energy particle precipitation occurs during disturbances, as well as the poleward substorm expansion. It is only this circumstance that, in our opinion, may account for the apparent paradox of the dynamics of the luminescence region during substorms mentioned by *Moore et al.* [1981]. Referring to some authoritative sources from the published literature, they assert that, in contrast to the poleward boundary of the oval, its equatorward boundary shifts little during substorms, which leads to the following formulation from *Moore et al.* [1981]:

> A long-standing mystery of substorm dynamics is the paradox presented by the prevalent poleward expansion of various low-latitude auroral substorm features despite the equally prevalent thinking that hot plasma is transferred radially from the magnetospheric tail, i.e. equatorwards, when mapped through a fixed magnetic geometry to low altitudes.

It is assumed that the paradox can partly be resolved by allowing for the change in magnetic field topology as an integral part of the substorm. The field lines are taken to be essentially attached to fixed points on the earth and to move simultaneously toward the earth in the equatorial plane.

From the auroral data it follows, however, that the earthward plasma motion in the equatorial plane of the magnetosphere is accompanied also by an equatorward shift of the low-latitude plasma penetration region (see Figures 1 and 4). Such motion can clearly be seen from the auroral dynamics during auroral substorms, the scheme for which was proposed by *Starkov and Feldstein* [1971]. In this respect, their scheme

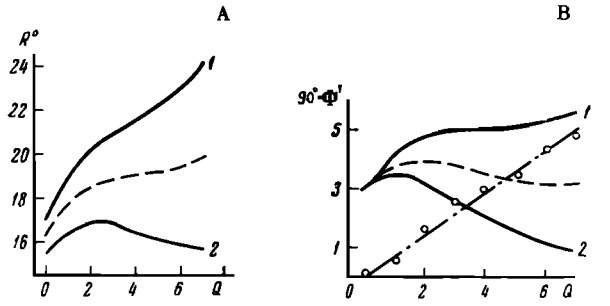

Fig. 4. The variations in the parameters of the circles approximating the equatorward (1) and poleward (2) boundaries of the auroral oval or the mean line of the oval (the dashed line) versus magnetic disturbance intensity [*Starkov and Feldstein*, 1967]. (*a*) The radius of the circle in degrees of latitude. (*b*) The shift of the circle's center from the geomagnetic pole along the midnight meridian. The circles and the dash-dot line denote the distance between the centers of the equatorward and poleward circles.

differs from the schemes proposed by *Akasofu* [1968] and *Montbriand* [1971]. The equatorward shift of the auroral oval boundary from $\sim 70°$ to $\sim 60°$ with the development of significant disturbances corresponds in the case of the dipolar field to a radial earthward shift of the inner boundary of the plasma sheet from $\sim 11\ R_E$ to $\sim 4\ R_E$ and to an even more significant shift in the case of the real extended configuration of the magnetospheric magnetic field. Of course, the shift of the equatorward boundary during an individual substorm is much less noticeable but is still sufficiently marked and does not contradict the available data on the shift of the "injection boundary" in the magnetosphere (see section 7 below). Thus the paradox mentioned by *Moore et al.* [1981] is probably a mere exaggeration. It should be admitted, however, that the physical processes relevant to the injection (heating or acceleration) of the plasma sheet particles near the inner boundary of the plasma sheet and to its radial earthward shift have still been insufficiently studied and deserve much more attention.

The mean position of the equatorward boundary of the auroral oval may be presented analytically. *Starkov* [1969] proposed the following dependence of the position of the equatorward oval boundary on the magnetic activity index Q and the geomagnetic local time t:

$$\theta_{eq}^{\circ} = 18° + 0.9Q + 5.1 \cos (t - 12°)$$

Here the colatitude $\theta_{eq}^{\circ} = 90° - \varphi$; Q is expressed in its nondimensional units; t is local time in degrees measured counterclockwise from midnight.

The analytical representation of the mean location of the auroral oval (of the positions of its poleward and equatorward boundaries) was given by *Holzworth and Meng* [1975]. The colatitude $\theta°$ of the auroral oval boundaries inferred from the data of *Feldstein and Starkov* [1967] is presented in the form

$$\theta° = A_1 + A_2 \cos (t + A_3) + A_4 \cos (2t + 2A_5) + A_6 \cos (3t + 3A_7)$$

Here t is the hourly angle in degrees; the coefficients $A_1, \cdots, A_7$ have been found by least squares fitting. From the table of coefficients it follows that already the first two coefficients of the expansion describe the location of the equatorward boundary down to $\sim 0.5°$ and the location of the poleward boundary down to 1.0°. The changes of the coefficients A_1 and A_2 are in excellent agreement with the data of Figure 4, namely, as Q changes from 0 to 6 for the equatorward (poleward) boundary, A_1 varies from 17.36° to 23.18° (from 15.22° to 16.1°), A_2 varies from 3.03° to 4.85° (from 2.41° to 0.37°), and A_3 is practically unchanged at $\sim 3.3°$ ($\sim 3°$). Thus the auroral oval boundaries may actually be considered as circles with centers shifted approximately along the midnight meridian, while the shifts and radii of the circles vary depending intimately on magnetic activity.

Examination of the photoelectric images of auroras obtained from DMSP has shown that the boundary of the auroral oval during magnetically quiet periods is marked with a bright arc [*Meng et al.*, 1977]. To within an accuracy better than 0.5°, the arc is described by a circle whose center was found from the data of 50 orbits to be shifted on the average of 4.2° along the 0010 meridian. These values are in excellent agreement with the above presented data on the position of the center of the equatorward boundary of the oval.

The arcs photographed from the satellite mark the equatorward boundary of the oval rather than its poleward boundary, as was assumed by *Meng et al.* [1977]. Indeed, in the DMSP photographs one can clearly see a diffuse luminosity band equatorward of the arc. The band borders the auroral oval in lower latitudes of the dusk-midnight sector. Such a subvisual homogeneous luminosity has not been identified with all-sky cameras and, therefore, was disregarded when determining the boundaries of the auroral oval. In these lower latitudes, magnetospheric processes resulting in a field-aligned acceleration of particles in localized regions (which give rise to discrete forms of auroras normally) become inoperative in the magnetospheric force tubes. Respectively, the maximal energy fluxes are much weaker in the diffuse luminosity latitudes equatorward of the auroral oval than in the oval, and their values generally are $\lesssim 1$ erg cm^{-2} s^{-1} (usually, tenths of 1 erg cm^{-2} s^{-1} and even smaller). Therefore the diffuse luminosity equatorward of the arc must be attributed to a physical phenomenon of a different type which will be discussed below. The most clearly defined and longitude-extended arc is often located just at the poleward boundary of the diffuse luminosity (see also *Murphree et al.* [1981*b*] and, therefore, marks the equatorward boundary of the auroral oval.

The radius of the circle which approximates the quiescent arc is a function of the B_Z component of the interplanetary magnetic field (IMF). Figure 5 shows the radii $\theta°$ of these circles inferred from the DMSP photographs [*Holzworth and Meng*, 1975]. Under magnetically quiet conditions ($B_Z > 0$), the resulting $\theta° \sim 16°$ for an arc and increases up to $\sim 23°$ during magnetic disturbances ($B_Z < 0$). These values are also in good agreement with the radii of the equatorward boundary of the auroral oval presented in Figure 4. As a rule, the poleward auroral boundary cannot be approximated by a circle of so great a radius.

Zverev et al. [1979] presented the location of the luminosity band in the northern hemisphere during various MLT intervals at $B_Z > 0$ and used the method of least squares to obtain the following relations of the mean values of φ_{eq}^{n} and φ_{p}^{n} to B_Z^m in the near-midnight sector 2200–0002 MLT:

$$\varphi_{eq}^{n} = 69.95° + 0.53B_Z^m - 0.02(B_Z^m)^2$$

$$\varphi_{p}^{n} = 72.93° - 0.24B_Z^m + 0.07(B_Z^m)^2$$

where φ_{eq}^{n} is the latitude of the equatorward boundary of the auroral oval at the moment of commencement of the substorm expansion phase; φ_{p}^{n} is the latitude of the poleward boundary of the auroral oval at the maximum of the substorm expansive phase; B_Z^m is the minimum value ($B_Z < 0$) of the

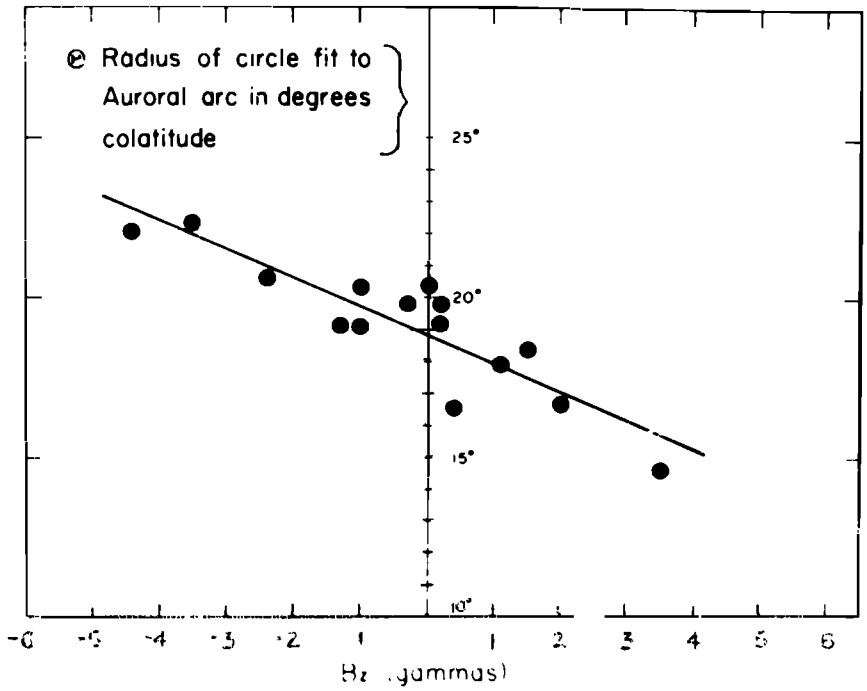

Fig. 5. The radii of the circles approximating the equatorward boundary of auroras within the oval versus the IMF B_Z component according to the DMSP observations [*Holzworth and Meng*, 1975].

IMF southward component prior to the commencement of the substorm expansion phase. *Vorobjev and Zverev* [1981] obtained the dependence of the positions of the equatorward $\varphi_{eq}{}^d$ and poleward $\varphi_p{}^d$ boundaries of the auroral oval on B_Z in the dayside sector described by the relations

$$\varphi_{eq}{}^d = 74.3° + 0.49B_Z - 0.02(B_Z)^2$$

$$\varphi_p{}^d = 75.7° + 0.57B_Z$$

where B_Z are hourly means in the solar magnetospheric coordinate system. Then, the radius of the poleward boundary of the auroral oval is 14.5° at $B_Z = +4$ nT and 15.8° at $B_Z = -4$ nT, which agrees with the date of *Starkov and Feldstein* [1967] for quiescent and disturbed conditions. The radius of the equatorial boundary of 16.2° at $B_Z = 4$ nT agrees with *Holzworth and Meng* [1975] and is ~20.5° at $B_Z = -4$ nT, i.e., smaller by 1.5°. The difference is due to the fact that *Zverev et al.* [1979] characterize the location of the boundary at the moment of substorm expansion phase commencement, whereas *Holzworth and Meng* [1975] made allowance for the shift of $\varphi_{eq}{}^n$ to lower latitudes during the expansion phase. The relations for the southern and northern hemispheres are practically the same; i.e., the positions of the boundaries of the northern and southern ovals in the φ (or Λ) and MLT coordinates coincide with each other to within the error involved. The position of the dayside poleward boundary of the oval for $B_Z > 0$ does not depend significantly on the value of the IMF B_Y component and is ~76.6° in a broad interval of variations in B_Y. The position of the equatorward boundary at $B_Y > 0$ remains constant at $\varphi_{eq}{}^d = 76.1°$ and shifts to lower latitudes for $B_Y < 0$. The shift is described by the relation

$$\varphi_{eq}{}^d(B_Z > 0) = 76.0° + 0.14B_Y - 0.02(B_Y)^2$$

The deformation of the poleward boundary of the auroral oval was qualitatively studied by *Lassen* [1979] and *Murphree and Cogger* [1981] in connection with the orientation of the IMF B_Z and B_Y components. In the periods with $B_Z > 0$, the polar cap arcs may directly adjoin the poleward boundary of the oval for $B_Y > 0$ in the dusk sector and for $B_Y < 0$ in the dawn sector. This circumstance affects the accuracy in determining the position of the boundary because of the observational difficulties of assigning auroras to different types.

The asymmetry in the latitudinal extension of the auroral oval in the dawn and dusk sectors (see Figure 1) is related in the work of *Atkinson and Hutchison* [1978] to the asymmetric convection pattern in the presence of an ionospheric conductivity gradient in the polar regions from sunlit to dark sectors of the polar cap. As a result, the antisolar convection is enhanced in the dawn sector of the polar cap. Outside the polar cap the return flow toward the dayside spreads over a wider latitude range on the dawnside than on the duskside. This may be one of the factors accounting for the asymmetry in the thickness of the auroral oval described by *Feldstein and Starkov* [1967].

It was noted above that *Lyatsky* [1978], *Galperin et al.* [1980], and *Whalen* [1981, 1983] proposed that the auroral coordinate system should be used in model descriptions of some geophysical phenomena. The pole of the system is shifted along the midnight meridian by 5° [*Lyatsky*, 1978; *Galperin et al.*, 1980] and by 4.2° [*Whalen*, 1981]. It follows from the above data that such a coordinate system should be fixed to the equatorward boundary of the auroral oval. The geophysical phenomena in the polar caps are better described using a coordinate system fixed to the poleward boundary of the oval which is shifted by 3° to the nightside in magnetically quiet periods and centered nearly at the corrected geomagnetic pole in disturbed periods. With the purpose of detailed simulation of particular data sets, such as preferred intervals of IMS, etc., more precise coordinates of the centers may be inferred from instantaneous images of the oval and from the instantaneous disturbance levels, if necessary.

Bond and Thomas [1971] and *Feldstein et al.* [1974] have inferred the positions of the poleward and equatorward boundaries of the auroral oval in the southern hemisphere at

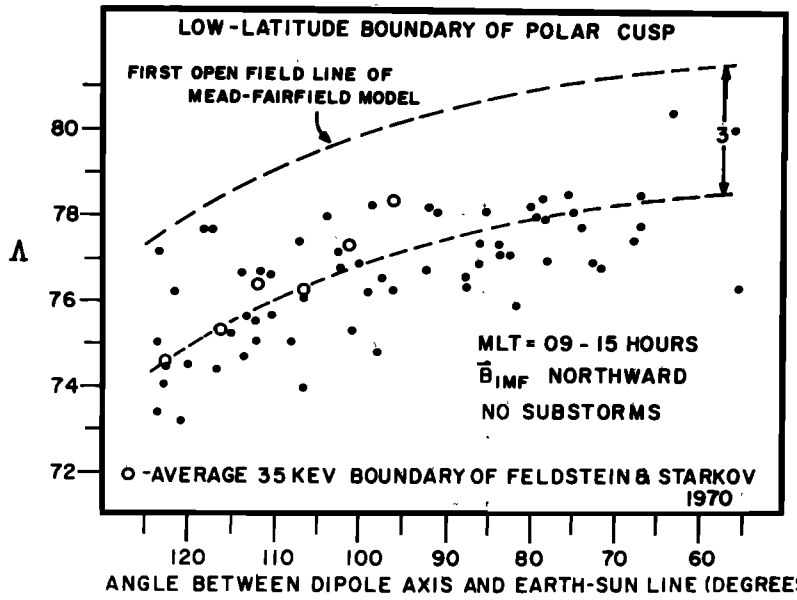

Fig. 6. Positions of the low-latitude boundary of the precipitation region of dayside cusp electrons at various angles of geomagnetic dipole tilt [*Burch*, 1972].

various magnetic disturbance levels from all-sky camera data. The comparison of the obtained location of auroral regions with the DMSP photographs has demonstrated excellent agreement between the results of the satellite and ground-based observations [*Bond and Akasofu*, 1979]. The auroral oval in the southern hemisphere was analytically described by *Thomas and Bond* [1977, 1978].

The diurnal variation in the geomagnetic dipole orientation with respect to the plane of the ecliptic results in a change of the positions of the low-energy electron precipitation region (*Machlum* [1968]; see also *Hoffman* [1972]). *Feldstein and Starkov* [1970] have shown that at identical angles of dipole tilt to the plane of ecliptic, the boundary of closed geomagnetic field lines φ_b in the noon sector inferred from the high-energy electron data will be mapped within the auroral oval. As the dipole tilt angle varies with season and UT, the position of the noon boundary φ_b changes by $\sim 4°$.

Burch [1972] has studied in detail the effect of the geomagnetic dipole orientation on the location of the low-energy electron precipitation region. If observation periods with the minimum values of IMF northward component are used, the mean latitude φ of the low-latitude boundary of the region of electron precipitation to the dayside cusp varies monotonically with the dipole tilt angle. In the northern hemisphere the boundary is located at the minimum invariant latitudes Λ in winter, when the dipole is tilted from the sun, and at the maximum invariant latitudes in summer, when the dipole is tilted to the sun (see Figure 6). The diurnal variation of the location of the noon sector of the auroral oval (and hence of the dayside cusp) does not exceed 2° in winter. Fairly good agreement is seen between the results obtained by *Feldstein and Starkov* [1970] and *Burch* [1972]. The expansion of the electron precipitation region in the noon sector by 2° to higher latitudes in the summer hemisphere compared with the winter hemisphere was inferred from the DMSP F2, F3, and F4 2-year observation data [*Makita and Meng*, 1982; *Makita et al.*, 1983].

Meng [1979*b*] has reported that the UT diurnal variations of the auroral oval size exist in the dawn and dusk sectors in connection with the daily precession of the geomagnetic pole. The minimum size of the oval is near 0600 UT, and its maximum size is near 1800 UT. However, *Gussenhoven et al.* [1980] assert that a very large portion of, if not all, the observed diurnal variations in the positions of the boundaries, rather than the true UT variations of the auroral oval size, reflect the daily shift of satellite orbits in the corrected geomagnetic latitude–MLT coordinates (see also *Meng* [1980]). According to *Gussenhoven et al.* [1980] the positions of the quiescent-time equatorward boundaries of the auroral electron precipitation regions observed by *Meng* [1979*b*] can very well be described by a $\sim 18°$ radius circle whose center is shifted by 4° with respect to the 0100 MLT meridian.

The atmospheric luminescence arising along the auroral oval in the dayside and nightside sectors differs in some of its parameters [*Feldstein*, 1969]. This is accounted for by the differences of the magnetospheric plasma parameters at the source altitudes resulting in the decreased mean values of the field-aligned potential difference which, in turn, give rise to generally softer particle fluxes in the dayside sector of the auroral oval [*Eather and Mende*, 1972]. As a result, the dayside auroras are located at higher altitudes (~ 200 km) than the nightside auroras (~ 110 km), with atomic emissions being prevalent in their spectra in the daytime compared with molecular bands at nighttime [*Sivjee and Deehr*, 1980; *Sivjee*, 1983; *Gault et al.*, 1981]. The results of satellite measurements permitted *Snyder and Akasofu* [1976] and *Akasofu* [1981*b*] to modify somewhat the above described schematization of the structure of the auroral form distribution along the oval for magnetically disturbed periods as proposed earlier. However, the main features of the distribution, namely, the prevalent radiant forms in the dayside sector and the extended homogeneous arcs and bands in the nightside sector, are preserved.

The dayside and nightside visual discrete auroras form different systems overlapping each other in local time and shifted in latitude in the dusk sector [*Akasofu and Kan*, 1980]. The different behavior of discrete auroras in the dayside and nightside sectors of the auroral oval in magnetically quiet periods and during magnetospheric substorms was described by *Vo-*

robjev et al. [1976]. *Rezhenov et al.* [1979] used the photographs taken with all-sky cameras to analyze in detail the character of connection of the discrete auroras extending to the dusk sector from both dayside and nightside sectors, namely, their overlapping in longitude and the typical directions of longitudinal and latitudinal drifts in the region. It has been shown that the two systems of auroral arcs may coexist in the noon-afternoon sector. In the case of a general amplification of the electric field of magnetospheric convection, the arcs of the different systems are shifted in latitude in opposite directions. The equatorward arc located near the poleward boundary of the region of closed field lines coshifts equatorward with this region, while the poleward rayed arc located poleward of this boundary shifts toward the pole. Therefore the meridional drift direction of the equatorward arc in the dusk sector is the same as that of the equatorward arc in the noon sector but may differ from the drift of the poleward arc. This is why they were assigned to different systems. *Murphree et al.* [1981*a*] described the appearance of the latitudinal discontinuities or abrupt shifts in latitude of the arcs in the dusk sector. However, the luminous intensity of the arcs in discontinuities is almost the same, and they are immersed in the continuous and smoothly varying diffuse aurora. Therefore *Murphree et al.* [1981*a*] concluded that the noon and dusk arcs belonged to a single topological entity. However, the necessity for a differential classification of the noon (dawn) and night auroras follows from not only the magnetospheric convection data but also from the statistical data on the frequency of occurrence of auroras over Greenland [*Lassen*, 1972; *Danielsen*, 1980; *Lassen et al.*, 1981]. However, this circumstance does not invalidate the concept of the single oval where energy fluxes maximize and inside which the homogeneous and rayed arcs and bands arise which may belong to different, but closely interrelated, structural formations in the magnetosphere.

Thus the various structural forms of auroras in different time sectors are combined to constitute a single oval encircling the geomagnetic pole in all longitudes. The general continuity of auroras along the oval is due to the topology of the magnetospheric magnetic field which feeds the oval with the electron fluxes precipitating into the atmosphere from a vast volume of the outer magnetosphere in all sectors of local time. In magnetically disturbed periods, discrete auroras are located along the oval in all longitudes. In magnetically quiet periods, discontinuities may arise in the auroral oval at the dusk or dawn hours [*Feldstein*, 1975; *Akasofu*, 1976] and/or in the near-noon sector [*Dandekar*, 1979]. The discontinuities are due to the characteristic features of a given particular plasma convection pattern at a given particular moment. As the disturbance enhances, the convection velocity (electric field) increases, and as the mean auroral intensity rises, the discontinuities in these sectors disappear. The noon discontinuity is filled by steady state moving fractions of arcs and by rays, while extended and strongly deformed arcs and bands are observed in the dusk and dawn sectors. The noon discontinuity expands in longitude during the intervals of the northward orientation of the IMF; in these cases, however, the discontinuity covers not more than 2 hours of local time centered at 1130 MLT.

The complicated distribution of the auroras in the dayside sector of the oval was studied in detail using ground-based observations and airborne and satellite measurements (see, for example, *Buchau et al.* [1972]). The Antarctic photometric experiment [*Eather et al.*, 1979] with a scanning photometer has shown that the precipitation band in the noon sector is found to be continuous if measurement data with a ~ 5 R threshold are used. If the equipment sensitivity is poorer, the luminosity proves in individual cases to be lower than the instrumental threshold which is perceived to be a discontinuity of the oval in the noon sector [*Dandekar*, 1979]. The optical data have failed to give any evidence for a systematic longitudinal limit for the soft electron precipitation into the dayside cusp. Luminosity spots appear sporadically equatorward of the continuous luminosity band. The spectral composition of the luminosity indicates that it is excited by electrons with only very feeble, if any, proton precipitation. Precipitation of high-energy electrons during their gradient drift after injection from the nightside after disturbances is the most probable source of such a luminosity. The luminosity resulting from such a precipitation will be examined in the next section in more detail. The permanent existence of auroras in the noon sector was confirmed by *Eather* [1981], who used a meridian slit camera working monochromatically at 6300 Å (a ~ 30-R threshold of sensitivity). The so called "midday gap in dayside auroras" here is missing and must be attributed to a limited sensitivity of the all-sky cameras and the DMSP pictures.

Detailed information on the emissions from the dayside sector of the oval in the winter of 1978–1979 was derived by *Deehr et al.* [1980] from photometric observations over Spitsbergen. The auroras were most intense in the 6300-Å emission and simultaneously shifted and expanded equatorward in the latitudes of the auroral zone. It has been concluded from the ratio of the emission intensities that the energies of the precipitating electrons range from below 100 eV to 2 keV. Higher-energy particles appear during disturbances in the generation region of rayed arcs, whereas the lower-energy particles form a widespread structureless precipitation region. The observed discontinuity of the luminosity isolines in the 5577-Å emission in the near-noon sector is probably due to a softer spectrum of precipitating particles in the sector. The proton aurora intensity was below the instrument sensitivity threshold which is 20 R in the H_α emission. The altitude of the structureless luminosity in the 6300-Å emission could not be determined; for short-lived rayed bands the 5577-Å emission maximum was located at 140-km altitude, and for 6300 Å, at an altitude of about 220 km.

Spectrophotometric data were used by *Sandholt et al.* [1980] and *Egeland et al.* [1980] to show that there exist two types of winter auroras in the noon sector of the oval, namely, the band in the 6300-Å emission and the relatively narrow short-lived arcs and bands in the 5577-Å and 4278-Å emissions. The width of the band ranges from 1.5° to 5° (a 2°–3° mean width), and its intensity varies from 0.2 to 2 kR for $76° < \varphi < 80°$ in magnetically quiet periods. The discrete auroras are most frequently located within, and at the equatorward edge of, the band. The 5577-Å emission intensity in these visually observable forms of auroras rises up to several kilorayleighs. As the magnetic disturbance level increases according to nightside ground-based data, the luminosity band in the noon sector shifts equatorward by $\sim 1°$ of latitude for a negative bay enhancement at midnight of -150 nT. These results are in good agreement with the data of *Vorobjev et al.* [1975]. The increase in the precipitating electron energy from 50–200 eV in the cusp to ~ 0.5 keV at its equatorward edge follows also from the statistical analysis carried out using the DMSP F2 observations in winter [*Candidi et al.*, 1983].

The data of the ESRO 1 AURORA measurements of electrons and protons in the noon sector of the auroral oval and

of the simultaneous high-altitude airborne observations of optical emissions were used [*Sivjee and Hultqvist*, 1975; *Sivjee*, 1976] to distinguish the $77.5° < \varphi < 80.5°$ region of the auroral oval (cusp) where soft particles precipitate from the $70° < \varphi < 77.5°$ region of precipitations of the higher-energy protons and electrons gradient drifting from the nightside sources. Such discrimination also agrees with the results of the statistical analysis of the ESRO 1 AURORA data [*Deehr et al.*, 1973].

The luminosity pattern in the dayside sector of the oval inferred from the ISIS 2 observations in the 6300-Å, 5577-Å, and 3914-Å emissions was described by *Shepherd and Thirkettle* [1973], *Shepherd et al.* [1976], *Murphree et al.* [1980], and *Cogger et al.* [1977]. *Murphree et al.* [1980] report the following:

1. At 1000–1200 MLT the intensity of the 6300-Å emission generated by soft electron precipitation is maximum, and the 5577-Å and 3914-Å emission intensity in this sector is minimum.

2. The red emission is not confined to the regions of the discontinuity or intensity maximum in discrete auroras at the dayside but may spread over a wide latitude region with the maxima both at noon and at prenoon and afternoon hours.

3. The 6300-Å emission appears also in the region of the closed magnetic field lines which seem to penetrate the entry layer on the magnetopause. This conclusion was drawn from the results of *Cogger et al.* [1977] which show that the daytime luminosity in the 5577-Å and 3914-Å emissions is analogous to the nightside aurora on closed magnetic field lines in the oval. In the dayside sector, such luminosity is located at the equatorward edge of the continuous band of red emission.

4. Not a single specific optical signature of the cusp was found in the specific luminosity features resulting from excitation by the solar wind particles entering the ionosphere directly from the magnetosheath plasma between the bow shock and the magnetopause and located at ionospheric altitudes poleward from the higher-energy precipitations giving rise to discrete forms in the 5577-Å and 3914-Å emissions. The same negative result was drawn by *Meng* [1981*a*] from the DMSP 38 observations of auroras.

However, more sensitive ground-based observations of auroras in the dayside sector of the oval have shown that the structured auroras are located at the equatorward boundary of the luminosity region [*Sivjee et al.*, 1982]. They spatially coincide with the higher-energy electron precipitations. A diffuse luminosity band of $\sim$1-kR intensity in the 6300-Å emission was observed poleward from $\varphi = 77° \pm 1°$. The band was due to precipitation of softer particles. Such diffuse luminosity which spread over the latitudes of the auroral oval and poleward of the oval was also observed by *Lassen et al.* [1981] on $\varphi = 77.5°$ at Godhavn, Greenland, and by *Peterson et al.* [1980] on $\varphi = 76.8°$ at Cambridge Bay, Canada.

The measurements of electron precipitation and convection direction on board the AE-C satellite [*Burch et al.*, 1976] have shown that the inverted V events generally characterizing the locations of auroral arcs from the satellite particle data are located in the dusk sector mainly in the sunward convection region but also in the region of velocity shear or even sign reversal, thereby suggesting their direct relevance to the magnetotail plasma sheet. In the region of the dayside cusp, where the direction of the large-scale ionospheric convection changes and becomes antisolar, inverted V events extending far into the dusk sector were observed. The mean electron energy in such dayside precipitation was 100–350 eV. The most intense discrete auroral forms in the dusk sector were also observed at the equatorward edge of the region of auroral precipitation of low-energy particles. All this suggests that the discrete auroral forms on the dayside are associated with the entry layer of the dayside magnetopause, i.e., that the discrete forms at the equatorward edge of the oval in the afternoon–early dusk sector are located at the latitudes where the closed geomagnetic field lines are mapped, but the convection is antisunward.

It is quite possible that the direct penetration of solar wind particles from the magnetosheath to the magnetosphere takes place in a longitude-limited region having a funnel-shaped pattern centered near noon [*Cambou and Galperin*, 1974; *Sauvaud et al.*, 1980], whereupon these particles are involved in the convection from dayside to nightside. In this case the low-latitude part of the funnel is located on closed geomagnetic field lines, i.e., in the entry layer, and the high-latitude part on open field lines, i.e., in the plasma mantle (see, for example, *Candidi and Meng* [1984]). *Meng* [1981*b*] and *Muliarchik et al.* [1982] have substantiated in more detail the above conclusion concerning the spot-shaped form of the region of instantaneous direct penetration of the solar wind particles on the basis of the data obtained by observing the electron and proton precipitations and hence their conclusion concerning the funnel-shaped pattern of the magnetospheric region of direct particle precipitations from the magnetosheath to the dayside sector of the auroral oval. The ESRO 1 AURORA satellite observed the azimuthal transfer of auroral electrons along the poleward border of the oval [*Hultqvist*, 1974], and the Cosmos 184 satellite measured the azimuthal convection in the dayside region showing a reversal with the sign of the B_Y component of the IMF [*Galperin et al.*, 1978]. The theoretical aspects of convection in the closed magnetospheric model at the dayside were discussed by *Vasyliunas* [1974]. The existence of such an azimuthal convection at the dayside makes it possible to account for the fact that the satellite-observed luminosity at the cusp is usually extended mainly in longitude and not in the form of a "tongue" toward the poleward region [*Foster et al.*, 1980]. Such a tongue of recombination luminosity in the 6300-Å line probably exists when the convection into the polar cap proceeds rapidly through the throat, as was described in some examples by *Heelis et al.* [1976] and *Reiff et al.* [1978]. However, the decrease with latitude in the auroral luminosity intensity of the 5577-Å emissions and in the bands of molecular nitrogen, etc., even in the presence of the poleward convection is associated with a sharp decrease of the auroral electron number density due to the rapidly increasing field tube volume while extending to the magnetospheric tail, as the excitation by these electrons defines the poleward boundary of the intense precipitation region. *Reiff et al.* [1978] relate the absence of the visible auroral arcs near afternoon and their presence in the oval away from noon on both the dawn and afternoon sides to the convection pattern on the cusp latitudes at the dayside near the cusp. Away from local noon the boundary between the sunward and antisunward convection is a pronounced tangential discontinuity (shear reversal), whereas near local noon the "boundary" is harder to define, since the flow paths display a rotational reversal. The auroral arcs appear at the boundary where the drift velocity suffers a simple shear reversal and field-aligned electric currents are generated. *Murphree et al.* [1980] failed to find any luminosity features associated with the particles entering directly through the funnel poleward from the high-energy electron trapping region. This is probably due to the fact that ISIS 2 measured the 6300-Å, 5577-Å, and 3914-Å emissions only

and did not measure the hydrogen emission (H_α or H_β). The former emissions are known to be generated in the dayside cusp mainly by electrons. According to *Sivjee* [1976], practically all the 6300-Å emission, 75% of the 5577-Å emission, and 70% of the 3914-Å emission are produced by the 0.1- to 1-keV electrons. At the same time the precipitation of such electrons in the noon sector is more uniform than the precipitation of soft electrons and protons with energies of <100 eV which form a spot of direct plasma penetration from the magnetosphere away from noon. It should be noted that there exist some possibilities for optical identification of such a spot on the basis of the Doppler shift in the spectral contour of the hydrogen lines excited by charge exchange protons precipitating in the cusp, but their intensity is very low for sufficient spectral resolution.

The fine structure of the luminosity in the dayside sector of the auroral oval was in fact observed during the expedition of 1981 in the Canadian part of the Arctic by taking measurements with meridional scanning photometers [*Creutzberg and McEwen*, 1983]. Evidently, such data deserve close attention to clarify the processes of the solar plasma penetration through the magnetopause.

4. The Diffuse Luminosity Region and Its Dynamics Equatorward of the Auroral Oval

Ground-based spectrographic studies of auroras indicated with certainty that a region of diffuse subvisual luminosity existed equatorward of the auroral oval [*Reid and Rees*, 1961; *Galperin*, 1963; *Sandford*, 1964, 1968; *Eather*, 1967, 1975; *Wiens and Vallance Jones*, 1969; *Evlashin*, 1971; *Fukunishi*, 1975].

The luminosity was considered to be due to proton precipitation in the dusk sector and to high-energy electron precipitation in the dawn sector. The high-energy particle precipitation equatorward of the auroral oval produces a number of geophysical phenomena, auroral absorption in particular [*Hartz and Brice*, 1967; *Hartz*, 1971].

The first satellite observations of auroras in integral light and in individual emissions confirmed the concept of the auroral oval [*Snyder et al.*, 1974; *Lui et al.*, 1975*a*; *Murphree and Anger*, 1980]. The discrete forms and the diffuse luminosity are concentrated within a single continuous oval band located eccentrically with respect to the geomagnetic pole. It has also been shown in the above work that another diffuse luminosity band, which is less eccentric with respect to the geomagnetic pole than the auroral oval, exists equatorward of the oval.

The diffuse luminosity equatorward of the auroral oval in the night sector having a fairly pronounced low-latitude boundary was inferred from ground-based and satellite data [*Lui and Anger*, 1973; *Akasofu*, 1974*a*; *Pike and Whalen*, 1974; *Lui et al.*, 1973; *Creutzberg*, 1976; *Snyder and Akasofu*, 1974]. It should be noted that the visual observations of the boundary at $L < 4$ have shown that it is characterized by short-term equatorward jumps of the luminosity by up to tens of kilometers which are accompanied by pulsations at the level of class 1. This small-scale instability of the nightside equatorward boundary has not been studied sufficiently as yet. As a rule, the width of the equatorward boundary varies gradually with longitude, but at finer scales feeble pulsating arcs and patches can be observed near the edge. In rare cases during magnetic storms, however, the boundary of the diffuse band is sharply bordered with large-amplitude undulations [*Lui et al.*, 1982]. The longitudinal wavelength of the undulations is $\sim$40–400 km, and they disappear within 0.5–3.5 hours after their appearance. It is natural to assume that the above described diffuse luminosity zone is adjacent to the auroral oval. It must be precisely stated that here we deal with the polar boundary of a specific auroral structure, the diffuse auroral belt, while the diffuse auroral luminosity, as was already mentioned above, extends inside the auroral oval existing between the arcs and even poleward of the auroral oval (see below).

The ISIS 2 spectral data [*Lui and Anger*, 1973; *Wallis et al.*, 1976; *Lui et al.*, 1977] indicate that the diffuse luminosity is due to low-energy (0.1–10 keV) electron precipitation. Comparison of the pictures from DMSP with the data of all-sky cameras [*Snyder and Akasofu*, 1974; *Akasofu*, 1974*a*] has shown that the diffuse band in fact includes some inhomogeneities. The observed intensity of the luminosity in the 5577-Å emission is sufficiently high that it cannot be attributed to proton precipitation. In an individual case the H_β intensity observed on the earth was $\sim$50 R and the intensity of λ5577 Å in the diffuse band was $\sim$7 kR [*Lui and Anger*, 1973]. *Mende and Eather* [1976] have also concluded that the major fraction of the energy in the diffuse luminosity region is supplied by electrons.

The equatorward boundary of diffuse luminosity is not located along a geomagnetic parallel, as was assumed by *Lui et al.* [1973] and *Akasofu* [1974*b*], but is frequently shifted to higher latitudes when going from night to day [*Evlashin and Evlashina*, 1981]. The high-energy electron precipitation giving rise to measurable luminosity in the 5577-Å and 3914-Å emissions takes place during and after intensive magnetospheric disturbances in the dawn sector. The luminosity is located mainly along a geomagnetic parallel (more strictly, along the line of the high-energy electron drift), thereby resulting in a complication of the luminous region structure due to spatial overlaps of the luminous entities due to processes of a different nature.

Akasofu [1974*b*] presented a summary of the characteristic features of various types of auroras and called the oval-aligned diffuse luminosity "the continuous aurora" with the view of distinguishing this auroral type from the diffuse luminosity equatorward of the auroral oval.

Because of the relative homogeneity and low intensity of the diffuse luminosity equatorward of the oval, it may be best studied using photometric observations from on board low-orbiting satellites and on the basis of data on the ionization of the subauroral ionosphere generated by such electrons in the night sector obtained as a result of oblique sounding of the ionosphere from the ground-based (or airborne) ionosondes [*Turunen and Liszka*, 1972; *Khalipov et al.*, 1977]. We shall consider these results below.

The photographs of the luminosity taken from DMSP [*Nagata et al.*, 1975; *Sheehan and Carovillano*, 1978; *Pike and Dandekar*, 1979; *Nakai and Kamide*, 1983] and from ISIS 2 [*Lui et al.*, 1975*b*] and ground-based photometric data [*Slater et al.*, 1980; *Alekseev et al.*, 1980] on the luminosity were used in these studies to obtain quantitative relations between the position of the equatorward diffuse auroral boundary (DAB) and magnetic activity in the dusk-night sector. DAB proved to shift systematically equatorward with increasing magnetic disturbance; at the same time, the width of the band increased rapidly. The compression and expansion of the diffuse auroral region are controlled by substorm activity and by the IMF B_Z component [*Pike and Dandekar*, 1979; *Nakai and Kamide*, 1983]. Besides that, as a disturbance expands, the equatorward DAB shift is more rapid than its reversed poleward recovery as the disturbance decays. This feature was explicitly

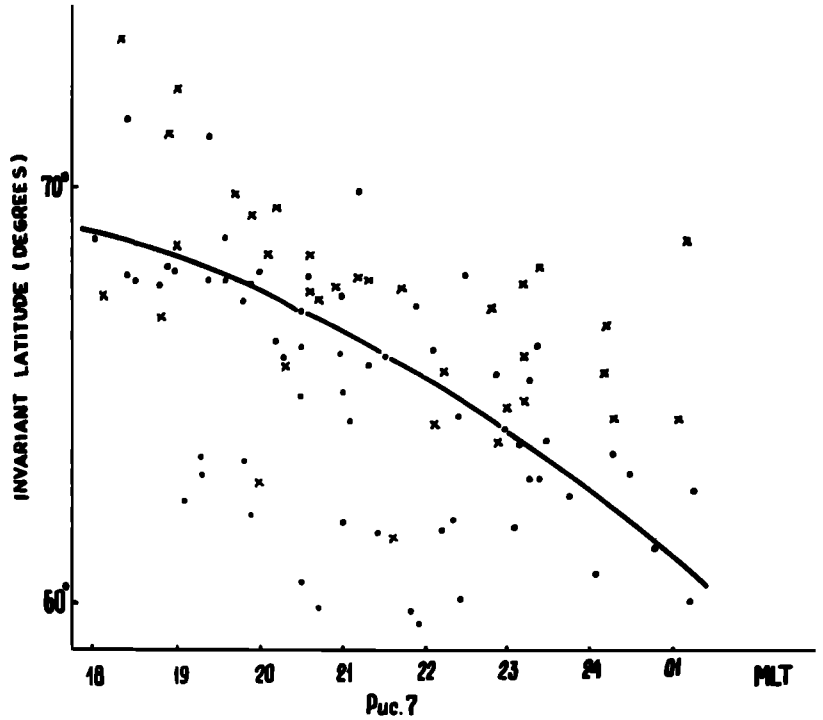

Fig. 7. Positions of the diffuse precipitation boundary (φ_{DPB}) in the dusk–near-midnight sector inferred from the AUREOL 1 and 2 measurements: dots, energy flux $E \geq 10^{-3}$ erg cm^{-2} s^{-1} sr^{-1}; crosses, energy flux $E \geq 10^{-1}$ erg cm^{-2} s^{-1} sr^{-1}. The solid line shows DPB according to *Galperin et al.* [1977] for the "oval" approximation at $Kp = 3-$.

demonstrated by soft electron observations from the AUREOL satellites by *Galperin et al.* [1977] so that its inertial displacements are ordered better by Kp than by instantaneous AE indices. We shall return to these results below. According to *Lui et al.* [1975*b*] the DAB in the emission λ5577 Å was located at midnight on $\varphi = 67°$ at $Kp = 1$ and on $\varphi = 62°$ at $Kp = 4$. The data presented by *Sheehan and Carovillano* [1978] indicated that as Kp increased, the DAB shifted monotonically equatorward at 0100 MLT and was observed on $\varphi = 67°$ at $Kp = 1$ and on $\varphi = 61.5°$ at $Kp = 5$, i.e., 1°–2° equatorward of the DAB positions obtained by *Nagata et al.* [1975] in the southern hemisphere for the disturbances with $Kp = 2$–4. The relationship of the DAB position to the AE index is more irregular than it is to the Kp index, but φ decreases on the average by 1° with a 100-nT rise in AE. At 2000 and 2200 MLT the monotonic trend of the equatorward shift of DAB with increasing Kp is violated; namely, the boundary shifts poleward with increasing Kp from 0 to 2, and only after that does it shift to lower latitudes.

The following relation for φ_{DAB} in the near-midnight interval of 2100–0002 MLT was inferred from ground-based observations of DAB in the λ6300-Å emission [*Slater et al.*, 1980]:

$$\varphi_{DAB} = 67.46° - 2.04Kp$$

The regression relations of the form $\varphi = \beta + \alpha Kp$ and $\varphi = C + BKp + AKp^2$ obtained for each hour in the 2100–0002 MLT interval have made it possible to find φ_{DAB} in this interval at various geomagnetic disturbance levels. Comparison with the results of *Sheehan and Carovillano* [1978] and *Lui et al.* [1975*b*] has shown that φ_{DAB} inferred from ground-based photometric observations is located farther equatorward by 2°–3°. This difference may be explained by the fact that *Slater et al.* [1980] determined φ_{DAB} to be the boundary of a 100-R excess of the 6300-Å emission intensity over night glow which coincides with the boundary of a 10^{-2} erg cm^{-2} s^{-1} sr^{-1} energy flux of precipitating electrons. The luminosity detection threshold was found to be ~1 kR in integral light [*Sheehan and Carovillano*, 1978] and ~1 kR in the 5577-Å emission [*Lui et al.*, 1975*b*]. At the same time, the energy flux of the precipitating soft electrons decreases toward lower latitudes [*Winningham et al.*, 1975]. It is quite obvious, therefore, that φ_{DAB} may also decrease with the lower luminosity threshold used.

It was noted above that the DAB position was closely related to the fluxes of the penetrating low-energy electrons. Therefore satellite measurements were extensively used to find the position of the diffuse precipitation boundary (DPB) of such particles [*Galperin et al.*, 1977; *Kamide and Winningham*, 1977; *Gussenhoven et al.*, 1981; *Hardy et al.*, 1981]. The latitude variations of auroral electron precipitation and their spectra were first studied systematically by *Frank and Ackerson* [1971, 1972] using Injun 5 data. They have shown that a structureless soft electron precipitation, whose spectrum is the same as the plasma sheet electron spectrum, exists equatorward of the discrete auroral region coinciding with the inverted V electron precipitation.

The form and position of the DPB were studied by *Galperin et al.* [1977], *Kamide and Winningham* [1977], and *Gussenhoven et al.* [1981] with respect to magnetic disturbance intensity and by *Kamide and Winningham* [1977], *Hardy et al.* [1981], and *Nikolaenko et al.* [1983] with respect to interplanetary medium conditions.

Galperin et al. [1977] determined the DPB position in the dusk and midnight sectors using the AUREOL 1 and 2 measurements of the 0.2- to 250-keV electron precipitations at a $< 10^{-3}$ erg cm^{-2} s^{-1} sr^{-1} flux threshold. The diffuse precipitation zone equatorward of the auroral oval was observed on every orbit, and its boundary DPB proved to be suf-

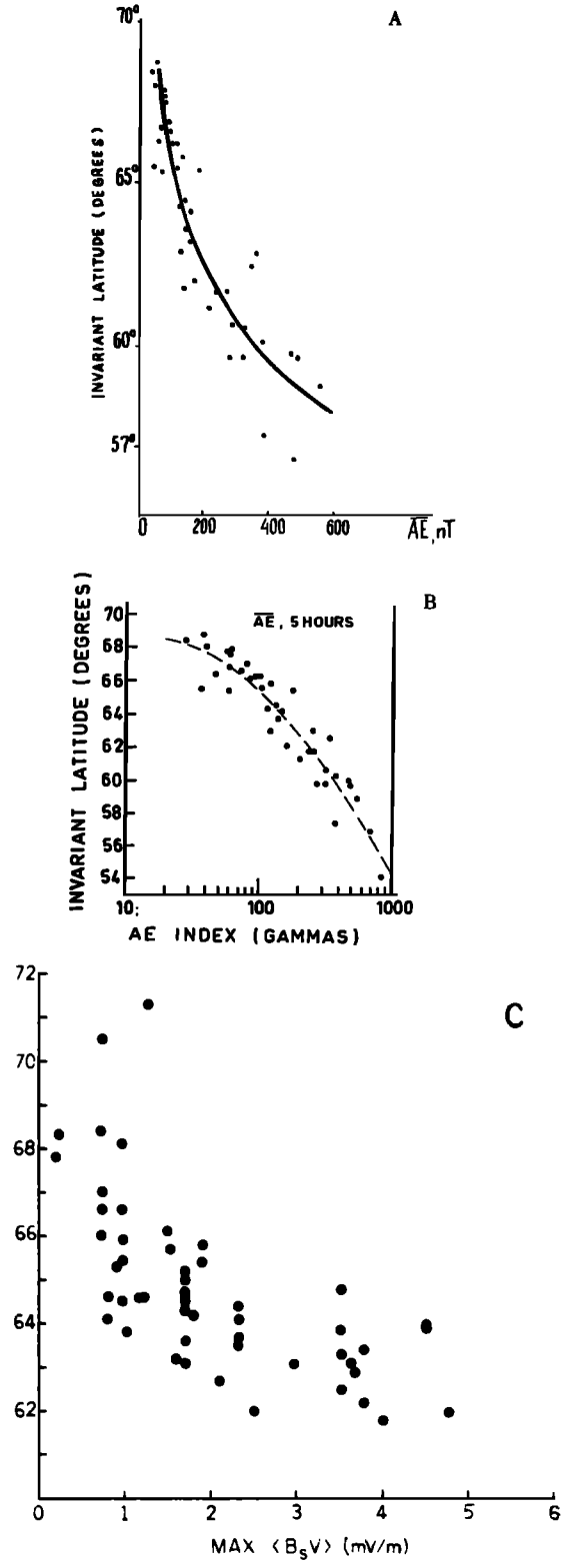

Fig. 8. (*a*) The dependence of φ_{DPB} on the *AE* index averaged over 5 hours preceding each DPB crossing by satellites for the near-midnight data area [*Nikolaenko et al.*, 1983]. The line corresponds to the regression equation $\varphi_{DPB} = 84.6° - 9.6 \log \overline{AE}(5 \text{ hours}) > 50$ nT and $\tau = -0.9$. (*b*) The dependence of the DPB on the *AE* index averaged over 5 hours preceding each DPB crossing. The dashed line indicates a quadratic fit determined by the standard method of least squares [*Sauvaud et al.*, 1983]. (*c*) Positions of the equatorward DAB versus the maximum 30-min averaged $B_s \times V$ value during 6 hours preceding the time of each DAB observation [*Nakai and Kamide*, 1983].

ficiently stable in time, so that its equatorward shift with rising activity occurred only within a period equaling two to three satellite orbits, that is, during several hours. The DPB position was inferred from the 1- to 2-keV electron flux intensity jump which coincides in magnetically disturbed periods with the latitude of the rapid rise of the precipitating electron energy flux ($E > 10^{-3}$, $>10^{-2}$, $>10^{-1}$ erg cm^{-2} s^{-1} sr^{-1} and in the quiet periods, when the rise of E with latitude is more gradual, with $E > 10^{-2}$ erg cm^{-2} s^{-1} sr^{-1}. The DPB latitude φ_{DPB} (in degrees) as a function of Kp in the $0 < Kp < 5$ interval within the 1800 < MLT < 2400 local sector is described by the following relations obtained using the least squares method:

Linear form

$$(90° - \varphi_{DPB}) = 18.53 + 1.25Kp + 0.018(Kp)^2 + [2.84 + 1.24Kp - 0.076Kp^2] \times \frac{\text{MLT}}{6} - 3 \pm 0.12$$

Oval form

$$(90° - \varphi_{DPB}) = 19.2 + 0.35Kp + 0.17(Kp)^2 + [1.30 + 2.56Kp - 0.34Kp^2] \times \cos(\text{MLT}) \pm 0.13$$

Figure 7 presents φ_{DPB} for the measurement thresholds $E > 10^{-3}$ (dots) and $E > 10^{-1}$ erg cm^{-1} s^{-1} sr^{-1} (crosses). The solid line shows the DPB of an oval form at $Kp = 3-$. All measurements have been plotted; therefore a large spread of values of φ_{DPB} is observed. However, it is seen that as E decreases, the boundary shifts to lower latitudes and its position shifts to smaller φ from dusk to midnight. The use of the hourly means of the *AE* index during the passage through the boundary to find φ_{DPB} gives a much larger spread between the observed and calculated values of φ_{DPB}, which is accounted for by a high inertia of the processes which determine the DPB position. Between or after the disturbances the *AE* index decreases while φ_{DPB} remains practically constant. Thus the equatorward DAB differs fundamentally from the equatorward boundary of the auroral oval in the character of the temporal relationship to magnetic disturbances. The position of the auroral oval boundaries is intimately, nearly functionally, related to the instantaneous and immediately preceding magnetic disturbance intensity without any noticeable time shift, whereas the DPB position is more inertial and proves to be closely related to the magnetic disturbances which occurred several hours prior to the moment of observation of the DPB position. This circumstance may account for a closer relationship of φ_{DPB} with the 3-hour mean of the Kp index than with the hourly mean of the *AE* index, as was found by *Galperin et al.* [1977].

The study of the effect of geomagnetic activity level on the DPB using AUREOL data was continued by *Sauvaud et al.* [1982, 1983] and *Nikolaenko et al.* [1983]. The relationships of φ_{DPB} to the magnetic activity indices Kp and *AE* were found for the dusk-midnight quadrant (1800–2400 MLT) or for the near-midnight interval 2148 < MLT < 0012 MLT only. The data obtained in the entire dusk sector for φ_{DPB} were corrected for the φ_{DPB} dependence on MLT according to the model proposed by *Galperin et al.* [1977] (see the solid line in Figure 7) and then correlated to other parameters.

The correlation coefficients τ are shown to depend heavily on the duration of the time interval for the determination of an index prior to the moment of boundary traversal. For the 3-hour mean of the Kp index, $\tau(\varphi_{DPB}, Kp) = -0.71$. For the hourly means of the *AE* index, $\tau(\varphi_{DPB}, AE) = -0.64, -0.65,$

-0.47, -0.35 if the AE index is determined in the same hourly interval (the 0-hour advance) or with the advances of 1, 2, 3 hours relative to the boundary traversal, respectively. As the time interval of the AE averaging increases, the values of $\tau(\varphi_{DPB}, AE)$ not only do not increase, but even increase somewhat, so that $\tau = -0.66$ in case of a correlation of φ_{DPB} with $\overline{AE}$(0–3 hours). The respective regression equation is

$$\varphi_{DPB} = 67.9° - 0.016AE(3 \text{ hours})$$

where AE in nanoteslas is the value of the AE index averaged over the 0- to 3-hour interval before the moment of boundary traversal.

This inertial behavior of the DPB is highly typical for the relation of the DPB position found in the near-midnight sector to the mean value of large $\overline{AE}$ within the intervals of 20 min, 2 hours, 3 hours, 5 hours, 10 hours, and 20 hours prior to the boundary traversal. The squared correlation coefficients $\tau^2(\varphi_{DPB}$, large $\overline{AE})$ are -0.77, -0.81, -0.86, -0.90, -0.76, and -0.61, respectively. Figure 8*a* shows the dependence of φ_{DPB} on the mean $\overline{AE}$ value within a 5-hour interval prior to the DPB traversal of energy flux when $\tau^2(\varphi_{DPB}$, large $\overline{AE})$ is maximum. It is seen that φ_{DPB} decreases rapidly with rising $\overline{AE}$ at small $\overline{AE}$ and that the equatorward shift slows with increasing $\overline{AE}$. The least squares fit gives the following relation for the linear dependence of φ_{DPB} on large $\overline{AE}$(5 hours):

$$\varphi_{DPB} = 84.6° - \text{large } \overline{AE}(5 \text{ hours})$$

at magnetic disturbances with intensities $50 < \overline{AE}(5$ hours$) < 600$ nT.

Figure 8*b* shows the position of φ_{DPB} determined from at least a threefold increase of the 1- to 2-keV electron flux over the apparatus threshold of AUREOL 1, 2 as a function of AE(5 hours). The nonlinear dependence is approximated from a least squares fit by the relation

$$\varphi_{DPB} = 64.11° + 3.7 \text{ large } \overline{AE}(5 \text{ hours}) - 0.75[\text{large } \overline{AE}(5 \text{ hours})]^2$$

and is shown with the dashed line in Figure 8*b*. Thus the DPB position in the near-midnight sector is determined mainly by substorm activity several hours prior to the boundary traversal rather than by the instantaneous disturbance level. In other words, the DPB position depends on the combined effects of several recent high-energy charged-particle injections from the plasma sheet to the inner magnetosphere. After being injected, the particles drift in the magnetosphere and precipitate slowly to the subauroral upper atmosphere. During this time the pattern of the particles' precipitation in the night sector retains the signatures of the previous injections within a sufficiently long period (several hours) because of the small latitudinal shift of the drifting particles. Therefore the distribution of the precipitating particles, which produce the diffuse auroras and the ionization in the subauroral ionosphere, is as if the development of the active processes occurring in the magnetosphere during several preceding hours were memorized. The relative stability of the quiescent auroral electron precipitations in the diffuse auroral region was also noted by *Tanskanen et al.* [1981] when this region was consecutively traversed by the DMSP F2 satellite. *Eather et al.* [1976] have paid attention to the fact that according to scanning photometer observations, the spatial distribution of auroral luminosity depends on previous injection events, an observation which is in line with the above described data.

Thus various observational data have shown that the entire auroral zone does not react synchronously with the magnetic activity variations. The boundaries of the discrete region, the oval, reflect immediately the development of disturbances, whereas the variations of the equatorward DAB and DPB are characterized by a significant inertia.

The statistical study of φ_{DPB} in the dusk (1600–2300 MLT) and dawn (0400–1000 MLT) sectors [*Gussenhoven et al.*, 1981] was based on the data obtained from several thousands of DMSP F2 orbits through high latitudes of the northern and southern hemispheres. According to earlier studies the DPB shifts equatorward with decreasing energy of the detected electrons. The position of the boundary was determined from a pronounced increase ($>10^7$ (cm^2 s sr)$^{-1}$) of the integral number flux of the 0.05- to 20-keV electrons. The linear regression dependence of φ_{DPB} on Kp was determined for each 1-hour interval of MLT. The dependence for the 2200–2300 MLT interval in the northern hemisphere is of the form

$$\varphi_{DPB} = 68.3° - 1.79° \, Kp$$

The high correlation coefficients ($\tau \sim 0.7$–0.8) indicate that the 3-hour Kp indices can properly order the variations of φ_{DPB}.

Meng [1979*b*] determined φ_{DPB} in the dusk sector on the basis of the DMSP F2 data obtained during prolonged, extremely quiet geomagnetic periods. At 1900–2100 MLT, $\varphi_{DPB} = 72°$–$69°$. After that, the boundary no longer shifted poleward with an increasing duration of the quiet geomagnetic period. These values of φ_{DPB} should probably be considered as maximum in the dusk sector. The zone of auroral particle precipitation after reaching this "ground state" apparently does not diminish to smaller dimensions.

Kamide and Winningham [1977] have correlated the DPB position in the night (2000–0400 MLT) sector with the IMF B_Z component from the ISIS 1 and 2 observation data. The boundary was determined to be the equatorward edge of the >0.1-keV electron precipitation region. Use was made of the values of the IMF B_Z component averaged over a 1-hour interval preceding a crossing of φ_{DPB}. The regression dependences relating φ_{DPB} to B_Z in the ± 4-nT interval of variations in B_Z were obtained for each 1-hour interval from 2000–2100 MLT to 0300–0400 MLT. The relations are

$$\varphi_{DPB} = 64.8° + 0.46° \, B_Z$$

for the 2300–2400 MLT interval and

$$\varphi_{DPB} = 64.5° + 0.6° \, B_Z$$

for the entire night sector 2000–0400 MLT.

Although *Kamide and Winningham* [1977] assumed that the IMF B_Z component was of major importance in controlling the DPB motion, the correlation coefficient $\tau \sim 0.55$ indicates that B_Z orders the φ_{DPB} position more poorly than does the Kp index (see above). A noticeable contribution to the variations of the equatorward position of the DPB is made by substorms. As a substorm develops, φ_{DPB} decreases rapidly. However, a quantitative relationship of φ_{DPB} to the AL index characterizing the westward electrojet intensity was not established definitely for the near-midnight sector (2300–0100 MLT). A noticeable spread of the values of φ_{DPB} takes place at any given value of AL. Nevertheless, there exists a trend for φ_{DPB} to shift to lower latitudes with increasing magnetic activity. The DPB position has been shown to depend on the dipole axis orientation, namely, that the φ_{DPB} night sector winter location is 1°–2° equatorward of the summer location.

The study of the effects of the interplanetary medium pa-

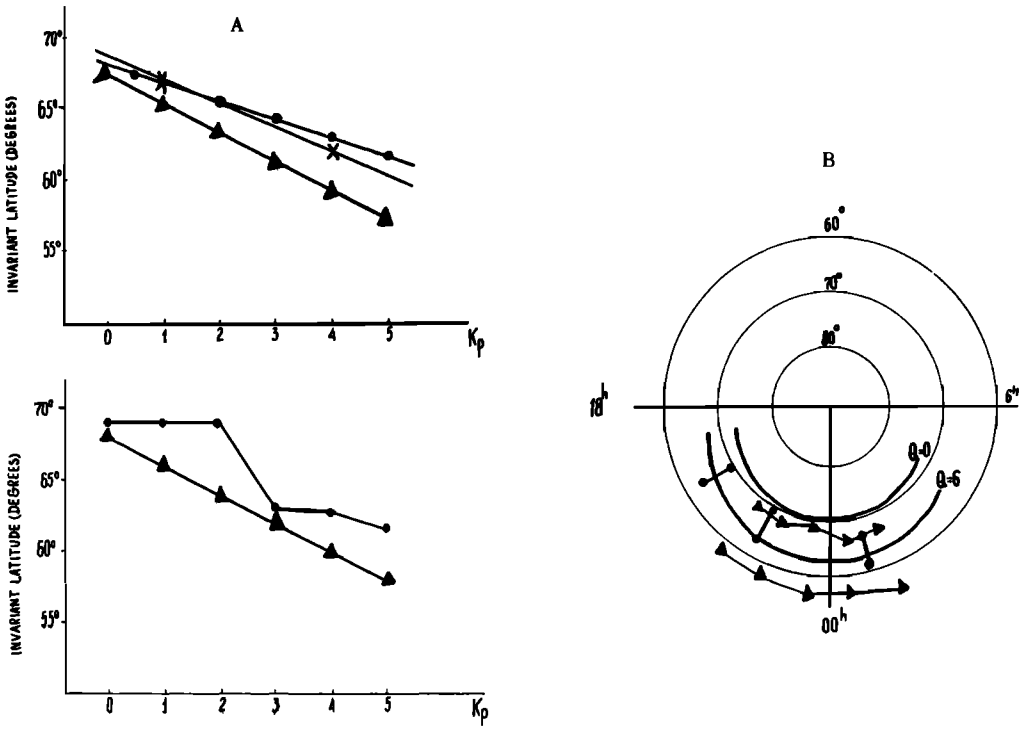

Fig. 9. The geomagnetic latitude of DAB inferred from the ground-based observations [*Slater et al.*, 1980] and from the ISIS 2 [*Lui et al.*, 1975*b*] and DMSP [*Sheehan and Carovillano*, 1978] data. (*a*) The dependence on Kp at (top) near-midnight hours and at (bottom) 2200 MLT. Triangles, *Slater et al.* [1980]; circles, *Sheehan and Carovillano* [1978]; crosses, *Lui et al.* [1975*b*]. (*b*) The dependence on MLT at $Kp = 0$ and $Kp = 5$. Triangles, *Slater et al.* [1980]; circles, *Sheehan and Carovillano* [1978]. The solid lines show the positions of the equatorward boundary of the auroral oval at the magnetic activity index $Q = 0$ and $Q = 6$ [*Starkov and Feldstein*, 1967].

rameters on the DPB and DAB positions was continued using DMSP F2 data [*Hardy et al.*, 1981], AUREOL 1 and 2 data [*Sauvaud et al.*, 1982; *Nikolaenko et al.*, 1983], and DMSP 7529, 8531, and 9532 data [*Nakai and Kamide*, 1983]. *Hardy et al.* [1981] determined φ_{DPB} to be the latitude where the >0.05-keV electron flux increases rapidly, which is close to the determination of φ_{DPB} by *Kamide and Winningham* [1977], namely, the latitude where $E > 10^{-3}$ erg cm^{-2} s^{-1} sr^{-1}, and by *Nakai and Kamide* [1983], namely, the equatorward DAB at midnight. According to *Hardy et al.* [1981], among four sets of the interplanetary medium parameters (B_Z, B_Z^2, $V \times B_Z$, $V \times B_Z^2$) the highest correlation of φ_{DPB} is with B_Z and $V \times B_Z$ ($\tau \sim 0.44$ and 0.47, respectively). The maximum τ is obtainable using the hourly means of B_Z and $V \times B_Z$ which are 1–2 hours ahead of the hour of determination of φ_{DPB}. The value of τ proved to depend significantly on the sign of B_Z; namely, in the data arrays with $B_Z < 1$ nT, the correlation is much higher than in the data array with $B_Z > 1$ nT. For example, in the 2100–2200 MLT interval

$$\varphi_{DPB} = 65.8° + 0.87B_Z \qquad B_Z < 1 \text{ nT}$$

$$\varphi_{DPB} = 66.6° - 0.15B_Z \qquad B_Z > 1 \text{ nT}$$

at $\tau = 0.68$ and -0.17, respectively. A special study has shown that the best correlation of φ_{DPB} with B_Z is obtainable if the boundary of the arrays runs through $B_Z = 1$ nT. In this case, φ_{DPB} correlates with B_Z in the data array with $B_Z < 1$ nT, and the correlation is practically absent in the data array with $B_Z > 1$ nT. Since the number of boundary traversals totaled ~ 2500, it proved possible to obtain regression relations for each hour in the dusk (1800–2200 MLT) and dawn (0400–0800 MLT) sectors of the northern hemisphere.

The AUREOL 1 and 2 data obtained in winter were used to select the boundary traversals in the dusk sector for which *King* [1977] provided the data on the IMF components and on solar wind velocity V. The regression relationships between φ_{DPB} and the interplanetary medium parameters (B_Z and $V \times B_Z$) were found. A correction for the φ_{DPB} shift with MLT was introduced as described above.

The study of the φ_{DPB} correlation with B_Z and $V \times B_Z$ has shown, in agreement with *Hardy et al.* [1981], that the correlation is absent at $B_Z > 0$ and is relatively small at $B_Z < 0$. The values of τ increase to ~ 0.5 when the values of B_Z averaged over previous hours are used. The linear regression equations obtained by a least squares fit are

$$\varphi_{DPB} = 64.0° + 0.4B_Z \qquad \tau = 0.22 \qquad B_Z > 0$$

$$\varphi_{DPB} = 64.4° + 0.5B_Z \qquad \tau = 0.54 \qquad B_Z < 0$$

when B_Z is averaged over several previous hours. Thus the DPB position in the dusk sector correlates more poorly with the IMP B_Z component than with the magnetic disturbance intensity (Kp, $\sum AE$). *Nakai and Kamide* [1983] have also shown that the low correlation of φ_{DAB} with B_Z at $B_Z > 0$ is due to a high inertia of the position of the equatorward DAB in the near-midnight sector after the previous magnetospheric disturbances. A trend exists for the DPB to be observed at low latitudes even during the periods of northward IMF if such periods followed the southward IMF intervals. The position of the equatorward DAB, in accordance with the data described above, proved to be determined by the time history of IMF rather than by the simple hourly means of IMF when the DAB is traversed. An interval of southward IMF may affect the position of φ_{DAB} for at least several hours. The correlation coefficients between φ_{DAB} and $B_Z \times V$ averaged over five different time scales (30 min, 1 hour, 2 hours, 3 hours, 6 hours)

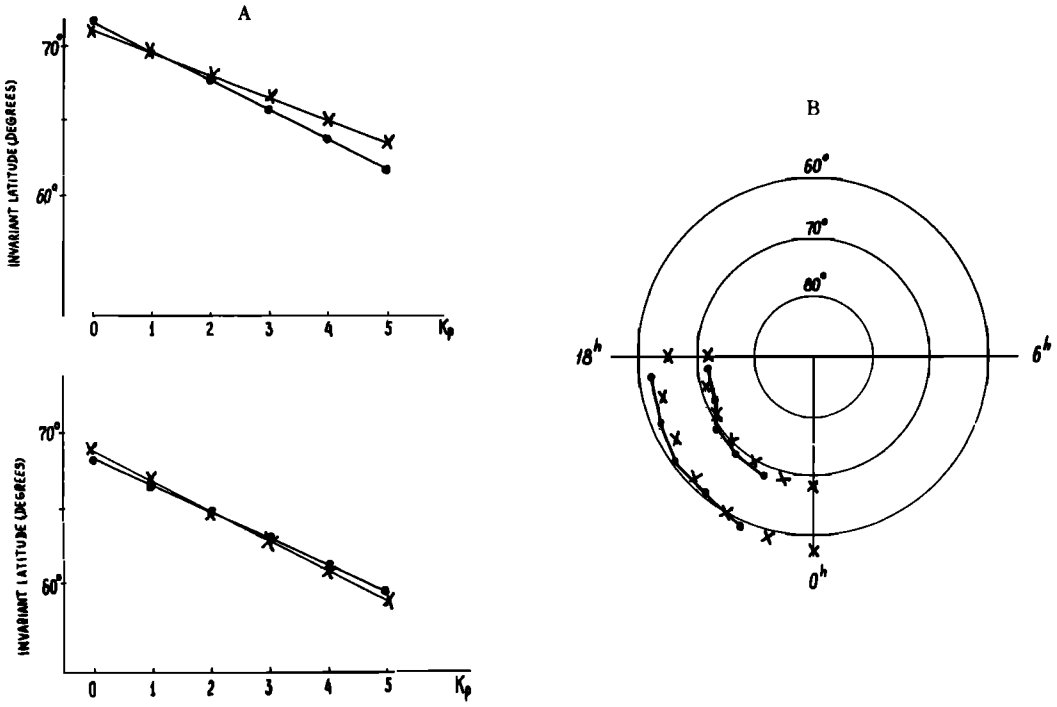

Fig. 10. The geomagnetic latitude of DPB inferred from the AUREOL 1, 2 [*Galperin et al.*, 1977] and DMSP/F2 [*Gussenhoven et al.*, 1981] data. (*a*) The dependence on Kp at 1900 MLT [*Galperin et al.*, 1977] and at (top) 1800–1900 MLT [*Gussenhoven et al.*, 1981] and at (bottom) 2300 MLT [*Galperin et al.*, 1977] and 2200–2300 MLT [*Gussenhoven et al.*, 1981]. Crosses, *Galperin et al.* [1977]; circles, *Gussenhoven et al.* [1981]. (*b*) The dependence on MLT at $Kp = 0$ and $Kp = 5$. Crosses, *Galperin et al.* [1977]; circles, *Gussenhoven et al.* [1981].

prior to observations of the boundary rise from ~0.3 to ~0.57. Figure 8*c* shows the φ_{DAB} positions plotted against the maximum 30-min average $B_s \times V$ value during 6 hours preceding the time of the boundary traversal. This parameter was found to correlate best with φ_{DAB}. The linear correlation coefficient $\tau = 0.64$.

Let us examine now the agreement of the values of φ_{DAB} and φ_{DPB} obtained in the dusk sector by various authors. Figure 9*a* presents the dependences of φ_{DAB} on Kp in the near-midnight sector (top) and at 2200 MLT (bottom) according to *Lui et al.* [1975*b*], *Sheehan and Carovillano* [1978], and *Slater et al.* [1980]. Fairly good agreement between the data inferred from the ISIS 2 and DMSP observations can be noted [*Lui et al.*, 1975*b*; *Sheehan and Carovillano*, 1978], while the DAB position inferred from ground-based observations is at lower latitudes [*Slater et al.*, 1980]. Such a difference was explained above by the fact that different auroral intensity thresholds were used by these authors to find φ_{DAB}. The values of φ_{DAB} obtained by *Sheehan and Carovillano* [1978] and *Slater et al.* [1980] are shown in Figure 9*b* for various MLT in the corrected geomagnetic latitude–MLT coordinates. The solid lines in Figure 9*b* show the position of the equatorward boundary of the auroral oval in magnetically quiet ($Q = 0$) and magnetically disturbed ($Q = 6$) periods according to *Starkov and Feldstein* [1967]. The DAB is located in lower latitudes than is the equatorward boundary of the auroral oval. The difference is ~2°–3° in magnetically quiet periods and increases up to ~5° in magnetically disturbed periods. According to *Sheehan and Carovillano* [1978], φ_{DAB} coincides closely with the boundary of the auroral oval in magnetically disturbed periods, a fact that may be explained by the increased auroral intensity and by the appearance of luminosity inhomogeneities within the diffuse auroral region. Such a luminosity is readily detected with all-sky cameras. The weaker diffuse luminosity equatorward of the auroral oval, which was observed from the earth's surface [*Slater et al.*, 1980], was not traced in the photographs taken on board DMSP because of a high measurement threshold. Figures 10*a* and 10*b* compare the average results on the DPB position as measured from AUREOL 1 and 2 [*Galperin et al.*, 1977] and from DMSP F2 [*Gussenhoven et al.*, 1981]. The dependence of φ_{DPB} on Kp in the dusk and near-midnight hours (Figure 10*a*) and the dependence of φ_{DPB} on MLT at $Kp = 0$ and $Kp = 5$ (Figure 10*b*) demonstrate excellent agreement between the results of independent observations. It is regrettable that *Gussenhoven et al.* [1981] are probably unaware of the similar results of *Galperin et al.* [1977] which were published 4 years earlier.

The comparisons between the DPB and DAB positions have shown that at $Kp = 0$ the values of φ_{DPB} and φ_{DAB} are approximately the same and that at $Kp = 5$ better agreement is observed with the data of *Slater et al.* [1980] than with the data of *Sheehan and Carovillano* [1978]. Thus the statistical data are also indicative of the spatial coincidence between DPB and DAB which was found in particular cases [*Deehr et al.*, 1976; *Lui et al.*, 1977; *Valchuk et al.*, 1979]. DPB is located equatorward of the boundary of the auroral oval by ~2° at $Kp = 0$ and by ~5° at $Kp = 5$. This difference is preserved in the entire MLT interval from 1800 to 2400, thereby confirming the conclusion [*Evlashin and Evlashina*, 1981] that the diffuse auroras in the dusk sector equatorward of the auroral oval are not located along a geomagnetic parallel but form an oval-shaped zone shifting to higher latitudes from midnight to dusk.

The region of diffuse precipitation of soft electrons equatorward of the auroral oval is not limited to 1800 MLT but extends further to the early dusk sector [*Burch et al.*, 1976;

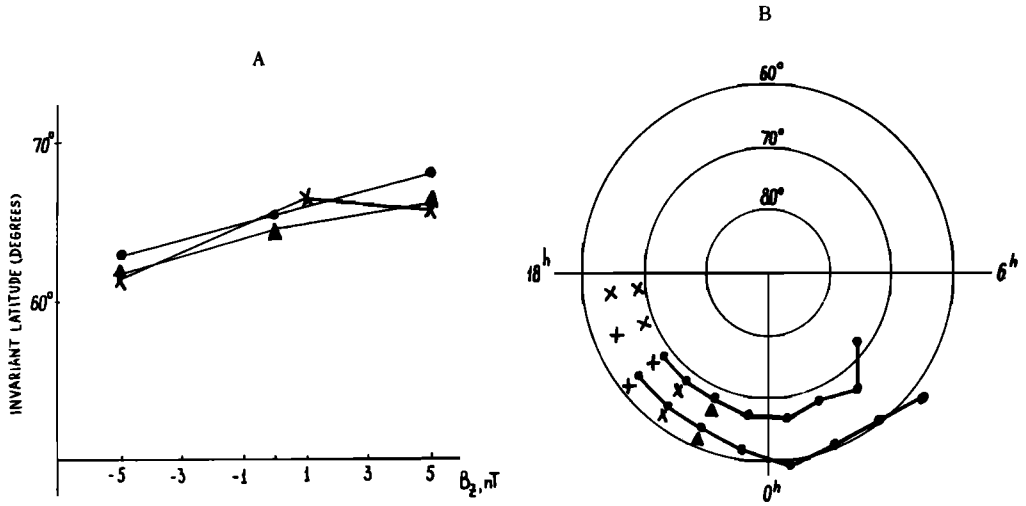

Fig. 11. Geomagnetic latitude of DPB inferred from the ISIS 2 [*Kamide and Winningham*, 1977] and DMSP/F2 [*Hardy et al.*, 1981] and AUREOL 1, 2 [*Nikolaenko et al.*, 1983] observations. (*a*) The dependence on B_Z: circles, at 2200–2300 MLT [*Kamide and Winningham*, 1977]; crosses, at 2100–2200 MLT [*Hardy et al.*, 1981]; triangles, at 2200–2300 MLT [*Nikolaenko et al.*, 1983]. (*b*) The dependence on MLT at $B_Z = +5$ nT and $B_Z = -5$ nT: circles, *Kamide and Winningham* [1977]; crosses, *Hardy et al.* [1981]; triangles, *Nikolaenko et al.* [1983].

Heelis et al., 1980]. The equatorward boundary of the region keeps shifting to higher latitudes and is located on $\varphi_{DPB} \sim 70°$ at 1500 MLT. The soft electron precipitations equatorward of the auroral oval were observed in the dusk sector up to afternoon hours from AUREOL [*Muliarchik et al.*, 1982] and DMSP [*Meng and Akasofu*, 1983; *Candidi et al.*, 1983] satellites. When approaching noon, the latitudinal extension of the region decreases. It is compressed to the dayside cusp which constitutes the noon sector of the auroral oval and is located on $\varphi \sim 77°$ at 1300 MLT under magnetically quiet conditions. *Muliarchik et al.* [1982] assume that soft electrons precipitate in the region extending continuously from the night to day sector through dusk hours. They did not detect soft electron penetrations in the prenoon sector equatorward of the auroral oval. The region of soft electron penetration equatorward of the auroral oval seems to be asymmetric with respect to the noon meridian; it spreads over the dusk sector and is barely noticeable in the dawn sector. The detection of the region at late dawn hours is probably hampered by the superposition of the intense fluxes of precipitating high-energy electrons which appear in this time sector during and after magnetic disturbances. The asymmetry of the 0.434-keV electron precipitation region with respect to the equatorward boundary of the auroral oval in the dusk and dawn sectors follows from the DMSP observations [*Candidi et al.*, 1983]. *Gussenhoven et al.* [1983] have statistically studied the position of the equatorward DPB in the day sector. Frequently, auroral electron precipitation was not detected in the prenoon sector at latitudes below the equatorward boundary of the dayside cusp. The absence of such penetrations in the day sector may be treated as additional evidence for the above mentioned asymmetry of the soft electron precipitation region with respect to the noon meridian. According to *Gussenhoven et al.* [1983], the equatorward DPB is located on $\varphi \sim 69.4°$ at 1200–1300 MLT at $Kp = 0$. This result presents the mean position of the boundary inferred from a great number of passes and is characterized by a large dispersion. Besides that, the difficulties in determining the positions of the boundaries on the dayside are very significant [see *Gussenhoven et al.*, 1983], and therefore the problem of the precise positioning of the equatorward boundary of the soft auroral electron precipitations in the day sector cannot be considered to be finally solved.

Figures 11*a* and 11*b* show the dependences of φ_{DPB} on B_z and on MLT, respectively, at various B_Z as obtained in the work of *Kamide and Winningham* [1977], *Hardy et al.* [1981], and *Nikolaenko et al.* [1983]. The results of all the above papers coincide with each other to within 1° of latitude, although the linear correlation of φ_{DPB} with B_Z was determined for the entire interval of $B_Z \lessgtr 0$ in one of the papers and for the intervals $B_Z > 0$ and $B_Z < 0$ separately in the other two. It should be noted that although the latitudes φ_{DPB} obtained by *Hardy et al.* [1981] and by *Nikolaenko et al.* [1983] at the extreme values of $B_Z = \pm 5$ nT are the same, disagreement between them is observed in the middle of the interval because of a difference in the behavior of φ at $B_Z > 0$ where the boundary shifts equatorward according to *Hardy et al.* [1981] and to higher latitudes according to *Nikolaenko et al.* [1983].

The diffuse luminosity equatorward of the auroral oval is observed not only in the dusk sector, as was discussed in detail above, but also in the dawn and near-noon sectors [*Sandford*, 1964, 1968; *Hartz and Brice*, 1967; *Snyder et al.*, 1972; *Eather et al.*, 1979]. In the dawn sector the luminosity is frequently superimposed on pulsating subvisual auroral patches [*Kvifte and Pettersen*, 1969; *Roldugin and Starkov*, 1970; *Siren*, 1975, 1978; *Chernouss*, 1977; *Royrvik and Davis*, 1977; *Cresswell and Davis*, 1966; *Stenbaek-Nielsen and Hallinan*, 1979]. The pulsating auroras are closely associated with the high-energy electron precipitation responsible for a rapid increase of the auroral absorption of cosmic noise in the ionosphere as measured with riometers. The diffuse luminosity and the pulsating auroral forms constitute an integral part of the auroral substorm pattern [*Akasofu*, 1968; *Starkov and Feldstein*, 1971].

The diffuse luminosity equatorward of the oval in the dawn sector seems to be of a complicated structure. The luminosity located in the immediate proximity to the equatorward boundary of the auroral oval exists simultaneously with the luminosity band whose equatorward boundary runs closer to the geomagnetic parallel from night to day (such luminosity was called the mantle aurora by *Sandford* [1964]). The re-

lationship between the two types of luminosity varies depending on the geomagnetic activity level and accounts for the observed diversity in the morphology of the phenomenon.

Lassen [1972] indicated a $\sim 8°$ latitudinal gap in the location of discrete auroras at dawn hours (some forms are located at $\varphi \sim 67°$, while others are located at $\varphi \sim 75°$). *Zverev et al.* [1976] have examined in detail the mutual positions of the discrete and diffuse auroras in the dawn sector at $63° < \varphi < 74°$ during magnetic disturbances. In such periods the intensity of diffuse auroras increases, so they sometimes can be identified using all-sky camera data. After weak substorms the diffuse auroras are located in immediate proximity to the equatorward boundary of the structured auroral region. As the substorm intensity rises, the latitude band covered by diffuse auroras expands and the intensity increases, especially in the equatorward part of the diffuse aurora zone. A latitude "slot" may appear between the bright structured auroras along the auroral oval and the more intense part of the diffuse auroras, as described by *Lassen* [1972]. The slot between the brighter auroras in the oval and in the diffuse zone arises from the fact that there exist two types of diffuse luminosity located along the equatorial edge of the oval and approximately along a geomagnetic parallel. However, the equatorward DAB shifts somewhat poleward from night to noon, in agreement with the results obtained by *Evlashin and Evlashina* [1981].

The diffuse auroras equatorward of the oval in the dawn sector are due to the intense electron precipitation which was observed by *Frank and Ackerson* [1972] and, in more detail, by *Frank et al.* [1976] using the Injun 5 data. The intensity of the precipitating fluxes decreased gradually from midnight to late dawn and noon hours and was fairly uniform in latitude.

The spectra of the precipitating electrons in diffuse auroras do not show a secondary maximum, thereby indicating that the field-aligned electron acceleration by the quasi-static field-aligned electric fields is absent on these magnetic field tubes. The pitch angle distribution of the electrons is nearly isotropic here during and shortly after a substorm injection, but a loss cone with slow pitch angle diffusion develops during the recovery phase and afterward. The energy flux in the dawn sector diffuse precipitation depends essentially on the disturbance level and may reach values of the order of 1 erg cm^{-2} s^{-1} sr^{-1} in the 0.05- to 15-keV electrons. The DMSP 32 observations [*Meng*, 1978] have shown, however, that the diffuse precipitation zone is rather inhomogeneous in the dawn sector; namely, rather hard and much softer electron spectra can be observed here in the equatorward part and at the poleward edge, respectively, of the diffuse zone with the energy flux in the precipitation band of about 0.2–0.5 erg cm^{-2} s^{-1} sr^{-1}.

Meng and Akasofu [1983] related the luminosity which appears in the day and late dawn sectors equatorward of the auroral oval to the 10- to 20-keV electron precipitation. The electron energy flux increases up to $\gtrsim 0.1$ erg cm^{-2} s^{-1} sr^{-1} after moderate and intense disturbances. The luminosity was identified with the mantle aurora in the 3914-Å and 5577-Å emissions which form a wide band from midnight through dawn to noon. It has been shown that the hard electron precipitation region is asymmetric in local time with respect to the noon meridian and extends from the dawn sector to the early afternoon sector only (1300–1400 MLT), while its equatorward boundary is located at $\varphi \sim 65°$–$70°$ irrespective of longitude. As was noted above, the absence of high-energy electron precipitation in the late afternoon sector at $\varphi \sim 70°$ is a spatial rather than a temporal phenomenon. The asymmetric position of the hard electron precipitation region was also inferred from the riometer observations of the auroral absorption of cosmic noise [*Berkey et al.*, 1974]. Model calculations have shown that the mantle aurora is produced by the precipitation of high-energy electrons drifting from midnight to noon in the radiation belt region during and after magnetospheric substorms [*Hoffman*, 1972; *Meng and Akasofu*, 1983]. The drift of the 5- to 20-keV electrons is limited to the dawn and day sectors, whereupon their drift trajectories emerge to the magnetopause and they leave the magnetosphere. It is this circumstance that distinguishes the mantle aurora from the diffuse luminosity which is located in immediate proximity to the equatorward boundary of the auroral oval in the region of the outer belt of trapped particles. The latter is due to the precipitation of soft suprathermal electrons transferred by the unsteady convection during disturbances from the plasma sheet to the magnetospheric interior.

According to *DeForest and McIlwain* [1971] and *Hultqvist* [1975*a*, *b*], the drifting electrons in a broad energy range are injected into the magnetosphere from its tail over the entire nightside. Simultaneous precipitation from the plasma sheet was observed by *Eather et al.* [1976] in the longitude interval from 1700 to 0300 MLT and by *Panasyuk et al.* [1978] in the longitude interval above 12 hours. However, the high-energy particle fluxes are maximal near midnight, and the variations of the keV electrons with local time are insignificant. Detailed descriptions of the electron spectra in diffuse auroras may be found in the work of *Meng* [1978].

Isolated auroral optical emission regions equatorwards of the diffuse auroras were observed on board ISIS 2 also in the dusk sector [*Anger et al.*, 1978; *Moshupi et al.*, 1979]. Such regions appear predominantly during the recovery phase from moderate geomagnetic activity, their intensity is lower in comparison with the diffuse auroras located further poleward, and the ratio of the 3914-Å and 5577-Å emissions is indicative of harder spectra of the precipitating electrons. The results obtained by *Wallis et al.* [1979] have shown that the optical emission is due to the precipitation of hard electrons at all energies up to 210 keV. The luminosity is produced by the outer belt electrons injected in the geomagnetic trap during previous short-lived disturbances and precipitating into the ionosphere during their drift around the earth.

Fjodorova and Knuth [1978] have observed intense precipitations of outer belt electrons causing measurable ionospheric absorption down to $L < 3$ at moderate Kp values. *Meng and Akasofu* [1983] failed to find any relationship of the equatorward boundary of the hard electron precipitation region to the Kp index. One of the reasons for their results is probably the effect of the previous activity on the position of this precipitation boundary at dawn hours which was disregarded in the data analysis. However, the processes relevant to high-energy electron precipitation from the radiation belt are of a specific nature and will not be discussed here.

The DPB position in the dawn sector was obtained by *Gussenhoven et al.* [1981] as a function of the Kp index and by *Hardy et al.* [1981] as a function of the interplanetary medium parameters. These relations for the northern hemisphere at 0700–0800 MLT are

$$\varphi_{DPB} = 70.2° - 2.15° \, Kp \qquad \tau = -0.83$$

$$\varphi_{DPB} = 66.2° + 1.25° \, B_z \qquad \tau = -0.62 \qquad B_z < 1 \text{ nT}$$

$$\varphi_{DPB} = 67.0° - 0.067° \, B_z \qquad \tau = -0.05 \qquad B_z > 1 \text{ nT}$$

It is seen that φ_{DPB} is closely related to Kp and B_Z in the intervals with $B_Z < 1$ nT and that such relationships are practically absent in the intervals with $B_Z > 1$ nT. The use of additional data [*Gussenhoven et al.*, 1983] has made it possible to alter somewhat the relation

$$\varphi_{DPB} = 68.9° - 1.91° \, Kp \qquad \tau = -0.76$$

Similar dependences were obtained for all hours of MLT. In the dawn sector, DPB is located in relatively low latitudes even at low magnetic activity ($Kp \sim 1$–2) and practically along a geomagnetic parallel at high Kp. Taking into account the adopted methods for boundary selection, the results indicate that the above relations can, to a great degree, describe the position of the equatorward boundary of the diffuse precipitation region of harder electrons (the mantle aurora). According to the observations on the Atmosphere Explorer satellite [*Heelis et al.*, 1980], the position of the equatorward boundary of the 0.2- to 25-keV electron diffuse precipitation at $\varphi \sim 70°$ and 1500 MLT shifts monotonically to $\varphi \sim 61°$ at 0200 MLT and, after that, ascends up to $\varphi \sim 66°$ at 0900 MLT. According to *Gussenhoven et al.* [1983] for $Kp = 2$, $\varphi \sim 69.3°$ at 1500 MLT, $\varphi \sim 62°$ at 0200 MLT, and $\varphi = 65.6°$ at 0900 MLT. A more accurate comparison between the results of the two works is difficult because *Heelis et al.* [1980] disregarded the data on the variations of the φ_{DPB} positions at different disturbance levels.

In the dawn sector the diffuse auroras coincide with the large-scale regions of enhanced ionization in the ionosphere [*Senior et al.*, 1982; *Sivtzeva et al.*, 1983]. In this case the complicated structure of the precipitation regions of the suprathermal and high-energy electrons in the dawn sector, which gives rise to two types of diffuse luminosity, has its signatures in the data of the oblique ionospheric sounding of the subauroral F layer.

Khalipov et al. [1977] have shown quantitatively that in the dusk-premidnight sector the poleward edge of the main ionospheric trough of the electron number density near the ionospheric F layer maximum just coincides spatially with DPB. This fact was subsequently extended and substantiated by systematic measurements and comparisons. It permits the DPB position to be traced nearly continuously by oblique soundings under the conditions of the dark ionosphere using the data from a latitudinal chain of subauroral ionosondes which bear visual signatures of the trace scattered from the sharp poleward wall, or cliff, of the main ionospheric F region trough.

In the dawn sector the ionization latitude structure in the F layer equatorward of the auroral oval is more complicated; namely, the latitudinal behavior of ionization may involve two bands of increased plasma density at the altitudes of the D layer [*Möller*, 1974]. *Khalipov et al.* [1983] and *Sivtzeva et al.* [1983] have described cases with two or even three steps of increased plasma density in the latitudinal profile of the F region in the dawn sector during magnetospheric substorms using the data from the meridional chain of vertical and oblique sounding stations in Yakutia and inferred similar structures in precipitation and in luminosity. The subauroral region, or step density increase, located at a higher latitude, appears as a continuation of the diffuse precipitation region from dusk to dawn, and the DPB position calculated from the model proposed by *Galperin et al.* [1977] for midnight coincides in the 0000 < MLT < 0500 interval with the equatorward boundary of this region of increased ionization. The equatorward boundary of the second region of increased ionization coincides with the poleward wall of the main ionospheric trough and with the equatorward boundary of a very feeble particle precipitation. Such particles seem to be of sufficiently high energies and to give rise to various geophysical phenomena not only at F layer altitudes but also at the E layer [*Evans and Moore*, 1979]. According to *Filippov et al.* [1980] the inhomogeneities of the anomalous ionization in the ionospheric F layer appear on the ionograms of vertical and oblique soundings most frequently in two regions in the dawn sector, one being located near the equatorward boundary of the auroral oval, and another being located in lower latitudes along the quasi-circular zone. This pattern agrees with the above described structure of the auroral electron precipitation regions. The results of vertical and oblique soundings in the dawn sector may be used with sufficient reliability to locate the position of the equatorward boundary of the diffuse precipitation region of suprathermal magnetospheric electrons. This is substantiated by good agreement of the DPB position obtained by *Heelis et al.* [1980] with the position of the poleward boundary of the main ionospheric trough obtained by *Benkova et al.* [1980] and by *Samsonov and Romaschenko* [1982].

Thus the observational data indicate that electron precipitation extends equatorward of the auroral oval in the dawn sector and that this precipitation gives rise to feeble diffuse luminosity and ionization of the subauroral ionosphere. In the dusk sector, where the structure of this region is relatively simple, consistent quantitative relations have been obtained between the DAB position, the magnetospheric disturbance intensity, and the interplanetary medium parameters. The extension of the region to the noon and dawn sectors, where the precipitation pattern is more complicated, has been studied much less. However, a noticeable asymmetry with respect to the noon meridian may well be established; namely, the soft electron penetration region (and hence the respective auroral luminosity region) spreads over the dusk sector, extends to afternoon hours, and is barely noticeable at the prenoon hours. In the dawn sector, apart from the soft electron precipitation region extending along the oval from the midnight sector, there exists a region of diffuse precipitations of the radiation belt hard electrons drifting eastward during, and within several hours after, magnetospheric substorms. The precipitations of such particles give rise to the mantle aurora and to the pulsating auroral patches in the postmidnight and dawn sectors. The precipitations of such a type are asymmetric with respect to the midnight meridian and are maximum in the dawn sector; i.e., the asymmetry patterns of two types of diffuse precipitations are opposite. The existence of two types of precipitations of a different nature in the dawn sector of the diffuse zone makes it difficult to study their characteristics on the basis of the measurements of auroral luminosity and of narrow energy range measurements of the electron precipitation. In particular, it is difficult to obtain quantitative data on the positions of the boundaries of the luminosity bands of two coexisting and partially overlapping types under various geophysical situations and on the longitudinal extension of the region of soft precipitation equatorward of the auroral oval into the dawn and noon sector. The differences in the spectral features of the precipitating electrons in the afternoon and prenoon sectors of the diffuse auroral region were considered by *Meng* [1978].

It seems to us that the changes of the position of the equatorward boundary of the diffuse precipitation region of auroral electrons during magnetospheric substorms may account

for the "mysterious" appearance of hot plasma inside the outer plasmasphere (on $L \sim 3$–4) observable in the postmidnight and dawn sectors [*Sivtzeva et al.*, 1983]. It is known from whistler data [*Carpenter et al.*, 1979] that the earthward radial drift of the thermal and soft auroral plasmas at the plasma sheet inner boundary at dawn is enhanced in these sectors during active phases of substorms. The radial inward drift, which lasts for 1–3 hours, introduces hot plasma from the plasma sheet to the shells down to $L \sim 3$ and, simultaneously, carries away thermal plasma from the same region of the outer plasmasphere. During the drift period (or as the magnetospheric disturbances get weaker), the plasma sheet electric field responsible for the radial plasma drift in the inner magnetosphere is shielded (or decreases). The smooth original form of the equipotential surfaces, which is characteristic of the quiescent plasmasphere, is restored, so that some hot quasi-trapped plasma finds itself inside the closed equipotentials, i.e., within the outer plasmasphere where cold plasma density is depleted. Electrons and ions of a few keV in energy caught in this sector of corotating outer plasmasphere have a low gradient drift velocity. So they nearly corotate with the earth and dissipate gradually to the subauroral atmosphere. We conclude that such nonadiabatic behavior of the convection electric field gives rise to the slowly precipitating population of the quasi-trapped hot plasma which resides for many hours in the local time–limited sector of the outer plasmasphere. Such hot plasma precipitation and quasi-trapping in closed field tubes lead to the accumulation in these tubes of the secondary electrons and suprathermal ions supplied from the ionosphere as a result of the rapidly developing ion outflow in the form of unsteady state "polar wind." Precipitations of such "remnant" auroral and suprathermal electrons may give rise to weak, though quite measurable, auroral emissions, to pulsating and burstlike strong diffusion events in the outer belt electrons, and to an additional steplike increase (or "cliff") of the F layer ionization in the subauroral ionosphere on the field tubes of the outer plasmasphere in the postmidnight sector. This scenario of the processes occurring after substorms holds in the postmidnight sector of the subauroral ionosphere, when and where a very unstable mixture of upflowing rarefied thermal plasma and suprathermal secondaries can give rise, because of precipitation of the remnants of the hot plasma injected from the plasma sheet, to unsteady state and spatially inhomogeneous enhancements in the precipitation of the outer belt hard electrons. Apparently, this is concordant with a variety of ground-based observation and spacecraft measurement data (see, for example, *Sivtzeva et al.* [1983]); however, this subject is beyond the scope of the present review.

5. The Diffuse Luminescence Region Poleward From the Auroral Oval

Eather [1969] and *Eather and Mende* [1971, 1972], based on the results of airborne photometric observations, have shown that a diffusive subvisual luminescence produced by suprathermal electron precipitations is observed in the night sector poleward from the auroral oval. The ratio of the emission intensities λ6300/4278 in this luminescence varies from ~ 2 at the auroral latitudes to 5 at $\varphi \sim 80°$. The latitude variation of the ratio is indicative of a softening of the precipitating electron spectrum down to several eV and lower toward the pole from the poleward boundary of the oval. Figure 12*a* presents the latitude variations of percentage occurrence of the precipitations of electrons with mean energies of < 1 keV and > 1 keV inferred from the data on the emission ratio [*Eather and Mende*, 1972]. As can be seen from the figure, the nighttime precipitation at $\varphi \gtrsim 80°$ is completely ($\sim 90\%$) due in practice to the < 1-keV electrons. This precipitation is characterized by a low luminosity in the emission λ4278 Å; i.e., it appears as a weak subvisual luminescence. This luminescence is observed during relatively quiet periods and is irrelevant to the possible occurrence, at $\varphi \sim 80°$, of the intense auroras which propagate poleward from the oval up to such high latitudes during active phases of magnetospheric substorms. The diffuse luminescence poleward from the auroral oval is less homogeneous than that observed equatorward of it. Isolated structural formations are observed in the former, and they are excited by the precipitation of softer electrons with considerably lower energy fluxes than those in the auroral oval.

During magnetically quiet periods, when the IMF B_Z component is northward, a weak diffuse luminescence with a < 0.5-kR intensity not only fills the entire region between the discrete auroral forms over the oval (see above) but also is observed inside the polar cap [*Murphree et al.*, 1982]. The red luminescence, which is due to soft electrons penetrating poleward from an auroral arc in the night sector, was reliably identified in high-sensitivity color photographs taken with all-sky cameras in various emissions [*Mende and Eather*, 1976].

Intense auroras propagating poleward in the night sector during active phases of substorms are contained within a border of diffusive luminescence [*Ievenko and Samsonov*, 1982]. The meridional scanning photometer data are indicative of an abrupt softening of the spectrum of the auroral electrons exciting the light emissions at the poleward boundary of the luminescence region [*Sandholt et al.*, 1982].

Starkov and Feldstein [1971] included this diffuse subvisual luminescence on the poleward side of the oval in their global pattern of auroral substorm development in the night sector. During magnetically quiet periods the boundary of such a luminescence is located at $\varphi \sim 80°$. During creation phases of substorms (~ 1 hour before active phase onset), the poleward boundary of the diffuse subvisual luminescence band shifts to lower latitudes with the outcome that the latitude region of the band narrows steadily, so that a much confined luminescence band exists at the moment of substorm active phase onset. The poleward boundary location and the locations of the oval boundaries respond in practice without any delay to the development of magnetospheric disturbances. It appears that the diffuse luminescence located poleward of the oval is characterized by a close time correlation with the disturbances and motions in the dynamical outer magnetosphere, and hence it differs radically from the equatorward diffuse luminescence which is due to inertial processes in the inner magnetosphere. However, the studies aimed at establishing quantitative relations characterizing the location of the poleward boundary of the diffuse luminescence at various disturbance levels (for a certain value of the energy flux to the ionosphere) are still in their initial stage.

Locations of the poleward boundaries of precipitation of electrons with $E > 0.05$ keV under extremely quiet geomagnetic conditions in the dawn and dusk sectors were analyzed by *Meng* [1981*b*] on the basis of the DMSP data. In this case the region of the diffuse precipitations extends up to $\varphi \sim 85°$–$87°$ for the electron flux of $\sim 10^8$ ergs cm^{-2} s^{-1} sr^{-1} and the energy flux of $\sim 2 \times 10^{-2}$ erg cm^{-2} s^{-1} sr^{-1}, i.e., spreads over almost the entire polar cap. The location of the poleward boundary for particle fluxes of $> 10^7$ ergs cm^{-2} s^{-1} sr^{-1} was

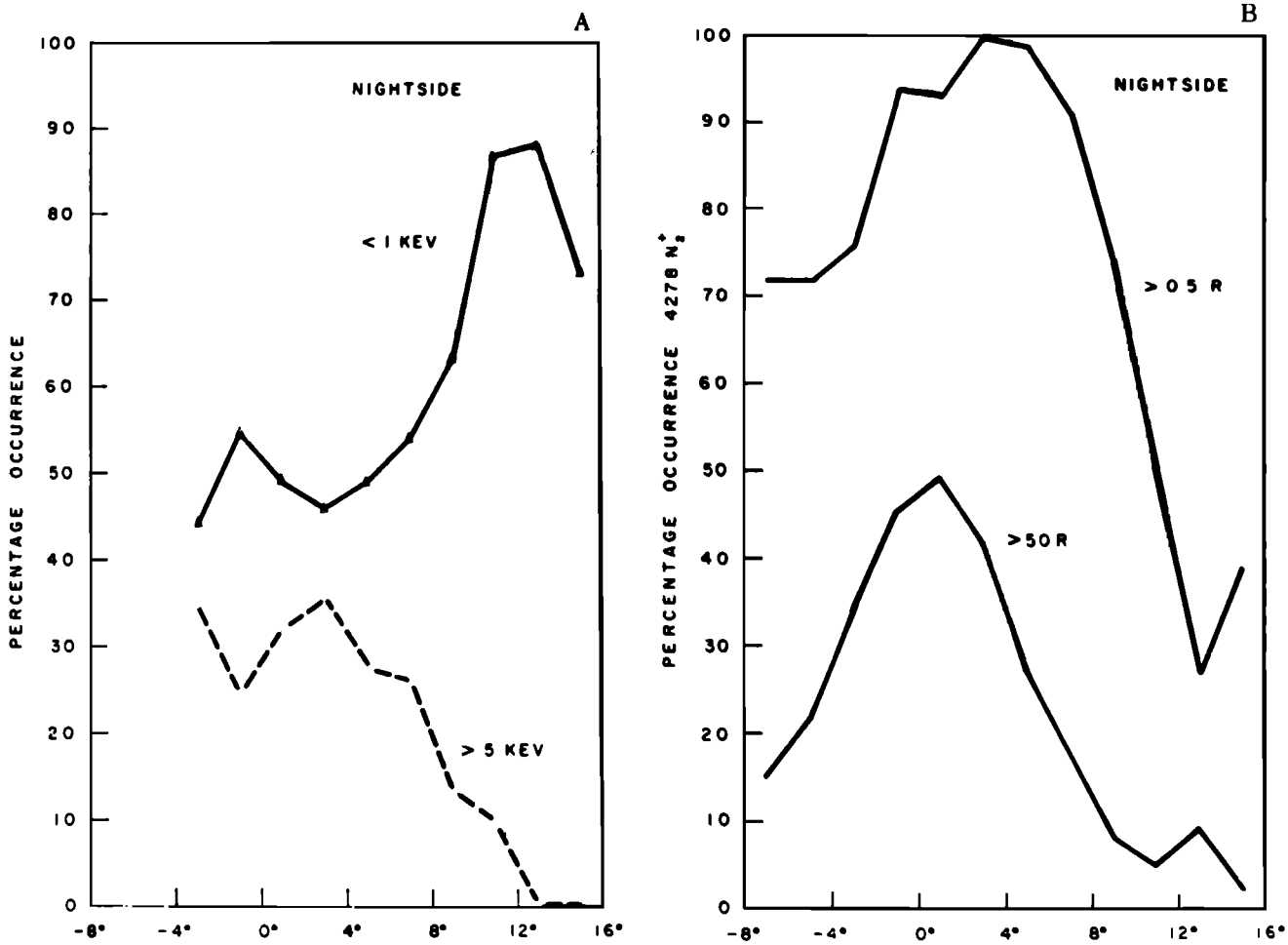

Fig. 12. (*a*) Percentage occurrence of electron precipitations with mean energies of <1 keV and >5 keV for auroral oval coordinates in the night sector [*Eather and Mende*, 1972]; 0° corresponds to the equatorward boundary of the auroral oval. (*b*) Percentage occurrence of the 4278 N_2^+ emission exceeding 0.5 R (detection threshold) and 50 R for auroral oval coordinates.

statistically determined by *Makita et al.* [1983] in all the MLT sectors. There is, however, a smooth intensity decrease (without any pronounced boundary) in low-energy (<500 eV) electrons on $\varphi > 80°$. In the near-polar region the <1-keV soft electrons can mainly penetrate. In this case the boundary shifts toward lower latitudes with increasing energy flux and approaches, but does not reach, the poleward boundary of the oval.

During long extremely quiet periods, apparently, nearly the entire polar cap (up to very high latitudes) is covered by weak electron precipitation, and a luminescence of the entire cap in the 6300-Å line emission may be expected. Such a luminescence was actually observed up to $\varphi \sim 85°$ by *Weill et al.* [1965] during magnetically quiet periods in the years of solar minimum. In the night sector the subvisual luminescence poleward from the auroral oval was observed from 1800 to 0500 MLT to be wide bands extended along a geomagnetic parallel. The luminosity in the bands increases poleward and then falls rather abruptly and forms a pronounced poleward boundary. Its location does not follow the line $\varphi = \text{const}$. It is supposed that the flux of soft electrons with energies ranging from 30 to 150 eV recorded on board Cosmos 261 [*Galperin et al.*, 1970] in the dusk sector up to $L \sim 20$–30 ($\varphi \sim 75°$–$80°$) should be responsible for this luminescence. The integral energy flux at these latitudes was 0.3 erg cm^{-2} s^{-1} sr^{-1}, i.e., was quite sufficient to induce the subvisual luminescence.

According to *Meng* [1981*b*] the expansion of electron precipitation up to the poles is due to an increase of the plasma sheet size and to a diminution of the high-latitude tail lobe in the magnetotail under extremely quiet magnetospheric conditions (see also *Murphree and Cogger* [1981] and *Murphee et al.* [1982]). Precipitation of plasma sheet electrons with energy of 0.434 keV into the upper atmosphere poleward from the oval was observed by *Candidi et al.* [1983]. Such penetration spreads over the dusk and dawn sectors under quiet magnetic conditions ($Kp \leq 2+$). The diffuse precipitation of soft electrons poleward from the oval was observed when the IMF B_Z component turned northward after active phases of substorms [*Hardy et al.*, 1982]. The authors supposed, however, that the interior cusp particles should be a source of these electrons.

The space-time localization of the 0.1- to 20-keV electron precipitation region was inferred by *Dyachenko et al.* [1980] from the Meteor 28 data. In particular, electron precipitation with soft monotonic spectra and energy fluxes $E \lesssim 10^{-1}$ erg cm^{-2} s^{-1} sr^{-1} were observed poleward from the typical "inverted V" structures. In the dusk-midnight sector, during magnetically quiet periods ($Kp \leq 1$), the boundary of the diffuse precipitation extends to $\varphi \sim 79°$, and the latitude extension of

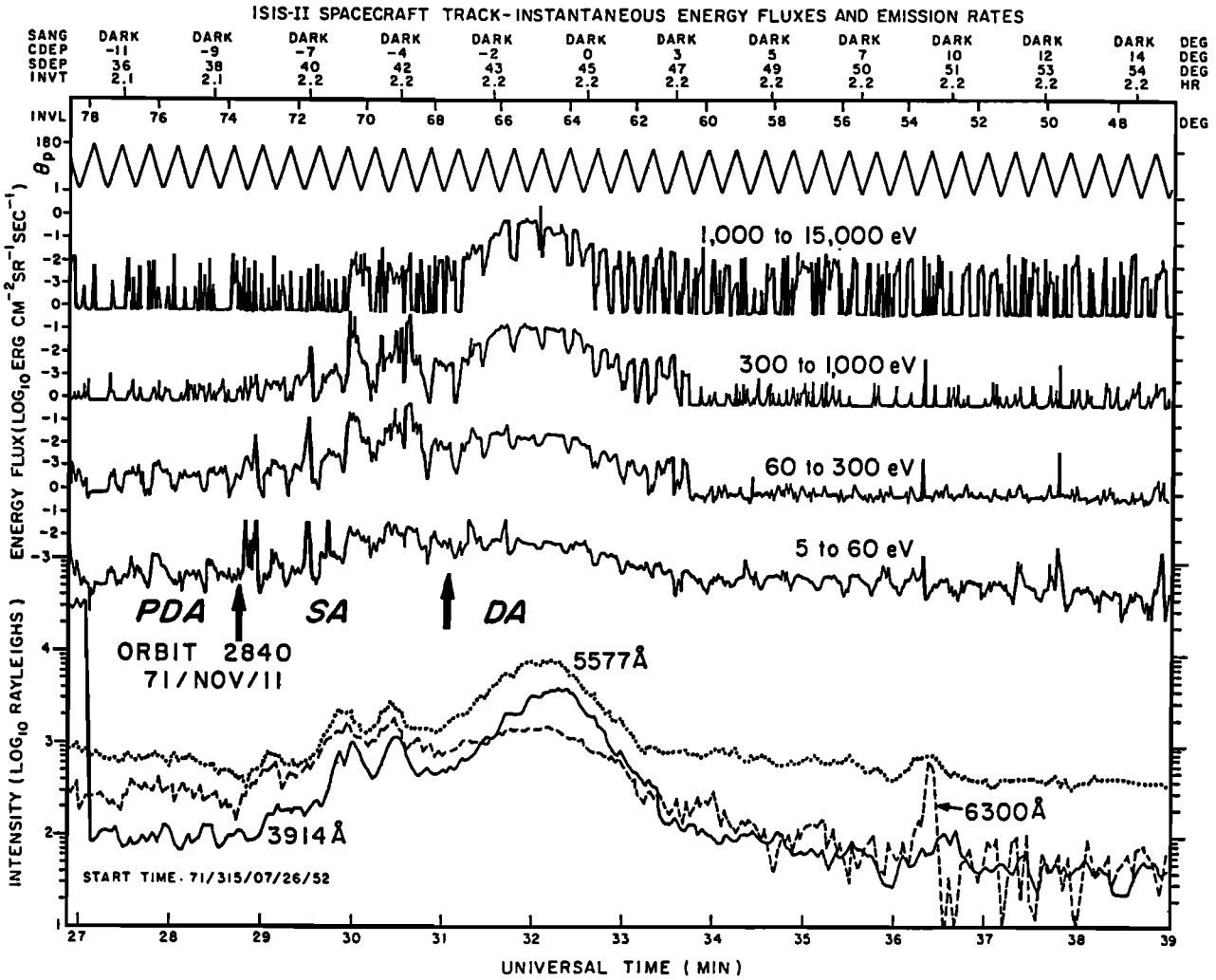

Fig. 13. Intensity variations of the precipitating electrons of various energies and of the auroral intensities during an ISIS 2 traversal of the night sector of the auroral oval at 0727–0739 UT on November 11, 1971 [*Shepherd et al.*, 1980]. The upper line shows the variations of the satellite pitch angle. Shown below are the intensity variations of the 6300-, 5577-, and 3914-Å emissions along the ISIS 2 trajectory. DA, diffuse auroras; SA, structured auroras; PDA, polar diffuse auroras. The arrows indicate the approximate positions of the boundaries between auroras of various types.

the region reaches $\sim 7°$. During magnetically disturbed periods ($Kp \sim 6$), the poleward boundary of the soft diffuse precipitation is located at $\varphi \sim 77°$, its latitude extension does not exceed $\sim 2°$, and the zone of soft monotonic electron spectra is adjacent to the poleward oval boundary which is shifted to the pole. The diffuse luminescence in the dusk sector poleward from the auroral arcs was observed systematically on board ISIS 2 [*Murphree et al.*, 1981*a*]. During the DMSP/F2 passes through the late dusk sector a bright luminescence was observed poleward from the "inverted V" [*Tanskanen et al.*, 1981]. Along the poleward boundary of the oval during magnetospheric substorms intense fluxes of soft electrons 10^9–10^{10} $cm^{-2}\ s^{-1}\ sr^{-1}$ with energies of $\lesssim 200$ eV and with steep and monotonic spectra were detected. It should be noted that the softening of the precipitating electrons and a decrease of their energy flux at the poleward side of the precipitation region were also observed on board some other spacecraft equipped with apparatus capable of measuring energy fluxes of electrons down to 10^{-3} erg $cm^{-2}\ s^{-1}\ sr^{-1}$ (*Galperin et al.* [1970] on Cosmos 261, *Frederick and Hays* [1978] and *Heelis et al.* [1980] on AE-C, *Valchuk et al.* [1979] on AUREOL 2, *Shepherd* [1979*b*, 1982] on ISIS 2, *Chiu and Gorney* [1983] on S3-3), and suggestions concerning their origin from the extended plasma sheet on closed field lines up to $\sim 80°$ from Cosmos 261 and even higher from some other satellites were made in these papers. Electron precipitation poleward from the oval, which should be related to the diffuse zone, is not always uniform. Even during magnetically quiet periods there are increases and decreases of particle intensity, and it is sometimes difficult to identify this zone unambiguously on the energy-time spectrograms. But the poleward diffuse zone differs from the precipitation along the oval in another important feature; namely, it is located in the region of antisolar convection. *Heelis et al.* [1980] have shown that a part of the region of the antisunward convection is usually found within the auroral particle precipitation region. *McDiarmid et al.* [1978] came to identical conclusions concerning the data from the dusk (1500–2100 MLT) and dawn (0300–0900 MLT) sectors: (1) the convection reversal from antisunward to sunward occurred within the region of auroral electron precipitations rather than at its poleward boundary; (2) the auroral electron precipitation takes place on closed field lines.

Hence it may be assumed that the poleward diffuse zone is located in the antisunward convection region, while the auro-

ral oval and the diffuse penetrations equatorward from the oval lie in the region of sunward convection. In this case the entire nightside region of auroral precipitation is located on closed geomagnetic force lines.

Figure 13 shows the results of measuring the 5-eV to 15-keV electron intensities in the night sector during an ISIS 2 pass in winter. Also shown are three optical auroral emissions [*Shepherd et al.*, 1980]. The observed spectra, the character of electron precipitations, and the emission intensities imply that the observed latitude interval can be divided into three distinct regions, namely, the equatorial region (DA) at $62° < \varphi < 67°$ corresponding to the diffuse luminescence region equatorward from the auroral oval, the auroral oval proper with structured forms (SA) at $67° < \varphi < 74°$ inferred from the peaks of structured emissions, and the poleward region of diffuse auroras (PDA) at $\varphi > 74°$ where soft electron fluxes prevail, while the 3914-Å N_2^+ band intensity falls to the instrumental threshold. The data of the measurements taken from 0727 to 0739 UT on November 11, 1971, were obtained during the magnetically quiet period which began at 0400 UT [*Allen et al.*, 1975]. It is quite possible that the poleward PDA zone boundary extends outside the data reception interval shown in Figure 13, i.e., to $\varphi > 78°$.

Thus according to various observational data, there exists a region of soft electron precipitations poleward from the auroral oval. The poleward boundary of the luminescence in this region undergoes temporal variations closely associated with the development of magnetospheric disturbances. The immediate task here is to obtain quantitative relations of the poleward PDA boundary location to the phase and intensity of these disturbances. PDA is to be located on closed field lines because a rather high degree of conjugation in the location of the luminescence poleward boundary was inferred from the observations in both hemispheres [*Makita et al.*, 1983]. Apparently, PDA is a projection of the high-latitude (outer) part of the nightside plasma sheet onto ionospheric latitudes.

6. Polar Cap Auroras

The polar cap is usually considered in the literature to be a near-pole region encircled by the poleward boundary of the auroral oval [*Akasofu*, 1968]. A special type of auroral luminescence observed there is called polar arcs (PA). In some model representations the polar cap is located inside a surface that consists of geomagnetic field lines which traverse the neutral line ($B = 0$) supposedly located around the magnetosphere [*Akasofu*, 1977*a*]. Along the neutral line the geomagnetic field lines are reconnected with the interplanetary magnetic field. The projection of this surface onto the ionosphere coincides approximately with the poleward boundary of the auroral oval. Apparently based on these model representations, *Meng et al.* [1977] have related an auroral arc during a magnetically quiet period to the poleward boundary of the auroral oval. It was, however, shown above that poleward from the nightside auroral oval a diffuse luminescence was located which is excited by soft electrons incoming from the periphery of the plasma sheet. Therefore a quiet auroral arc along the oval is to be projected inside the plasma sheet on closed field lines and, therefore, cannot be considered a neutral line projection. This circumstance proves to be very important in connection with the discussion in the literature of the generation mechanism of magnetospheric substorms, in particular, with a localization of the magnetospheric region where a substorm commences, and with the problem of the origin of stable auroral arcs inside the oval. That is why this morphological problem proves to be one of the problems of key importance in the magnetospheric physics.

It is useful to define the polar arcs as a special type of luminescence because the polar caps are mapped along magnetic field lines on the special structural region of the magnetosphere called tail lobes. The tail lobes are located just outside the plasma sheet of the tail, and plasma density there is extremely low. The intensity of the auroral luminescence in the polar caps is usually slightly higher than the level of airglow. That is why it is especially interesting to study discrete forms of polar cap auroras because their mapping inside the depth of the plasma sheet seems impossible, so the abundant source of hot particles exciting the luminescence is still to be identified.

During magnetically quiet periods, as was already described, the diffuse luminescence poleward from the oval extends up to very high latitudes. This means that the plasma sheet, receding from the earth by its inner part, expands simultaneously at its outer (poleward) boundary. In such a way, the volume of the part of the tail which is mapped on the night sector of the polar cap decreases [*Meng*, 1981*c*].

The plasma mantle which, according to various magnetospheric models, is mapped on the dayside polar caps becomes, at the same time, narrower [*Sckopke et al.*, 1976], thereby reflecting the gross reconfiguration of the magnetosphere. During the periods with $B_Z > 0$, a considerable region inside the poleward boundary of the oval is covered by the subvisual luminescence produced by weak "drizzling," precipitation of soft electrons with energies of up to 0.1–1 keV (except only for some limited areas near geomagnetic poles).

This testifies strongly that some hot plasma drifting toward the earth and undergoing adiabatic acceleration in the tail is present here, because the 0.1- to 1-keV electrons are absent in the solar wind. The polar cap boundaries during the periods with $B_Z > 0$ can hardly be distinguished if they are inferred from the data on feeble diffuse auroral luminescence. In a similar way, the projections of the boundaries between the tail lobes, plasma sheet, and plasma mantle were not determined unambiguously by the luminescence and particle measurements. We suggest that such projections might be found from magnetic field variations due to the field-aligned currents flowing in this region. The magnetic field lines in the polar caps are supposed to be open (i.e., to be connected to the IMF). During periods with $B_Z > 0$ the total flux of open magnetic field lines proves to decrease significantly, and the position of the remaining polar cap proper is controlled by the IMF B_Z and B_y components. Considering these experimental difficulties involved in boundary determination, we adopt the tentative definition of the polar cap as a spatially limited high-latitude region located poleward from the auroral oval within which (1) polar cap arcs are located at the typical orientation approximately along the earth-sun line and (2) the diffuse auroral luminescence is feeble, i.e., does not exceed some level compatible with the available observational evidence (say, about 10^{-2} erg cm^{-2} s^{-1}). Such a definition implies a temporal expansion of plasma sheet and radical diminution of the tail lobes in some intervals of $B_Z > 0$.

A relatively rare, but striking, feature of the polar caps is the existence of very long narrow regions of auroral emission which are often called sun-aligned arcs. The main morphological features of this type of auroral luminescence were described in their reviews by *Feldstein et al.* [1969] and *Cogger* [1980] and were summarized by *Akasofu and Roederer* [1983]. These features are as follows:

1. Auroras occur in single or multiple arcs with rayed structure. The lifetime of single arcs is usually several minutes. Extended arcs, however, occur in satellite images during successive passes of DMSP in every 100 min in 42.5% of the cases [*Gussenhoven*, 1982]. The average length of an arc was $\sim 1.5 \times 10^3$ km [*Ismail et al.*, 1977] or $\sim 10^3$ km [*Ismail and Meng*, 1982]. However, *Frank et al.* [1982*a*] observed an arc which extended through the polar cap from the day to the night sector of the auroral oval (θ auroras) (see also *Lassen* [1972] and *Anger* [1979]). Such extended arcs are rare because polar cap arcs of any type were only observed in 6% of ISIS 2 and in 4% of DMSP passes. According to the ground-based International Quiet Sun Year observation data, the percentage occurrence of discrete auroras in the zenith at the near-pole region was ~5% [*Belousov et al.*, 1968]. Furthermore, such an arc usually terminates inside the polar cap and fails to reach the night sector of the auroral oval. The width of an arc is ~30–40 km as inferred from the ground-based photometric observation data [*Romick and Brown*, 1971] and ~70 km as estimated from spacecraft observations [*Ismail et al.*, 1977]. *Frank et al.* [1982*a*, *b*] observed ~15 examples of the θ auroras within a month. The time duration of this auroral configuration can reach at least several hours.

2. The arcs are mainly oriented along the noon-midnight meridian, which results in their rotation by 360° during a day as observed from the earth's surface [*Mawson*, 1925; *Davis*, 1960; *Feldstein*, 1960; *Denholm and Bond*, 1961].

3. The arcs appear mainly during magnetically quiet periods [*Feldstein*, 1962; *Davis*, 1963; *Lassen*, 1963] when the IMF B_Z component is positive [*Berkey et al.*, 1976; *Ismail et al.*, 1977; *Lassen and Danielsen*, 1978; *Frank et al.*, 1983] and the solar wind velocity is high [*Gussenhoven*, 1982].

Figure 14 presents the occurrence frequency of the arcs in the southern polar cap for different orientations of the IMF according to *Yakhnin and Sergeev* [1979]. As can be seen from Figure 14*a*, the occurrence frequency grows approximately linearly with B_Z for northward IMF, and it is very small for southward IMF orientations. Figures 14*b* and 14*c* demonstrate a prevalence of auroral occurrences in the polar cap in the cases when the azimuthal component $B_Y < 0$ and the radial component $B_X > 0$ (with the simultaneous condition $B_Z > 0$). Thus the occurrence frequency of auroras in the southern hemisphere is increased when the IMF is sunward. The additional study made by *Sergeev and Yakhnin* [1979] has shown that the arcs appear mainly at $B_Y < 0$ in the southern hemisphere and at $B_Y > 0$ in the northern hemisphere. The effect of the radial IMF component (B_X) direction on the occurrence of arcs in polar caps was confirmed by *Ismail and Meng* [1982], namely, that the arcs appear mainly during $B_X > 0$ periods in the southern polar cap and during $B_X < 0$ periods in the northern cap. The effect of the IMF B_X component on polar cap auroral occurrence agrees with the results of *Burch et al.* [1979], who recorded the structured precipitations of electrons in the northern polar cap when the IMF was characterized by the component $B_Z > 0$ and $B_X < 0$ (the IMF was directed away from the sun). The effect of the B_Y component is also characterized by the fact that in the dawn (dusk) sector of the polar cap the occurrence frequency of the arcs is higher for negative (positive) B_Y [*Lassen*, 1979; *Gussenhoven*, 1982].

4. The spectral ratio of the emissions 5577 Å/3914 Å in the polar arcs varied from 1 to 3, and the ratio 6300 Å/3914 Å was about 7 [*Cogger*, 1980]. A comparatively high intensity of the emission 6300 Å in the polar arcs, which was noticed earlier

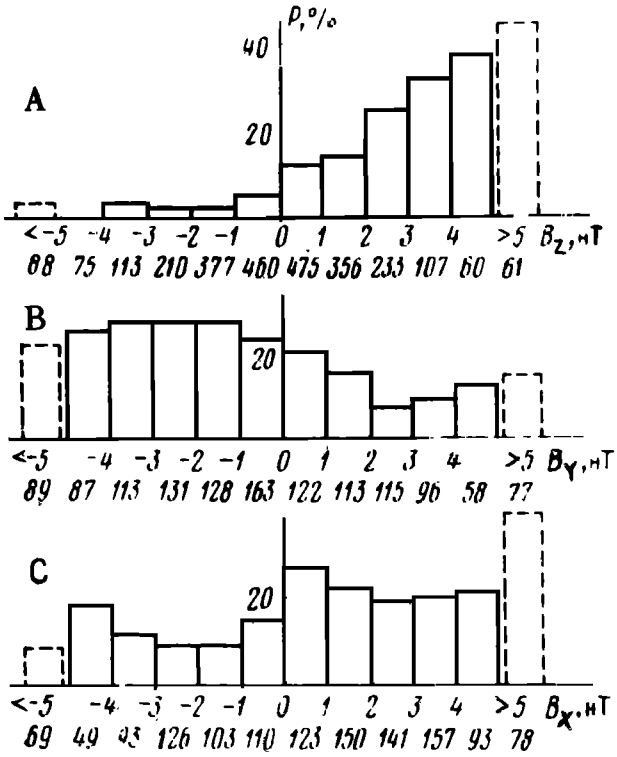

Fig. 14. Percentage occurrence of polar cap arcs versus the intensity and direction of the IMF (*a*) B_Z component, (*b*) B_Y component at $B_Z > 0$, and (*c*) B_X component at $B_Z > 0$ [*Yakhnin and Sergeev*, 1979, 1981]. The numbers under the histograms indicate observation periods in hours for the relevant intervals of the values of the IMF components.

by *Eather and Akasofu* [1969], indicates that the luminescence in the arc is excited by a precipitation of 0.2- to 1-keV electrons the energy flux of which reaches 1–10 ergs cm^{-2} s^{-1} sr^{-1}. This is confirmed by the measurement data of several other studies [*Whalen et al.*, 1971; *Meng and Akasofu*, 1976; *Meng*, 1978]. No proton flux was observed above the arcs (it proved to be below 10^{-3} erg cm^{-2} s^{-1}). These values are in agreement with direct measurements [*Murphree et al.*, 1983]. But recent low-energy particle measurements from AUREOL 3 (the ARCAD 3 project; see *Galperin et al.* [1982*a*, *b*] and *Galperin and Reme* [1983]) made it possible to measure the soft proton precipitation above the polar caps. For "drizzle" proton precipitation the 50- to 100-eV protons reach intensities of about 10^5 $(cm^2\ s\ sr\ keV)^{-1}$. Proton intensity drops are usually observed simultaneously with intensifications of soft electrons, thereby indicating field-aligned potential differences associated with polar cap discrete auroral formations.

Except for their position and a somewhat lower associated average electron energy, the polar cap arcs bear a strong resemblance to the oval-aligned arcs [*Murphree et al.*, 1982]. *Frank et al.* [1982*a*, *b*] have found a similarity of the electron spectra above the θ aurora both in the dawn and in the dusk sectors of the auroral oval, and *Weber and Buchau* [1981] have identified subvisual polar arcs at *F* layer altitudes excited by electrons with energies of several hundreds of eV.

5. Appearance and disappearance of auroral arcs in the polar cap is closely associated with development of magnetospheric substorms [*Starkov and Feldstein*, 1971]; namely, the discrete auroras in the polar cap disappear suddenly at the onset of an expansion phase and reappear during a recovery phase. *Hardy et al.* [1982] have shown that during intense

substorms, for southward IMF, only a homogeneous flux of soft electrons with energy fluxes of 10^{-3}–10^{-2} erg cm^{-2} s^{-1} sr^{-1} ("polar rain," according to *Winningham and Heikkila* [1974]) is observed in the polar cap. Within an hour after the IMF turns to the north ($B_Z > 0$) and a substorm decays, the electron precipitation into both polar caps increases abruptly and auroral arcs appear in the winter polar cap. If the B_Z turns southward, the polar cap arcs disappear again. The electron spectra in the arcs are characterized by a maximum at $\sim$1 keV. These narrow regions of intense fluxes of keV electrons known as "polar showers" [*Winningham and Heikkila*, 1974] appear as a result of the field-aligned acceleration in the potential drop of $\sim$1 kV [*Burch et al.*, 1979; *Hardy et al.*, 1982; *Burke et al.*, 1982]. This is also consistent with AUREOL 3 measurements of low-energy protons and electrons inside the polar caps (see above). Thus the polar cap arcs prove to be an optical signature of the "polar shower" precipitations. During the substorm recovery phase, $\sim$20-keV electron fluxes exceeding 10^5 el cm^{-2} s^{-1} sr^{-1} keV^{-1} were observed in the polar caps [*Dyachenko et al.*, 1980; *Foster and Burrows*, 1976]. *Yakhnin and Sergeev* [1981] assume that the disappearance and occurrence of the polar cap arcs during various phases of a substorm are controlled by the IMF B_Z component rather than by the geomagnetic disturbance level.

6. The polar arcs are followed by small-scale field-aligned currents [*Saflekos et al.*, 1978; *Dolginov et al.*, 1981; *Burke*, 1981; *Burke et al.*, 1982; *Zanetti et al.*, 1982]. According to *Lassen* [1979], they may be related to upward field-aligned currents, while *Feldstein and Vorfolomeeva* [1980] have found that the polar cap arcs are preferably observed in the region of large-scale currents flowing into the ionosphere.

7. The large-scale magnetospheric convection in the region of polar cap discrete arcs may be either antisunward or highly irregular or sunward [*Burke et al.*, 1982; *Lassen*, 1979; *Burch et al.*, 1979; *Frank et al.*, 1983]. Originally, polar cap arcs were supposed to exist in the antisunward convection region. Direct spacecraft observations have, however, shown that during periods with sufficiently intense $B_Z > 0$, the direction of polar cap convection, at least in its central part, may sometimes be changed to sunward. It is, therefore, not surprising that the polar cap arcs were sometimes observed within the sunward convection region. This interpretation differs from that proposed by *Murphree et al.* [1982] according to which the arc location in the region of sunward convection is due to the auroral oval shift poleward during periods with $B_Z > 0$. In a close proximity to a discrete arc, the convection velocity increases and the convection reversal is observed. In this case, electric fields converge to the core of an arc, thereby implying the existence of a field-aligned current flowing out of the ionosphere above the arc [*Burch et al.*, 1979]. According to *Lassen* [1979], who develops the ideas of *Reiff et al.* [1978], the auroral arcs arise in shear flow regions at the boundaries of convection cells and may be used to define qualitatively a pattern of polar cap convection.

8. Polar arcs may drift in the direction perpendicular to their alignment direction at velocities of about 100–400 m/s. *Feldstein et al.* [1968] and *Akasofu* [1972] have shown that the dawnward and duskward motions are of equal probability. *Danielsen* [1969] has found a prevailing dawn-to-dusk motion, while *Sergeev and Yakhnin* [1978] observed the motion from the borders to the center of the polar cap in both the northern and southern hemispheres.

The necessary condition for auroral arc generation is the occurrence of a field-aligned electric field in the magnetosphere above the arcs (see a review by *Chiu et al.* [1983]). Such a potential drop above polar cap arcs is usually $\lesssim$0.7 kV [*Hardy et al.*, 1982]. According to S3-3 observations [*Chiu and Gorney*, 1983] in polar arcs, intrusions of hot plasma from the plasma sheet and of the magnetosheath plasma do occur. Above the arcs, inverted V events are observed in satellite particle data; besides that, ion beams moving upward and abrupt gradients of electric field in the regions of its sign reversal are also observed. These are conditions similar to those for usual auroral arcs in the dusk sector of the oval. This, together with other experimental evidence cited above, allows us to conclude that a field-aligned potential drop is the necessary condition for generating polar cap arcs. Meanwhile, the detailed physical mechanisms of the polar arc–generating field-aligned potential drop may, however, be distinct if open field lines are involved here.

Sergeev and Yakhnin [1979] assume that electrons are accelerated along open magnetic field lines (for an open magnetospheric model) when the density of field-aligned currents (closed through the magnetosheath) exceeds a critical value and an instability is developed, resulting in the generation of a field-aligned potential drop. Field-aligned currents with sufficient current density must be provided by nonuniformity of the polar cap electric field which is controlled by the IMF B_Y component. But observational evidence for nearly complete disappearance of the polar cap auroras during the intervals with $B_Z < 0$ when the magnetosphere appears to be open contradicts the above scheme.

Inside the polar cap, intense field-aligned currents are observed, and as their direct result, the polar cap arcs may be generated by the occurrence of the separating boundaries between closed and open field lines during magnetically quiet periods [*Atkinson*, 1982]. *Akasofu et al.* [1981] and *Akasofu and Roederer* [1983] believe that such separating boundaries arise in the polar cap owing to the existence of regions with open field lines in the dusk or dawn sectors. These regions arise in the dawn or dusk sectors depending on the sign of the IMF B_Y component. In the northern hemisphere the open field line region is located in the dawn sector when $B_Y > 0$ and in the dusk sector when $B_Y < 0$. As a result, the dawnside or duskside of the polar cap will be connected to the IMF. When the IMF tangential discontinuity passes by the magnetosphere and the sign of the IMF B_Y component reverses on this discontinuity, the open field line regions will alternately appear in different regions of the polar cap. Just at the boundary between these regions, field-aligned currents arise which are connected with the polar cap arcs. This mechanism, though attractive, can hardly provide an explanation for the commonly observed simultaneous occurrence of several arcs.

A mechanism based on another possibility of field-aligned potential drop formation inside the magnetosphere is discussed by *Alekseeva et al.* [1979]. Electric field inhomogeneities in the polar cap and small-scale field-aligned currents arise, according to the authors, from the polarization field of a plasma cloud penetrating the magnetosphere from the solar wind. A similar idea was originally put forward by *Pikelner* [1956]. The cloud motion to the magnetospheric interior corresponds here to auroral motion toward the polar cap center. But when one tries to apply these ideas to observations of polar cap arcs, it is not clear why such clouds penetrate the magnetosphere exclusively during the periods of northward IMF when the polar cap arcs arise and disappear as the IMF turns southward; additional suppositions are needed here. *Lyatsky* [1982] has proposed an original concept connecting the

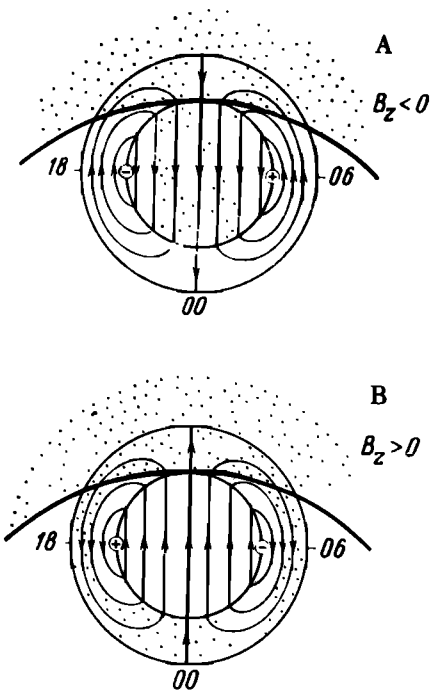

Fig. 15. Magnetospheric convection systems in the northern hemisphere (arrows) and the cold plasma distribution in the magnetosphere (the dots cover the regions of increased cold plasma concentration) at different signs of the IMF B_Z component. The thick line shows the terminator in winter. The auroral arcs avoid the regions covered with dots [*Lyatsky*, 1982].

formation and spatial distribution of auroral arcs with the cold plasma density in the underlying ionosphere. According to this concept, a magnetospheric field-aligned electric field accelerating electrons arises only if the ionospheric density in the underlying F region is sufficiently low; otherwise the ionospheric conductivity will short circuit the field-aligned electric field. In this case a low plasma density in the auroral force tube is not a result of its depletion due to a field-aligned current, as is assumed in a majority of other works on the subject, but, instead, is merely a condition to form a field-aligned potential drop. This assumption results, however, in the conclusions concerning the location of polar cap arcs concordant qualitatively with observations.

Figure 15 presents the expected plasma distribution for different directions of the convection controlled by the IMF B_Z component direction. At $B_Z < 0$, the intensified plasma convection is from the sunlit side of the earth to its nightside. A high plasma density in the polar cap prevents the field-aligned electric fields and polar cap auroras from appearing. When the B_Z component is reversed northward, the velocity of convection from day to night decreases with conservation of the convection direction [*Burch et al.*, 1979]. This results in a decrease of plasma density in the polar cap and in a growth of the occurrence probability of the polar cap auroras (Figure 14*a*). At high positive B_Z (as estimated by *Afonina et al.* [1982] at $B_Z \gtrsim 10$ nT) the convection of plasma over the whole polar cap is reversed to the sunward direction. According to the above scheme, it is just then that the most frequent occurrence of the polar cap auroras should be expected. Considering the IMF B_Y component effect on the polar cap convection pattern and, hence, on the polar ionosphere plasma density, one can also explain the observed differences in the occurrence of the polar cap arcs in the dusk and dawn polar cap sectors for different signs of B_Y. Further progress in the theory of auroral arc formation mechanisms has to be made, however, before one can appraise the role of the initial ionospheric conductivity in the field-aligned potential generation and its time stability to check the above ideas against experimental evidence.

7. Relevance of the Auroral Luminescence Regions to the Large-Scale Magnetospheric Structure

Akasofu [1966], *Feldstein* [1966, 1969, 1972], and *Vasyliunas* [1970, 1972] emphasized a close relationship between the auroral oval and the gross magnetospheric structure. Therefore the global distribution of auroras and their dynamics yield useful information on the variations in the magnetosphere during magnetospheric disturbances. The magnetosphere is formed as a result of solar wind plasma interaction with the earth's magnetic field, and therefore the various aspects of this interaction affect the character and distribution of the auroral luminescence at high latitudes where the remote magnetosphere regions are mapped. In connection with the complicated structure of the auroral luminescence at high latitudes, we shall consider the present-day concepts concerning the plasma distribution in the magnetosphere. The distributions of plasma with energies from tens of eV to several keV in the equatorial plane are presented schematically in Figures 16*a* and 16*b* according to *Vasyliunas* [1970] and *Frank* [1971*a*].

Figures 17*a* and 17*b* show the data in the noon-midnight magnetospheric cross section from *Frank* [1971*b*] and *Aubry et al.* [1972]. In the latter paper, observations of high-energy ($E_e > 50$ keV) electrons were used. The suprathermal plasma distribution in the night sector is characterized by the presence of the inner boundary of the plasma sheet at which a dramatic softening of the electron spectrum begins with decreasing radial distance (instead of a mean energy rise inward due to adiabatic acceleration of hot plasma with increasing magnetic field). Simultaneously, the energy density of hot electrons also decreases. The region where these variations are observed is located between the inner boundary of the plasma sheet and the plasmapause and is marked in Figure 16*b* as the earthward edge of the plasma sheet. The plasma sheet extends to the day sector [*Burrows et al.*, 1976; *Candidi and Meng*, 1984]. At high altitudes this region is detected on the equatorial dayside magnetopause [*Tsurutani et al.*, 1981]. As can be seen from Figure 16*b*, the inner boundary of the plasma sheet nearly coincides with the trapping boundary for high-energy electrons with energies ≥ 40 keV. The trapping boundary was identified with the position of the major rapid decrease of high-energy electron intensity as the radial distance increases. As can be seen from the meridional cross section of the magnetosphere shown in Figure 17*a*, the low-latitude and high-latitude parts should be distinguished in the plasma region of the magnetotail; namely, in the high-latitude part the fluxes of soft electrons and of their energy are much lower in comparison with the low-latitude part. The outer radiation belt (trapping region) is adjacent to the plasma sheet. The behavior of high-energy ($E \geq 50$ keV) electrons is much different from the behavior of suprathermal plasma (Figure 17*b*). The maximum fluxes are observed earthward from the stable trapping boundary φ_s separating the C and B regions. The C region (sometimes called the night cusp) is the outer radiation belt with a maximum hard electron flux of $> 10^5$ el cm^{-2} s^{-1}. It is the stable trapping region that is marked as the ring current trapping region in Figure 17*a*. In the low-latitude

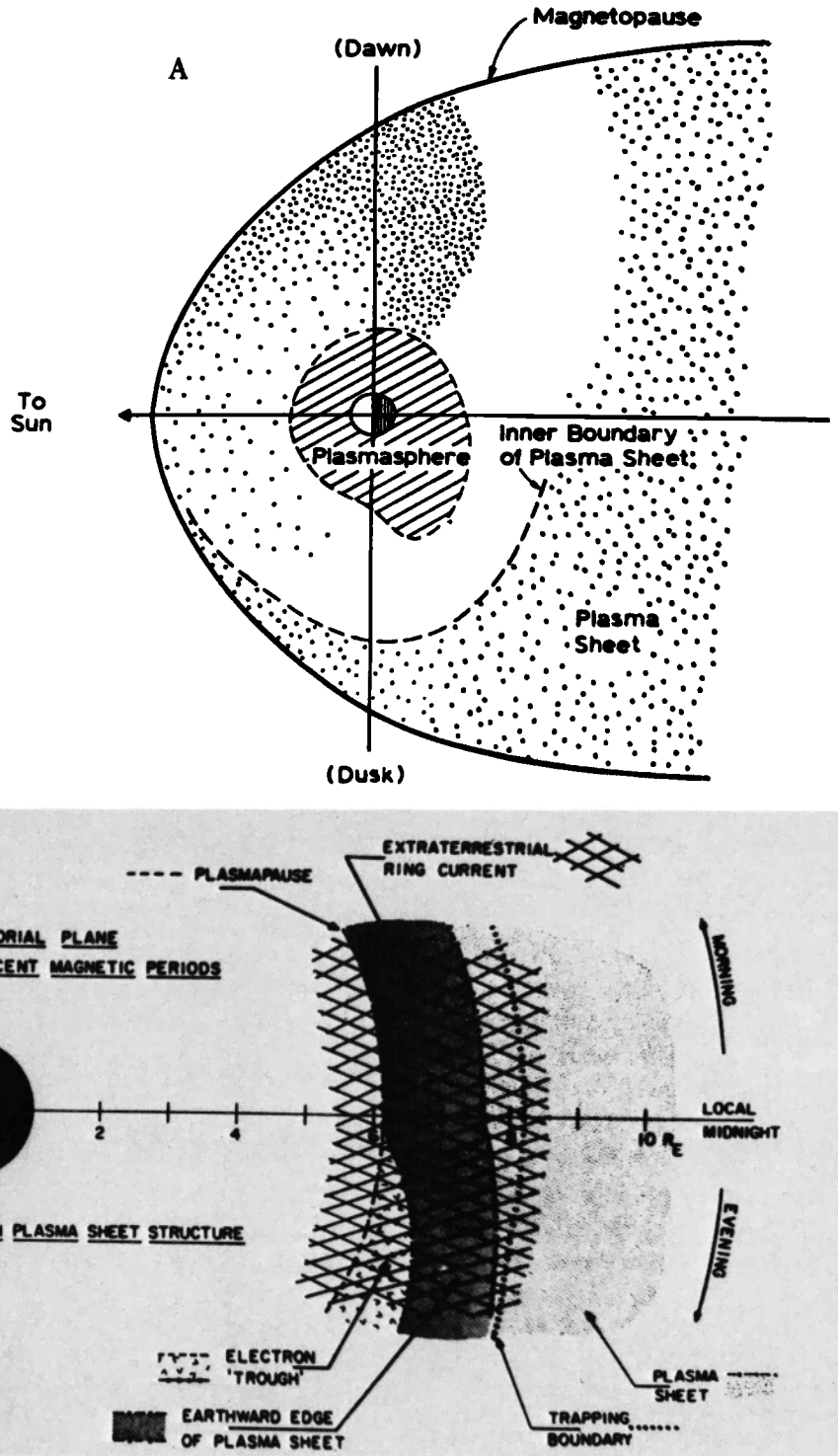

Fig. 16. (*a*) The average low-energy electron distribution in the equatorial magnetospheric region inferred from the OGO 1 and 3 data viewed from the north pole [*Vasyliunas*, 1970]. The density of dots is qualitatively indicative of the electron flux with energies from 100 eV to several keV. The unshaded region in the predawn sector has not yet been studied in detail; it is, however, known that strong electron fluxes are present within this sector. (*b*) Graphic summary of the structure of the near-earth plasma sheet in the night sector of the magnetosphere at the magnetic equator inferred from the OGO 3 data [*Frank*, 1971*a*] during periods of relative magnetic quiescence.

plasma sheet (*B* region), which is adjacent to the radiation belt, the fluxes of energetic electrons are considerably lower ($\sim 3.10^3$ el cm^{-2} s^{-1} sr^{-1}). The high-latitude part of the plasma sheet was never identified for electrons of such high energies and is related to the tail lobes (during substorms, however, bursts of high-energy electrons and ions also occur here).

In Figures 18*a* and 18*b*, variations with geocentric distance in the earth's radii (L) of the energy density, mean energy, and number density of auroral electrons are presented following

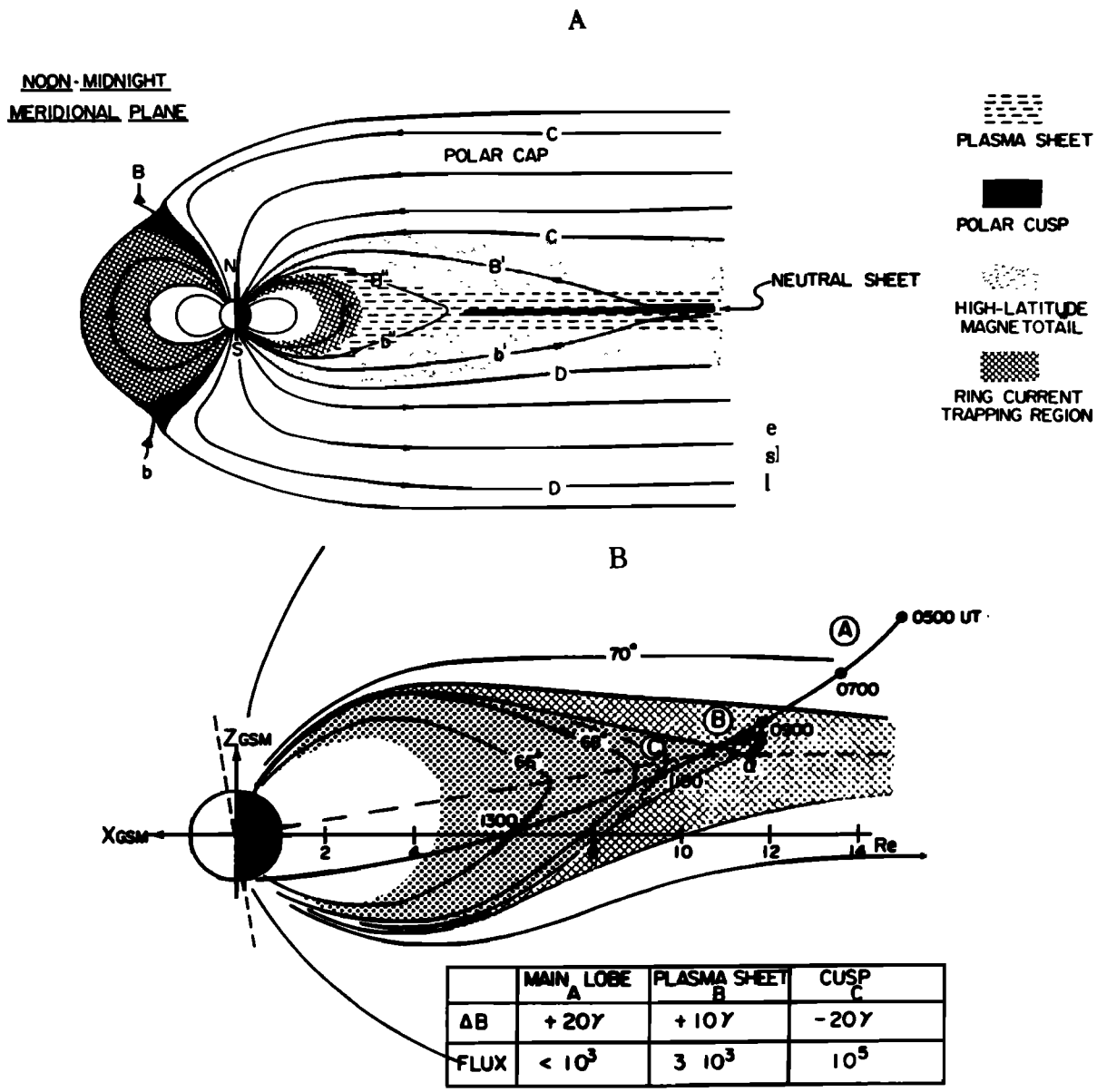

Fig. 17. (*a*) Schematic diagrams of the structure of the magnetospheric plasma domains in the noon-midnight meridional plane [*Frank*, 1971*b*]. (*b*) The structure of the plasma sheet near the earth in the night sector of the magnetosphere inferred from OGO 5 measurements of high-energy (> 50 keV) electrons [*Aubry et al.*, 1972]. The solid line is the satellite trajectory.

Vasyliunas [1972] for the night magnetospheric sector during a magnetic storm and during a quiet period.

Figure 18*c* shows the plasma sheet energy flux of auroral electrons at various distances from the neutral sheet. As the distance from the neutral sheet increases, the parameters of plasma sheet electrons vary in a manner very similar to that of decreasing radial distance in the near-earth region between the inner plasma sheet boundary and the plasmapause; that is, the mean energy of the electrons and their energy density decrease in a similar way (see also *Hones et al.* [1971]).

Vasyliunas [1970] determined the location of the inner edge at relatively low altitudes in the high-latitude horns of the plasma sheet. He concluded that the location of the inner edge of the plasma sheet corresponded to that of the equatorial boundary of the auroral oval (Figure 19*a*). A similar conclusion was also drawn by *Feldstein and Starkov* [1970] and by *Lassen* [1974]. Figure 19*b* presents the location of the auroral oval in the night sector (shaded area), the stable trapping boundary φ_s of >35-keV electrons (squares), and the boundary φ_b of the region where the counting rate of the >35-keV electrons falls to the cosmic ray background level (open circles) as functions of magnetic disturbance [*Feldstein and Starkov*, 1970]. The boundaries φ_b and φ_s were determined according to *McDiarmid and Burrows* [1968].

Latitudes φ_s for all the disturbance levels coincide with those for the equatorial boundary of the auroral oval within the limits of a few tenths of a degree. Therefore the oval is located at higher latitudes than the outer radiation belt L shells but is adjacent to these L shells on its low-latitude side. At low altitudes in the night sector the projections of the plasma sheet inner boundary and of the stable trapping boundary coincide, just as in the equatorial cross section of the magnetosphere.

According to *Lassen* [1974] (Figure 19*c*), the outer bound-

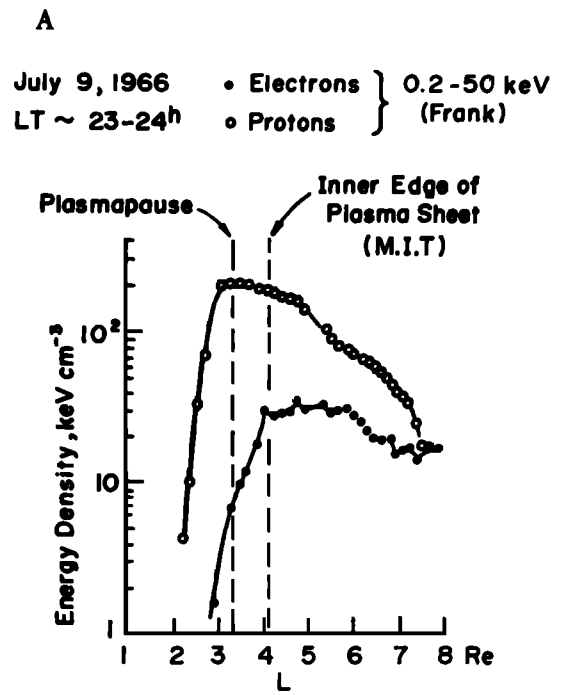

Fig. 18*a*

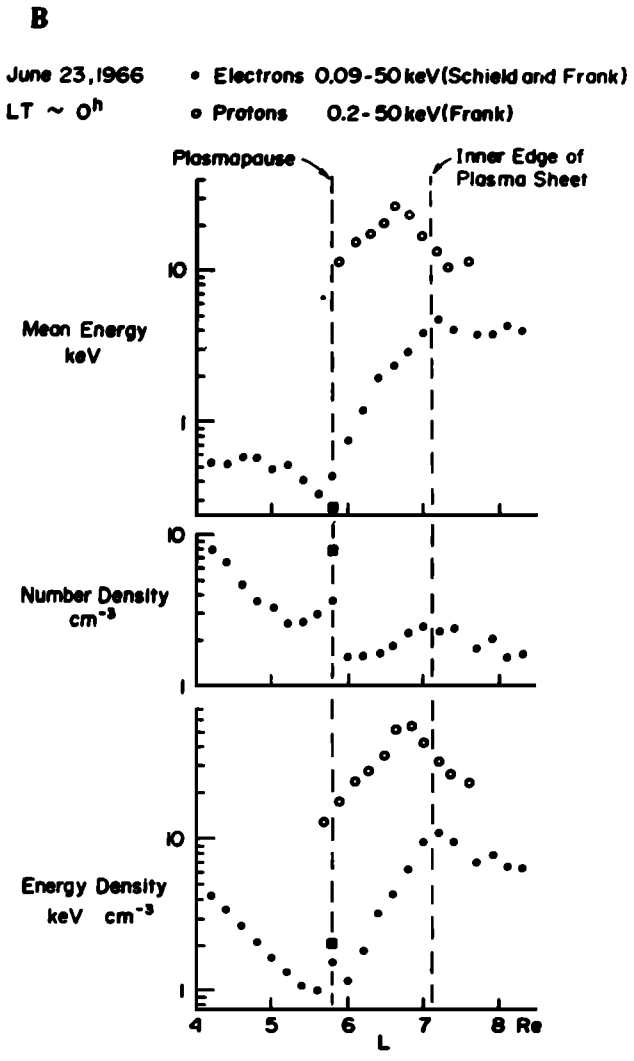

Fig. 18*b*

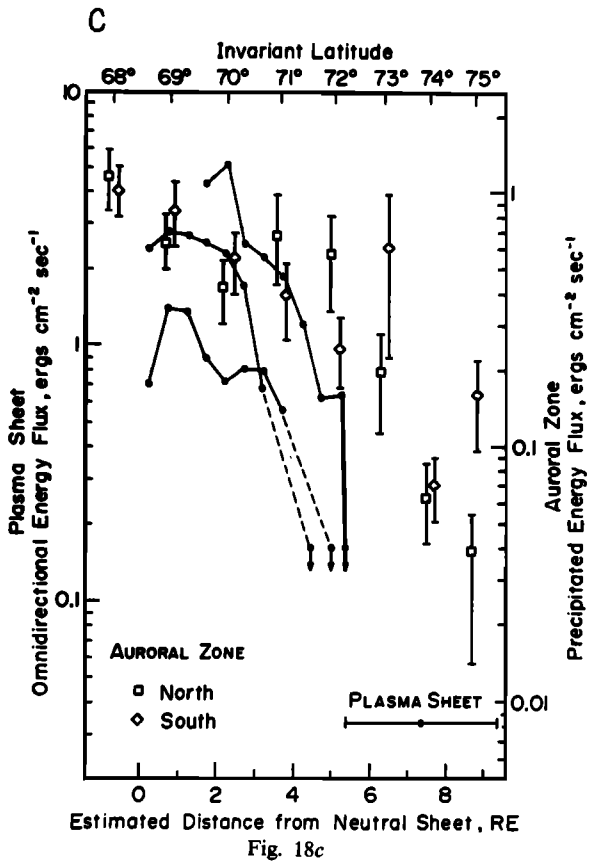

Fig. 18*c*

Fig. 18. (*a*) Rapid radial distance variations of electron and proton energy density during the main phase of a magnetic storm inferred from OGO 3 observations [*Frank*, 1967]. The plasmapause and plasma sheet inner edge positions have been inferred from simultaneous OGO 3 observations [*Vasyliunas*, 1972]. (*b*) The variations of the electron and proton properties across the inner edge of the plasma sheet (quiet conditions). The electron energy density, number density, and the plasmapause and inner edge positions are shown according to *Schield and Frank* [1970]. The proton energy density is from *Frank* [1967]. The squares are the anomalous values right at the plasmapause [*Vasyliunas*, 1972]. (*c*) Comparison of the average precipitating electron energy flux in the auroral oval [*Sharp et al.*, 1969] with the electron energy flux within the plasma sheet at different distances from the neutral sheet [*Vasyliunas*, 1972]. Three curves shown are from three OGO 3 traversals of the plasma sheet during quiet periods. The values of precipitating fluxes are averaged over 1° latitude intervals.

ary and the inner edge of the plasma sheet coincide with the poleward and equatorward boundaries of the auroral oval, respectively, which are determined by the statistical pattern of auroral arcs.

Thus the concept of Vasyliunas-Feldstein and Starkov-Lassen (VFSL) is essentially that the auroral oval is mapped on the magnetosphere in the low-latitude part of the plasma sheet (which can be called its main part). The equatorward boundary of the oval is geometrically conjugate through magnetic force lines to the inner boundary of the plasma sheet, and the poleward boundary is conjugate to the outer boundary of the plasma sheet. The subvisual luminescence poleward of the poleward boundary of the oval is produced by the diffuse precipitation of soft electrons which are mapped on the periphery of the plasma sheet (the high-latitude, or outer, part of the plasma sheet).

Another concept (FA) was proposed by *Frank and Ackerson* [1971, 1972] and *Ackerson and Frank* [1972]. From the thorough analysis of a great number of individual passes of Injun

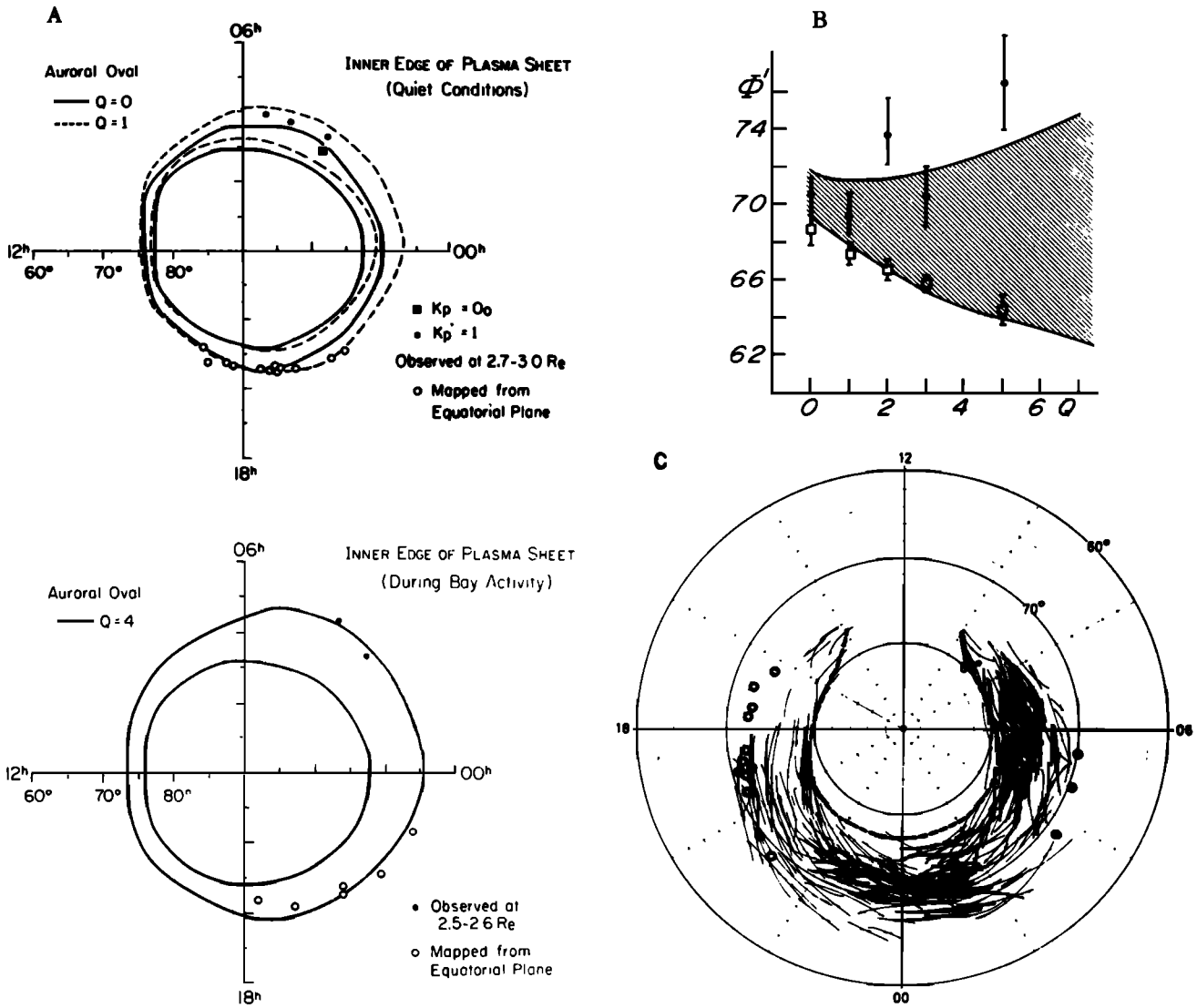

Fig. 19. (*a*) Observed positions of the inner edge of the plasma sheet, mapped to the ionosphere, and to the auroral oval [*Feldstein and Starkov*, 1967] for different values of geomagnetic activity. Shown to the left and to the right are magnetically quiet and disturbed conditions, respectively [*Vasyliunas*, 1970]. (*b*) The change of the location of the auroral region appearance in the zenith of the midnight sector during the IQSY with the level of magnetic disturbances [*Feldstein and Starkov*, 1968] (shaded area); the stable trapping boundary φ_a for electrons with energies of >35 keV inferred from the Alouette 2 data (squares); φ_b is the poleward boundary of the region where the >35-keV electron counting rate falls to the cosmic ray background level [*Feldstein and Starkov*, 1970]. (*c*) The auroral arc location observed from Greenland during quiet periods ($Kp = 0, 1$); also shown are the mapped inner edge of the plasma sheet (open circles and closed circles) and the mapped outer boundary of the plasma sheet at $X = -18\ R_E$(dashed line) [*Lassen*, 1974].

5 they deduced that all the important characteristics of charged-particle distributions can be described in terms of two major precipitation zones and that the trapped >45-keV electron boundary is a natural coordinate which separates the two zones. The trapping boundary is defined as coincident with the high-latitude termination of measurable high-energy electron intensities. The position of the trapping boundary is interpreted as delineating the location of the high-latitude termination of closed field lines; i.e., all field lines above the trapping boundary are directly connected to the interplanetary magnetic field ("open"). Moreover, the position of the trapping boundary is coincident with the reversal of the convective electric fields from sunward convective flow (equatorward from the trapping boundary) to antisunward flow (poleward from this boundary) as shown in Figure 20. Poleward of the trapping boundary, intense discrete bands of electron precipitation (inverted V events) coincident with the visible auroral arcs were detected [*Ackerson and Frank*, 1972]. During magnetically quiet periods, less intense, structureless soft electron precipitation was located in the dusk sector in the form of a relatively narrow zone adjacent to, and equatorward from, the trapping boundary. In the midnight and dawn sectors this zone of diffuse precipitation occupies a broad latitude region, especially during and after magnetic disturbances. If one assumes that the discrete precipitation is mapped on the plasma sheet and that the diffuse precipitation is mapped into the region between the inner boundary of the plasma sheet and the plasmapause, the trapping boundary on the nightside will coincide with the inner boundary of the plasma sheet. In this case the results of the FA concept would have coincided completely with the VFSL results. Contrary to this viewpoint, however, Frank and Ackerson have come to the conclusion

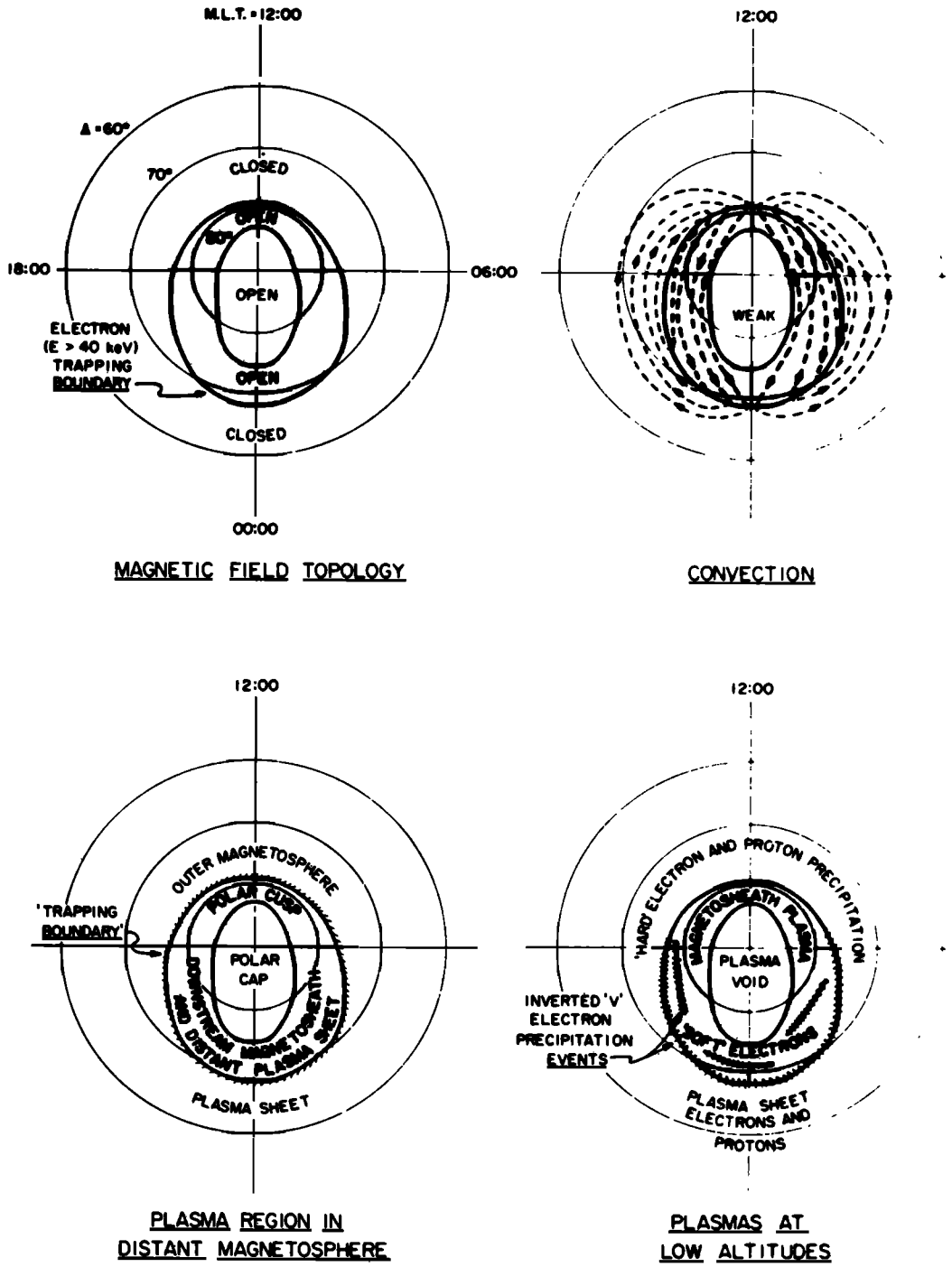

Fig. 20. The interpretative diagram for the auroral zones and polar caps including the low-altitude signatures of plasma in the distant magnetosphere, the major convection zones, and the magnetic field topology [*Frank and Ackerson*, 1972].

that the diffuse electron precipitation equatorward of the trapping boundary is from the plasma sheet, whereas the source of the discrete precipitation is in a distant part of the plasma sheet and in the downstream magnetosheath, i.e., at the boundary with the tail lobes. This means that the oval of discrete auroral forms is mapped on open field lines of the plasma sheet and that the diffuse auroras equatorward from the oval are mapped on the central part of the plasma sheet. In this case the poleward boundary of the oval also constitutes the equatorward boundary of the polar cap where electron precipitation is absent. The only reason for such an interpretation of the data was that the trapping boundary was assumed to be a boundary between closed and open field lines also separating the regions with sunward and antisunward convection. However, *Isaev and Pudovkin* [1972] argued that the nightside auroral plasma (including the region of discrete auroras) is located entirely on closed geomagnetic field lines. However, subsequent studies have shown that inverted V events are observed in the region of closed field lines [*Burrows*, 1974; *Venkatarangan et al.*, 1975; *Lin and Hoffman*, 1979] and the convection reversal occurs poleward of the boundary separating the diffuse and discrete precipitation

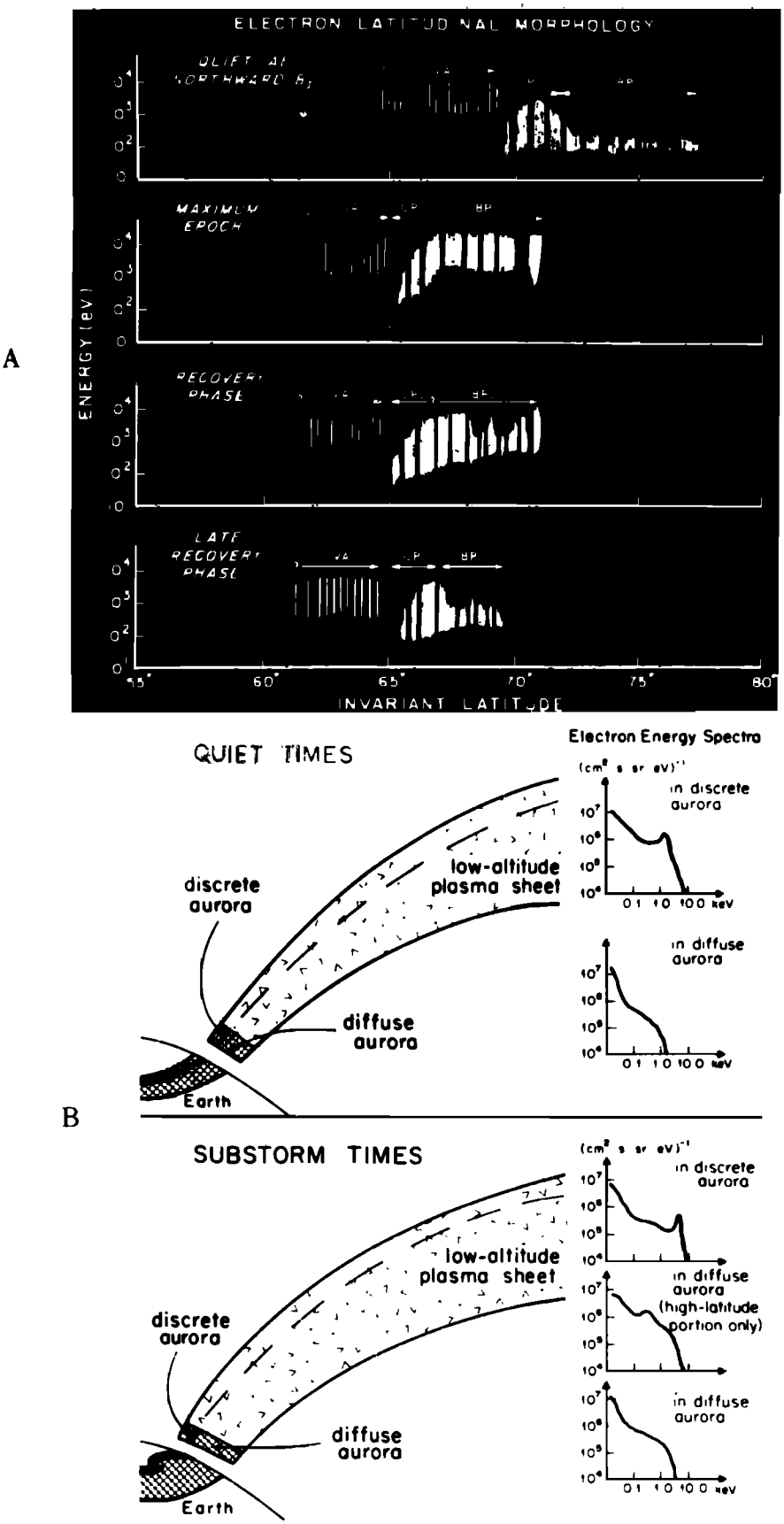

Fig. 21. (*a*) Schematic representation of the latitudinal morphology of electron precipitations in the night sector during various substorm phases [*Winningham et al.*, 1975]. VA is radiation belt, CPL is the central plasma layer, and BPL is the boundary plasma layer. (*b*) Schematic diagram to illustrate spatial relationships between the plasma sheet and the two types of auroras [*Lui et al.*, 1977]. Also presented are characteristics of the differential electron energy spectra for the two types of auroras in the quiet and substorm periods.

[*Burch et al.*, 1976; *Heelis et al.*, 1980]. The source of precipitating electrons in the inverted V events proves to be the plasma sheet and the neutral sheet [*Lin and Hoffman*, 1979] or the part of the plasma sheet with the sunward convection and the region of antisunward convection adjacent to the plasma sheet on the high-latitude side. The latter region appears to be "open," i.e., connected with the IMF in the magnetosheath [*Burch et al.*, 1976; *Heelis et al.*, 1980]. It should again be emphasized that the VFSL and FA concepts are based on consistent experimental data. The only difference is in the assumption of the relationship of specific types of auroral luminescence and precipitating auroral electrons at low altitudes to plasma domains in the magnetosphere.

Later, the two concepts relating the large-scale precipitation structures at low latitudes to different plasma domains in the magnetosphere (VFSL and FA) were extended. The FA concept was developed by *Akasofu* [1974*b*], *Winningham et al.* [1975] and *Lui et al.* [1977], and the VFSL concept by *Feldstein* [1974], *Valchuk et al.* [1979], *Feldstein et al.* [1979], and *Cambou and Galperin* [1982]. The relationship of the particle precipitation zones to the magnetospheric structure, proposed by *Pudovkin et al.* [1977], are close to the VFSL concept.

Akasofu [1974*b*], using earlier studies of auroral scanner and particle spectrometer data from ISIS 2 and also data from the Injun 5 satellite, studied the characteristics of discrete and diffuse forms of auroral luminescence and their relationship to precipitating auroral particles and plasma domains in the magnetosphere. He reached the following conclusions: (1) the diffuse luminescence region is associated with the central part of the plasma sheet (the main part of the plasma sheet); (2) the discrete luminescence region is associated with the upper (northern hemisphere) and lower (southern hemisphere) boundary layers of the plasma sheet; (3) the trapping boundary is located between the two auroral systems.

Winningham et al. [1975] summarized the morphology of precipitating particles in the midnight sector using ISIS 1 and 2 data and related the particle precipitation during substorm phases in various parts of the magnetotail to auroral oval morphology.

Lui et al. [1977] confirmed a close relationship between the luminescence at high latitudes and the auroral electron precipitation using simultaneous observations from ISIS 2 of auroral emissions and particle precipitation in the 1900–2400 MLT sector. In Figure 21*a* a schematic summary of the observed latitude distributions of electron precipitation with energies from 10 eV to 10 keV is presented according to *Winningham et al.* [1975]. The following four regions of electron precipitation differing in their mophological features were identified: (1) electrons of the outer radiation belt (VA) observed equatorward of the zones of auroral precipitation; (2) diffuse auroral electron fluxes whose spectrum becomes harder with increasing latitude; they are supposed to be associated with the central plasma sheet (CPS) and adjacent to the outer radiation belt; (3) structured fluxes of precipitating electrons which are characterized by inverted V events that are supposed to be related to the upper (in the northern hemisphere) and lower (in the southern hemisphere) boundary regions of the plasma sheet and adjacent to the tail lobe. They are called the boundary plasma sheet (BPS) and are denoted as BPL in Figure 21*a*; (4) frequent noticeable precipitation poleward of the BPS region which are defined as polar rain (PR) of electrons in the polar cap.

The locations of these regions and their latitude extensions change substantially from magnetically quiet to magnetically disturbed conditions. The diffuse and discrete precipitation of auroral electrons shifts to lower latitudes, the structured precipitation region expands markedly, and the soft precipitation region on the poleward edge of the auroral zone decreases (the latter zone is denoted BPL in Figure 21*a*). All of these factors result in a shift of the polar cap boundary toward lower latitudes on the nightside. During quiet times the shapes of the electron spectra in the BPL are not appreciably different from those at the dayside cusp, but the fluxes are weaker. In disturbed periods, electron precipitation from the BPL is characterized by considerable increases in the mean energy, number flux, and energy flux of particles. During disturbances the electron number flux from the CPS increases and significant spectral hardening is observed.

Lui et al. [1977] have confirmed that the diffuse and discrete auroras seen in the dusk sector are related respectively, to the regions of comparatively uniform and highly structured precipitation, respectively. Uniform precipitation is usually characterized by lower energy fluxes compared with those in the structured precipitation. The optical intensity of diffuse auroras was found to be produced mainly by uniform precipitation of 0.1- to 10-keV electrons. Protons precipitate in both discrete and diffuse auroral regions but contribute little to the total energy flux and even less to the number flux. The diagram in Figure 21*b* illustrates, according to *Lui et al.* [1977], the relationships between the plasma sheet and two types of auroras in magnetically quiet and disturbed periods ("FA concept"). It is assumed there that the discrete auroras in the oval are mapped on the BPS and the diffuse auroras are mapped on the CPS. The relationships of the diffuse auroral luminescence to the CPS are supported as follows: (1) the inner edge of the plasma sheet corresponds closely to the equatorward edge of diffuse auroras; (2) the electron energy spectra in diffuse auroras are reasonably well comparable with those measured in the plasma sheet; (3) the plasma sheet source alone can support the permanently existing uniform electron precipitation.

Since the discrete auroras usually occur in the poleward part of the diffuse aurora region, they must be mapped on the magnetosphere, based purely on geometrical considerations, in a region located somewhere near the poleward boundary of the plasma sheet.

Detectors of high-energy electrons made it possible to identify the >22-keV and >40-keV electron boundaries φ_b and φ_s. It appeared that φ_b corresponded to the poleward boundary of the structured precipitation, while φ_s was found somewhat equatorward of the high-latitude boundary of the diffuse zone. During magnetically disturbed periods a variation was noted in the spectral shape across φ_s; namely, the monotonically falling differential energy spectrum equatorward of φ_s and spectra with a significant maximum in the 0.1- to 10-keV energy range poleward of φ_s were observed. Thus from this scheme it follows that the main part of the CPS is presumably located inside the outer radiation belt, whereas the discrete auroras are located on closed magnetic field lines.

The zone of soft precipitation poleward of the oval, which occupies a wide latitude range in the late dusk–night sector during magnetically quiet periods (see Figure 21*a*), is absent in the scheme shown in Figure 21*b*. The source of this soft precipitation must be located geometrically in the tail lobes. In Figure 21*b*, however, such precipitation is not indicated. Here, as was already mentioned, the diffuse auroral luminescence is presumed to be generated by plasma particles from the inner, or central, plasma sheet [*Akasofu*, 1977*a*], and the discrete

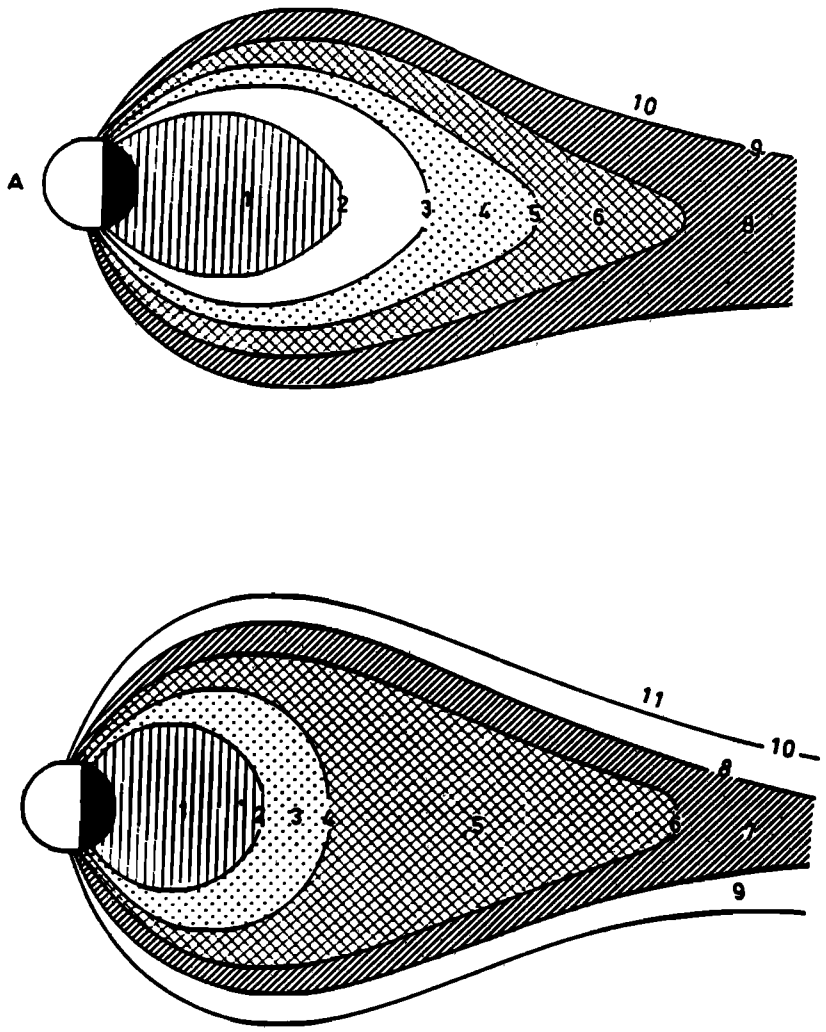

Fig. 22. Schematic representation of the relationships between the distant magnetosphere and the various types of auroras (~2200 MLT) inferred from the ARCAD experiment on AUREOL 1 and 2 satellites [*Valchuk et al.*, 1979]. (*a*) Magnetically quiet conditions ($Kp = 1$): 1, plasmasphere; 2, plasmapause ($R \sim 5\ R_E$, $\varphi = 63.5°$); 3, inner boundary of the remnant layer ($R \sim 6$–$8\ R_E$, $\varphi = 66°$–$69°$); 4, remnant layer connected via the geomagnetic field lines to the diffuse auroral zone; 5, inner boundary of the plasma sheet mapped on the equatorward boundary of the auroral oval ($R \sim 11\ R_E$, $\varphi = 70°$); 6, the central (low latitude) part of the plasma sheet mapped on the auroral oval; 7, external boundary of the low-latitude plasma sheet mapped on the poleward boundary of the auroral oval ($\varphi = 72°$); 8, the outer (high latitude) part of the plasma sheet mapped on the poleward soft electron precipitation zone; 9, the external boundary of the plasma sheet mapped on the poleward boundary of the soft electron precipitation zone ($\varphi \gtrsim 80°$); 10, magnetospheric tail lobes mapped on the polar cap. (*b*) Magnetically disturbed conditions ($Kp = 5$): 1, plasmasphere; 2, plasmapause and inner boundary of the remnant layer ($R \sim 4\ R_E$, $\varphi = 60°$); 3, remnant layer connected via geomagnetic force lines to the diffuse auroral zone; 4, inner boundary of the plasma sheet mapped on the equatorward boundary of the auroral oval ($R \sim 5\ R_E$, $\varphi = 63.5°$); 5, the central (low latitude) part of the plasma sheet mapped on the auroral oval; 6, the external boundary of the low-latitude part of the plasma sheet mapped on the poleward boundary of the auroral oval ($\varphi = 74°$); 7, the outer (high latitude) part of the plasma sheet mapped on the poleward soft electron precipitation zone; 8, the external boundary of the plasma sheet mapped on the poleward boundary of the soft electron precipitation zone ($\varphi = 75.5$); 9, the electron flux void region during magnetospheric storms (between the poleward boundary of the soft electron precipitation and the polar cap); 10, the equatorward boundary of the polar cap ($\varphi \sim 77°$); 11, the magnetospheric tail lobes mapped on the polar cap.

auroral forms are produced by particles from the boundary layers of the plasma sheet, in line with the FA concept.

At the same time, in summarizing the observations of auroral luminescence and particle precipitation fluxes relative to the magnetospheric structure in the night sector, *Feldstein* [1974] continued to defend the earlier VFSL concept concerning the relationship between the auroral luminescence zones and the plasma domains in the magnetosphere:

1. The discrete auroral forms along the oval are excited by electron precipitation of the inverted V event type located generally poleward of the trapping boundary of hard electrons (with energies of several tens of keV). This auroral region is presumed here to be magnetically projected onto the magnetotail plasma sheet.

2. During magnetically quiet periods, poleward of the auroral oval, diffuse red luminescence is observed which must be associated with lower-energy particle precipitation. This region is assumed to be magnetically projected onto the plasma sheet outer periphery.

3. A diffuse luminescence observed equatorward of the auroral oval is due to soft electron precipitation from the region of the outer radiation belt located between the plasma sheet

inner edge and the plasmapause. During a substorm expansion phase, hot plasma sheet electrons are injected into this region and drift to the dawnside. The precipitation of these accelerated (heated) electrons during a substorm recovery phase and some period after magnetic field recovery produces an intense diffuse luminescence in the late dawnside-dayside sectors along the zone located equatorward of the auroral oval.

In summary, the VFSL concept of the relationships between the auroral luminescence zones and plasma domains in the night sector of the magnetosphere has been developed by including, in addition to the diffuse luminescence poleward of the oval, the luminescence along the auroral oval and the diffuse glow equatorward of it. The equatorward diffuse auroral glow by that time (1974) had been studied from ISIS 2 and DMSP. The respective scheme of spatial relationships was finally developed by *Valchuk et al.* [1979] by comparing simultaneous observations of the luminescence from the DMSP 7529 satellite and the measurements of auroral electrons from the AUREOL 2 satellite (the ARCAD project). From the analysis of data made for a variety of geomagnetic conditions and auroral forms encountered by the satellites during their various passes in the dusk sector of the magnetosphere, the following conclusions were drawn:

1. Equatorward of the discrete forms of the auroral oval, there always exists a region of diffuse precipitation of low-energy electrons which is directly associated with the diffuse luminescence region.

2. The equatorward boundary of the diffuse luminescence region (DAB), which is especially distinct during substorms, coincides with the equatorward boundary (DPB) of diffuse precipitation of electrons with energies $\gtrsim 0.2$ keV and energy flux $E \gtrsim 0.01$ erg cm^{-2} s^{-1} sr^{-1}. Under more quiescent conditions, the latitude variations of E near DPB may prove to be smoother if softer electrons prevail. In this case the estimate of the DPB location depends on a particular method adopted for its experimental determination and on the instrument sensitivity threshold.

3. When a satellite crosses the DPB and moves to higher latitudes (but is still inside the zone of diffuse precipitation), the energy flux and the mean energy of precipitating electrons increase and reach 0.1–0.5 erg cm^{-2} s^{-1} sr^{-1} and ~ 0.4 keV, respectively, near the edge of the auroral oval. This region up to the most equatorward discrete arc in the dusk sector of the oval is located, according to simultaneous high-energy electron measurements, inside the outer radiation belt, i.e., within the stable trapping zone.

4. The stable trapping boundary φ_s is located close to the poleward boundary of the diffuse precipitation but is already in the region of discrete auroral forms, i.e., in the auroral oval proper.

5. The width of the diffuse precipitation band from DPB to bright discrete forms, i.e., to the equatorward boundary of the auroral oval, may extend from 1° to 5° of latitude.

6. Over a quiet auroral arc with the brightness of IBC II the electron energy flux is several ergs cm^{-2} s^{-1} sr^{-1}, while a secondary maximum arises in the differential energy spectrum at electron energies of 3–12 keV. In this region, high-energy electron fluxes of low intensities are still observed, but their intensity falls to the sensitivity threshold near the poleward auroral arc. Therefore the background boundary of high-energy electron precipitation φ_b coincides approximately with the poleward auroral arc.

7. Poleward of the auroral arcs, electrons with a softer spectrum and without a secondary maximum are usually observed at energies of <1 keV. This poleward band of diffuse electron precipitation extends usually along the poleward boundary of the auroral oval. During disturbed periods the extension is $\sim 1°$ of latitude and the energy flux of soft electrons is $\sim 10^{-2}$ to 10^{-1} erg cm^{-2} s^{-1} sr^{-1}.

Figure 22 presents the diagrams illustrating the spatial relationships of the auroral luminescence types to the boundaries of various plasma domains in the magnetospheric night sector according to *Valchuk et al.* [1979]. In this case, not only geometrical considerations for projection to the magnetospheric domains but also the hot plasma parameters in different regions of the magnetosphere and the spectra of precipitating electrons were taken into account, in particular:

1. Diffuse luminescence equatorward of the oval in the dusk sector is characterized by a gradual softening of the spectra of precipitating electrons and by a decrease of the electron energy flux with decreasing latitude [*Kamide and Winningham*, 1977; *Valchuk et al.*, 1979; *Winningham et al.*, 1975, 1978; *Tanskanen et al.*, 1981; *Gussenhoven et al.*, 1981]. The behavior of the electron component mean energy at radial distances between the inner plasma sheet boundary and the plasmapause is the same [*Vasyliunas*, 1968, 1972; *Schield and Frank*, 1970]. Also, the spectra of soft electrons in the diffuse luminescence and in the equatorial cross section of the magnetosphere along the same line of force at $R_E \sim 6.6$ are practically identical [*Eather et al.*, 1976; *Meng*, 1978; *Meng et al.*, 1979]. This fact suggests that the diffuse luminescence region is relevant to the magnetosphere region between the inner boundary of the plasma sheet and the plasmapause.

2. The separating boundary between the diffuse and discrete auroras, which corresponds to the equatorward boundary of the auroral oval, is the inner boundary of the plasma sheet [*Vasyliunas*, 1970] and, at low altitudes, is the stable trapping boundary of the >40-keV electrons [*Feldstein and Starkov*, 1970; *Akasofu*, 1974*b*; *Deehr et al.*, 1976; *Valchuk et al.*, 1979]. Thus the diffuse luminescence is mapped in the outer radiation belt region located at geocentric distances which are substantially less than the distances to the central plasma sheet.

3. Along the auroral oval the maximum electron energy flux is injected to ionospheric altitudes [*Spiro et al.*, 1982], while in the plasma sheet the prevailing energy densities of electrons and protons are concentrated at low latitudes near the so-called neutral sheet [*Hones*, 1968; *Vasyliunas*, 1972], and it is this particle energy that is necessary for the auroral oval energy fluxes to be sustained. The intensity ratios of emissions in the auroral spectrum at the oval indicates a gradual softening of the mean spectrum of precipitating electrons from the latitudes of the equatorward oval boundary (the mean electron energy of ~ 1–1.5 keV) to higher latitudes (~ 0.5 keV) [*Eather and Mende*, 1972; *Eather*, 1975]. Such spectral softening is also observed in the diffuse precipitation along the oval [*Winningham et al.*, 1978]. At the same time, a very similar general softening was found in the plasma sheet with increasing distance from the neutral sheet, namely, the mean electron energy decrease from 1.2 keV in the sheet center to 0.4 keV near the outer boundary of the plasma sheet [*Hones*, 1968; *Hones et al.*, 1971]. This circumstance permits one to relate the auroral oval to a projection to ionospheric altitudes of the central (low latitude) part of the plasma sheet.

4. The high-latitude part of the plasma sheet is characterized by electrons with a soft spectrum and by an almost complete absence of slowly varying precipitation of hard electrons (with energies $\gtrsim 40$ keV) because the poleward boundary of the auroral oval is in practice coincident with the back-

ground boundary, φ_b, of trapped high-energy electrons [*Feldstein and Starkov*, 1970; *Lui et al.*, 1977]. Thus it is natural to relate the soft zone of diffuse luminescence poleward of the oval to the periphery of the plasma sheet in the magnetospheric tail [*Eather and Mende*, 1972; *Feldstein*, 1973]. During magnetically quiet periods the diffuse luminescence poleward of the oval spreads over a wide latitude range but is transformed into a very narrow strip during disturbances. These variations are closely associated with the dynamics of the outer boundary of the plasma sheet in the tail during disturbed periods [*Akasofu*, 1977*a*]. Evidently, they deserve further thorough study.

5. Comparisons of particular structures of the field-aligned currents at plasma sheet altitudes and at ionospheric levels can be used to test their magnetic conjugacy in the real magnetosphere. Indeed, intense and localized field-aligned currents at the expanding outer boundary of the high-altitude plasma sheet were studied in detail by *Fairfield* [1973] for 57 orbits of IMP 4 and 105 orbits of IMP 5 in the night hemisphere. It was shown that these currents are observed during the recovery phase of substorms and are in the form of localized sheets with the flow direction toward the earth (inward) in the midnight and morning sectors and away from the earth in the evening sector for a single sheet or for one of several if multiple sheets are observed. The mapping of these field-aligned currents to ionospheric levels was performed using the magnetospheric field model MF73Q [*Mead and Fairfield*, 1975]. It appeared that all the crossings of the expanding plasma sheet boundary occurred on field lines mapping close to the polar boundary of the nightside auroral oval for $Q = 3$ according to *Feldstein and Starkov* [1967]. (If more appropriate models MF73D or MF73SD are used, the latitude of the ionospheric projection changes by no more than 2°, which does not change the above conclusion.) This is to be compared with the identification of the equatorial border of the auroral oval with the inner edge of the plasma sheet [*Vasyliunas*, 1970].

Recent high-altitude measurements from the ISEE 1 and 2 satellites allowed one to substantiate and extend these data on field-aligned currents at the plasma sheet outer boundary [*Frank et al.*, 1981*b*, 1984]. Measurements from the proton cross-field convection velocity at ISEE 1 and independent particle measurements from ISEE 2 gave a cross-field expansion velocity of 14 km s^{-1} and allowed one to calculate the widths of three adjacent current sheets alternating in direction and mapping to 25-, 39-, and 52-km widths at the ionospheric level (in order of decreasing latitude). Current densities of 0.3–1.3 $\times 10^{-8}$ A m^{-2} were directly measured by integration of three-dimensional distributions of electrons, and they correspond to exceptional current densities of the order of $\gtrsim 10^{-5}$ A m^{-2} at ionospheric levels. These characteristics of the field-aligned currents correspond to very intense discrete forms at the polar boundary of the expanded active auroral oval. Such bright auroras at the oval polar boundary are usually present during the active phase and recovery phase of an intense substorm. At the same time, active auroral forms typically are present inside the oval at lower latitudes. Very similar results were shown by *Akasofu et al.* [1971], who compared high-altitude particle measurements of the expanding plasma sheet boundary from VELA satellites with auroral all-sky camera data.

Thus these observations show conclusively that during a substorm the polar boundary of the nightside aurora projects close to the outer boundary of the expanding plasma sheet. Hence the auroral oval must be projected onto the central, or the main, plasma sheet in full accord with the VFSL concept.

In the same paper by *Fairfield* [1973] it was shown that such intense and localized field-aligned currents do not exist at the plasma sheet periphery when there is no substorm. From this an "apparent conclusion is that the expanding plasma sheet boundary is very sharp and characterized by the presence of field-aligned currents, whereas at other times the boundary is broader and more diffuse with no narrow region of currents." Thus in the outer plasma sheet during quiet times a smooth decrease of plasma pressure can be deduced indirectly from these data (which is also reflected in the data on $|\mathbf{B}|$ due to the plasma diamagnetism). This is in qualitative agreement with the poleward expansion of the smooth polar diffuse zone during such conditions. This character may be compared with the narrow latitudinal strip at the oval polar boundary during disturbed times when respective low soft particle intensities at the plasma sheet outer boundary could be difficult to measure directly.

6. The last but not the least argument on plasma sheet mapping to the auroral oval by the field-aligned currents can be deduced from quite general theoretical considerations concerning the generation of large-scale field-aligned currents by plasma pressure gradients in the plasma sheet. According to *Tverskoy* [1982], supposing plasma pressure P to be isotropic for the large-scale vertical current density $j_\parallel$ at ionospheric levels, we have for these conditions

$$j_\parallel = \tfrac{1}{2}c\mathbf{n}[\nabla W + \nabla P]$$

where $\mathbf{n}$ is the unit vector normal to the ionosphere, W is the volume of a field tube with unit magnetic flux, and W and P are regarded as functions of coordinates at the ionospheric level. On the nightside, ∇W is directed nearly sunward while ∇P in the main plasma sheet is closer to the radial direction. Thus for the equatorial (closed) plasma sheet outward from the line of maximal plasma pressure P (that is, for ∇P nearly radially inward) it can be deduced from the above formula that a downward directed large-scale $j_\parallel$ must flow in the postmidnight and morning sectors while upward directed current exists in the evening and premidnight sectors. This is grossly consistent with the directions of the large-scale field-aligned currents flowing out in the evening auroral oval and flowing downward in the poleward portion of the morning auroral oval according to *Akasofu* [1977*a*, *b*] and *Kamide and Rostoker* [1977] (this structure of the field-aligned currents was designated as region I by *Iijima and Potemra* [1978]). The region II currents are located equatorward from that. Thus they must be projected onto the diffuse auroral zone in the evening sector and onto the equatorward portion of the oval and the diffuse zone in the morning sector. And according to the above considerations they must map in the plasma sheet to the near-earth region where the plasma gradients in the plasma sheet and respective auroral regions were successfully used in global simulations of the magnetospheric substorm by *Harel et al.* [1981] and *Anistratenko and Ponomarev* [1981]. This is also consistent with the "VFSL concept."

The diagrams of the meridional cross section of the night magnetosphere through the 2200 MLT meridian are presented in Figure 22 separately for magnetically quiet ($Kp = 1$) and magnetically disturbed ($Kp = 5$) periods according to *Valchuk et al.* [1979]. The regions filled with hot electrons differing in their macroscopic parameters and mapped along magnetic field lines onto the auroral ionosphere are marked with different dashes. Identification of precipitation zones of electrons having different characteristic parameters as the low-altitude projections of certain plasma domains on the magnetosphere

makes it possible to apply the accumulated rich information on the dynamics of the auroral precipitation zones to quantitative studies of large-scale dynamic variations in the magnetosphere. Hereinafter we present such an identification from *Valchuk et al.* [1979].

To avoid any semantic misleading (as will be discussed below), it was proposed that the region which, according to *Frank* [1971*a*], was designated as the earthward edge of the plasma sheet, be called the remnant (or transitional) layer. The inner (earthward) boundary of the remnant layer corresponds to the equatorward boundary of the diffuse auroras [*Valchuk et al.*, 1979; *Cambou and Galperin*, 1982].

Under magnetically quiet conditions (Figure 22*a*) the plasmapause 2 is located at $L \approx 5$–6 ($\varphi \sim 63.5°$–$66°$). The inner boundary of the remnant layer 3 is mapped on the equatorward boundary of the diffuse zone located at $\varphi \sim 67°$–$68°$ for $Kp = 1$ [*Galperin et al.*, 1977]. Now the inner boundary is separated from the ionospheric projection of the plasmapause by a $\sim 2°$ gap in latitude. The remnant layer 4 is mapped along magnetic field lines on the diffuse auroral zone. The poleward boundary of the diffuse zone coincides with the equatorward boundary of the auroral oval and is a projection of the inner boundary of the plasma sheet onto the ionosphere. It is located at $\varphi \sim 70°$ [*Feldstein and Starkov*, 1967] and practically coincides with the sharp trapping boundary φ_s. Poleward boundary 7 of the central (low latitude) part of the plasma sheet 6 is mapped on the poleward boundary of the auroral oval proper ($\varphi \sim 72°$). The poleward boundary of the extended soft electron precipitation zone 9 (poleward of the oval) separating the soft auroral zone 8 from polar cap 10 is located at $\varphi \gtrsim 80°$.

During magnetically disturbed periods (Figure 22*b*) the inner boundary of the remnant layer 2 coincides with the plasmapause and is mapped on $\varphi \sim 59°$–$60°$, while the inner boundary of the plasma sheet 4 is also shifted toward the earth and its projection onto the ionosphere is shifted to $\varphi \sim 63°$. The central (low latitude) part of the plasma sheet 5, filled with hotter plasma, compared with magnetically quiet periods, is substantially widened. Its poleward boundary 6 is mapped on $\varphi \sim 74°$. The soft auroral zone 7 poleward of the oval is, on the contrary, narrowed and its poleward boundary 8 is located at $\varphi \sim 75.5°$. During magnetic storms there appears a latitude gap of $\sim 1°$ between the boundaries of auroral radiation 8 and polar cap 10 [*Meng and Kroehl*, 1977]. The polar cap boundary is located now at $\varphi \sim 77°$.

Figures 21 and 22 show considerable differences in the large-scale patterns of auroral electron precipitation relevant to the characteristic regions in the magnetosphere:

1. The band of soft diffuse precipitation and of diffuse auroral luminescence equatorward of the discrete auroras (the diffuse auroral zone) is mapped in the region of the outer radiation belt between the inner boundary of the plasma sheet and the plasmapause (in the remnant layer) according to the scheme shown in Figure 22 or in the central part of the plasma sheet according to the scheme in Figure 21.

2. The zone of discrete precipitation and structured auroral forms (auroral oval) is mapped in the main central (low latitude) region of the plasma sheet (Figure 22) or in the upper (the northern hemisphere) and lower (the southern hemisphere) boundary portions of the plasma sheet (Figure 21). The difference in the two schemes means that the inner edge of the plasma sheet corresponds to the equatorward edge of the diffuse aurora according to *Lui et al.* [1977] or to the equatorward edge of discrete auroras (auroral oval) coinciding with the poleward edge of the diffuse aurora [*Valchuk et al.*, 1979].

3. The zone of soft electron precipitation poleward of the auroral oval is mapped on the polar cap (Figure 21) or in the high-latitude (boundary) parts of the plasma sheet (Figure 22). This soft zone is connected with a periphery of the plasma sheet where the electrons originate from the particle fluxes in the form of polar rain in the tail lobes (Figure 21) or from the magnetosheath (Figure 22). We believe that the diagram in Figure 22 corresponds better to the available observational data: (1) the auroral oval is mapped on the main central part of the plasma sheet where the maximum number and energy fluxes of auroral electrons are located; (2) the soft low-latitude diffuse zone is connected with the magnetospheric region where the mean energies and the energy flux of auroral electrons decrease with decreasing distances to earth; (3) the soft high-latitude zone is connected with the periphery of the plasma sheet where a softening of the electron spectrum takes place with increasing distance from the neutral sheet to the abrupt boundary with the tail lobe.

Similar correspondences were not found in the identification scheme of *Lui et al.* [1977] (Figure 21).

The diagram in Figure 22 is based on the plasma sheet structure summarized in Table 1 according to the early synoptic surveys from high-orbiting satellites. Also presented in Table 1 is the terminology proposed here for various structural features in the outer magnetosphere according to *Valchuk et al.* [1979].

The scheme of the auroral electron precipitation relevant to magnetospheric plasma domains shown in Figure 22 has a characteristic feature in common with the schemes proposed by *Eather and Mende* [1972], *Feldstein* [1973], and *Pudovkin et al.* [1977]; namely, the plasma sheet consists of two regions of which one is mapped on the structured auroral oval and another on the diffuse auroras poleward of the oval. At the same time the scheme proposed in the above works differs significantly from Figure 22 in that the remnant layer connected via geomagnetic field lines to the diffuse auroral zone equatorward of the oval is absent. In spite of the differences outlined by the schemes shown in Figures 21 and 22, the authors of numerous papers adhered to the concept of the inner boundary of the plasma sheet as the equatorward boundary of the auroral oval and, simultaneously, the idea that the diffuse auroras are connected with the central plasma sheet and that the discrete auroral forms are relevant to the boundary plasma sheet. Such a situation has led to chaos in the terminology used to describe the same regions, which can be seen in Table 2.

Following the terminology summarized in Table 1 (and repeated for the sake of convenience in the upper part of Table 2), we used Table 2 to present the observational results and respective notions of several authors cited here concerning the relationships of the magnetospheric structure to various types of auroral luminescence and auroral electron precipitation.

To facilitate further usage of the extensive observational data presented and summarized in the respective papers, we made an attempt to systematize the reasons for the differences between the results of several authors as follows:

1. The same term was used to designate different subjects, or conversely, the same structural region of the magnetosphere is related to different types of auroral luminescence: "The equatorward boundary of the auroral oval" is considered the equatorward boundary of the region of discrete auroral forms according to *Feldstein and Starkov* [1970], *Eather and Mende* [1972], *Feldstein* [1973], and *Lassen* [1974] but is used to designate the equatorward boundary of the diffuse luminescence bordering the region of discrete forms

at lower latitudes according to *Eather et al.* [1976], *Kamide and Winningham* [1977], *Gussenhoven et al.* [1981, 1983], *Lui et al.* [1982], and *Horwitz et al.* [1982, 1983]. "The auroral oval" is considered the region of discrete auroral forms according to *Feldstein and Starkov* [1970], *Eather and Mende* [1972], *Feldstein* [1973], and *Lassen* [1974] but is considered the region of diffuse luminescence on the poleward side of which the discrete auroral forms are usually embedded according to *Kamide and Winningham* [1977] and *Meng and Akasofu* [1983]. "The inner boundary (edge) of the plasma sheet" is considered a surface along the magnetic field inward from which a softening of the mean auroral electron spectrum begins. This boundary is mapped on the equatorial boundary of the discrete auroral oval according to *Vasyliunas* [1972], but the same term was used to designate the minimum radial distance in the equatorial plane where soft auroral electrons are observed with a spectral softening inward; this boundary is mapped on the equatorial boundary of the diffuse luminescence [*Eather et al.*, 1976; *Lui et al.*, 1977, 1982; *Kamide and Winningham*, 1977; *Gussenhoven et al.*, 1983]. According to *Galperin et al.* [1977] and *Horwitz et al.* [1982, 1983], the inner edge of the plasma sheet (for which, in fact, the inner boundary of the remnant layer was taken) coincides with the plasmapause on the nightside during disturbed conditions and in the dawn sector (the data from ISEE 1). For quiet times ($Kp \leq 2$) there is a gap between them in the dusk sector (the AUREOL 1 and 2 data and the DE 1 and 2 data; see also *Fairfield and Vinas* [1983]. "The central (low latitude) part of the plasma sheet" is mapped on the oval of discrete auroras according to *Vasyliunas* [1970], *Feldstein and Starkov* [1970], *Eather and Mende* [1972], *Feldstein* [1973], and *Lassen* [1974], whereas according to *Akasofu* [1974*b*], *Winningham et al.* [1975], and *Lui et al.* [1977] it is mapped on the diffuse luminescence equatorward of the oval. "The boundary plasma sheet" is mapped on the subvisual diffuse luminescence poleward of the discrete auroral forms according to *Eather and Mende* [1972], *Feldstein* [1973, 1974], and *Valchuk et al.* [1979], whereas it is mapped on the region of discrete auroras according to *Akasofu* [1974*b*], *Winningham et al.* [1975], and *Lui et al.* [1977], while *Tanskanen et al.* [1981] identify its low-altitude mapping with the regions of both discrete and diffuse auroras. Indirect evidence for the occurrence of the convection reversal inside the BPS precipitation region [*Burch et al.*, 1976; *Heelis et al.*, 1980] indicates independently that the boundary plasma sheet can hardly be associated with the discrete auroral region only, as the high-latitude portion of the BPS precipitation region is presumably connected through magnetic field lines to the boundary layer on the magnetopause. This list may be continued.

2. Sometimes the same structural feature in the magnetosphere is defined by different terms. For example, the region between the plasma sheet and the plasmapause (the remnant layer in our description) is defined as (1) the inner edge of the plasma sheet [*Schield and Frank*, 1970]; (2) the earthward edge of the plasma sheet [*Frank*, 1971*a*]; (3) the near-earth plasma sheet [*Evans and Moore*, 1979]; (4) the near-earth plasma sheet, or the inner plasma sheet, or the inner part of the plasma sheet [*Moore et al.*, 1981]; (5) the earthward equatorial plasma sheet [*Slater et al.*, 1980]; (6) the inner (earthward) edge of the plasma sheet [*Nakai and Kamide*, 1983].

3. The experimental data are sometimes interpreted in favor of one of the commonly adopted concepts concerning the association of certain types of auroral luminescence with the characteristic region in the magnetosphere, apparently without sufficient justification. For example, the observations by *Deehr et al.* [1976] indicate that the diffuse precipitations equatorward from the discrete auroras are observed in the stable trapping region of high-energy electrons, i.e., at the latitudes of the outer radiation belt. *Deehr et al.* [1976], however, relate them to precipitations from the central plasma sheet (CPS) and the discrete auroras, and precipitations located in the region adjacent to and poleward from the stable trapping boundary (i.e., presumably at the latitudes of the central plasma sheet) were assigned by *Deehr et al.* [1976] to the precipitations from the boundary plasma sheet.

Similar phrasings can be found in many other papers, and this probably justifies such a detailed examination. Additional difficulties in the analysis of the observational data sometimes arise when describing the measurements taken inside a certain characteristic low-altitude structure. Some authors adopt its projection to the magnetospheric domains according to one of the above concepts but also quote the works where other concepts are assumed to be valid.

For example, *Hardy et al.* [1981], relating the equatorward boundary of the auroral electron precipitations to the inner edge of the plasma sheet, simultaneously quote *Vasyliunas* [1970], *Lassen* [1974], *Winningham et al.* [1975], and *Lui et al.* [1977] (see also *Nakai and Kamide* [1983]). It should be noted that *Lassen* [1974] has emphasized the substantial difference in identifying the inner boundary of the plasma sheet as the equatorward boundary of discrete or diffuse auroras. A similar situation with quotations can be found even in the otherwise excellent monograph by *Akasofu* [1977*a*]. In the section "magnetospheric plasmas and auroral particles" (see p. 165, point 3) one can read, "*Lassen* [1974] showed that the upper boundary and the inner edge of the plasma sheet coincided, respectively, with the poleward and equatorward boundaries of the auroral oval which are determined by a statistical study of auroral arc alignment." At the same time he writes (see p. 166, point 6), "It is quite likely that the projection of the inner boundary of the plasma sheet along the geomagnetic field lines coincides with the equatorial boundary of the diffuse aurora."

Gussenhoven et al. [1983] believe that there is widespread agreement that the immediate source of precipitating diffuse auroral electrons is the central plasma sheet. In this case the authors quoted *Vasyliunas* [1970], *Lassen* [1974], *Winningham et al.* [1975], *Lui et al.* [1977], and *Meng et al.* [1979], although the first two authors related the oval of discrete auroral forms to the center of the plasma sheet, whereas in the latter three papers it was associated with the diffuse luminescence equatorward of the discrete auroral forms.

The classification of the plasma sheet structure in the magnetosphere proposed in Table 1 may be treated, in our opinion, as a proposed tentative basis for the commonly used magnetospheric and auroral terminology open, clearly, to criticisms, improvements, and experimental verifications before being presented to the International Association of Geomagnetism and Aeronomy.

The pattern shown in Figure 22 has recently found its further confirmation in observations of the auroral luminescence from Intercosmos 19 [*Gogoshev et al.*, 1981*a*, *b*]. The emissions λ6300 Å, λ5577 Å, and λ4278 Å were measured with a high sensitivity and compared with other on-board measurements. Figure 23 shows the results of the measurements taken in the southern hemisphere at dusk hours during the magnetic storm of April 4, 1979. The λ6300-Å emission intensity begins

TABLE 1. Structure of the Magnetospheric Plasma Sheet

Author	Term 1	Term 2	Term 3	Term 4	Term 5	Term 6	Term 7	Term 8
Vasyliunas [1968]			inner boundary of the plasma sheet					
Schield and Frank [1970]	the separation between the plasmapause and the earthward edge of the plasma sheet	the earthward edge of the plasma sheet, inner edge of the plasma sheet						
Frank [1971*a*]	inner boundary of the earthward edge of the plasma sheet coincides with the plasmapause in the postmidnight sector while electron trough exists in the premidnight sector	the earthward edge of the plasma sheet	trapping boundary for energetic electrons >40 keV usually coincident with, or beyond, the outer boundary of the earthward edge of the plasma sheet					
Frank [1971*b*]		ring current trapping region		plasma sheet		high-latitude magnetotail		polar cap
Vasyliunas [1972]		soft electrons' fluxes	inner boundary or the inner edge of plasma sheet	plasma sheet	plasma sheet	plasma sheet	plasma sheet	high-latitude magnetotail (polar cap)
Aubry et al. [1972]	outer radiation belt (night cusp)	outer radiation belt (night cusp)	outer radiation belt (night cusp)	plasma sheet		main lobe	main lobe	main lobe
Proposed nomenclature	inner boundary of the remnant layer	remnant layer	inner boundary of the plasma sheet	central (low latitude) plasma sheet	external boundary of the central (low latitude) plasma sheet	outer (high latitude) plasma sheet	external boundary of the plasma sheet	tail lobes

TABLE 2. Relationships Between Large-Scale Structure of the Plasma Sheet and Various Types of Auroral Luminosity According to Different Authors

Author	Plasma Sheet Structure							
	Inner Boundary of the Remnant Layer	Remnant Layer	Inner Boundary of the Plasma Sheet	Central (Low Latitude) Plasma Sheet	External Boundary of the Central (Low Latitude) Plasma Sheet	Outer (High Latitude) Plasma Sheet	External Boundary of the Plasma Sheet	Tail Lobes
Vasyliunas [1970]			equatorial boundary of the auroral oval	auroral oval and diffuse aurora poleward of the oval	auroral oval and diffuse aurora poleward of the oval	auroral oval and diffuse aurora poleward of the oval	auroral oval and diffuse aurora poleward of the oval	
Feldstein and Starkov [1970]			the boundary of the stable trapping of energetic electrons (ϕ_s) coincides with the equatorward boundary of the auroral oval	auroral oval	background boundary of the energetic electrons (ϕ_b) coincides with the poleward boundary of the auroral oval			
Ackerson and Frank [1972]				weak diffuse electron and proton precipitation adjacent to, and equatorward of, the trapping boundary	trapping boundary of $E > 45$ keV electrons; the boundary between magnetic field lines closed within the magnetosphere and open field lines connected to the interplanetary medium	inverted V precipitations poleward of and adjacent to the trapping boundary		
Frank and Ackerson [1972]				diffuse electron precipitation from the distant plasma sheet and its earthward extension	trapping boundary of $E > 45$ keV electrons; the boundary between magnetic field lines closed within the magnetosphere and open field lines to the interplanetary medium; the trapping boundary is coincident with the reversal of convection electric fields—sunward flow equatorward of the boundary and antisunward flow poleward of it	inverted V precipitation bands in the zone of strong antisunward convection; projected to the distant plasma sheet and downstream magnetosheath adjacent to polar cap		polar cap, which is distinguished by the absence of low-energy particle fluxes and by slow convection

Another possible interpretation of the observations by *Ackerson and Frank* [1972], *Frank and Ackerson* [1972]		diffuse precipitation from the remnant layer	trapping boundary for electrons of $E > 45$ keV, boundary between diffuse and discrete auroras	inverted V events in the auroral oval					
Eather and Mende [1979]			equatorward boundary of the auroral oval	auroral oval		high-latitude soft zone (poleward subvisual luminosity)		polar cap	
Lassen [1974]			equatorward boundary of the auroral oval	auroral oval	poleward boundary of the auroral oval				
Akasofu [1974*b*]				central part of the plasma sheet (main part) connected with the diffuse aurora	diffuse and discrete auroral belts are separated by the trapping boundary for hard electrons	discrete (structured) auroras connected with the upper (northern hemisphere) and lower (southern hemisphere) layer of the plasma sheet			
Feldstein [1974]		diffuse aurora equatorward of the auroral oval	equatorward boundary of the auroral oval	auroral oval	poleward boundary of the auroral oval	diffuse subvisual aurora			
Winningham et al. [1975]		outer radiation belt	outer radiation belt	diffuse precipitation originates in the central plasma sheet (CPS) adjacent to the outer radiation belt		variable precipitation with inverted V; originates in the boundary plasma sheet (BPS) adjacent to the tail lobe		polar cap, appreciable precipitations of soft auroral electrons	
Liu et al. [1977]			the equatorward edge of the diffuse aurora	diffuse aurora corresponds to CPS	ϕ_a, stable trapping boundary	discrete auroras correspond to the BPS	ϕ_b, background boundary	polar cap	
Another possible interpretation of the observations by *Lui et al.* [1977] and by *Winningham et al.* [1975]	equatorial boundary of the diffuse aurora	diffuse aurora	trapping boundary for hard electrons ϕ_a	discrete auroras	trapping boundary for hard electrons ϕ_b	diffuse aurora		polar cap	
Burch et al. [1976]		diffuse precipitations, nonaccelerated electrons from the plasma sheet (sunward convection)		inverted V events projected to the plasma sheet (sunward convection)		higher-latitude duskside precipitation region projected to the magnetosheath (antisunward convection)			

TABLE 2. (continued)

Author	Plasma Sheet Structure							
	Inner Boundary of the Remnant Layer	Remnant Layer	Inner Boundary of the Plasma Sheet	Central (Low Latitude) Plasma Sheet	External Boundary of the Central (Low Latitude) Plasma Sheet	Outer (High Latitude) Plasma Sheet	External Boundary of the Plasma Sheet	Tail Lobes
Deehr et al. [1976]				diffuse aurora referred to as diffuse precipitation from CPS in the region of stable trapping of energetic electrons	stable energetic electrons trapping boundary ϕ_s ($E > 40$ keV)	discrete auroras referred to as structured precipitation from BPS is poleward of the stable electrons trapping boundary ϕ_s	background trapping boundary ϕ_b of energetic electrons ($E > 40$ keV)	very narrow (in latitude) region of soft (energy, ≤ 1 keV) particle precipitation on poleward edge of the structured precipitation region
Eather et al. [1976]			the equatorward edge of weak subvisual aurora	the region of weak subvisual diffuse aurora	the lowest latitude of new precipitation, the injection boundary, projected, to low altitudes	discrete aurora associated with injection events		
Another possible interpretation of the observations by *Eather et al.* [1976]	equatorial edge of the sub-visual diffuse aurora	subvisual diffuse aurora	injection boundary corresponding to the equatorward boundary of the auroral oval	zone of injection corresponding to the auroral oval				
Kamide and Winningham [1977]			equatorward boundary of the diffuse auroral particle precipitation was identified in terms of the equatorward boundary of the auroral oval	region of diffuse precipitation from the CPS		region of intense and highly structured precipitations from the BPS		
Pudovkin et al. [1977]			equatorial boundary of the auroral oval	auroral oval	poleward boundary of the auroral oval	diffuse subvisual aurora	poleward boundary of polar cap aurora, located near the plasma sheet external boundary but not coincident with it	
Meng [1978]		diffuse auroras produced by electrons from the CPS and/or the outer radiation zone	diffuse auroras produced by electrons from the CPS and/or the outer radiation zone	diffuse auroras produced by electrons from the CPS and/or the outer radiation zone		discrete and variable auroras were produced from the BPS		

Lin and Hoffman [1979]				inverted V precipitating electrons projected to the plasma sheet and neutral sheet				
Evans and Moore [1979]		diffuse aurora is the direct consequence of the pitch angle diffusion of particles in the near-earth plasma sheet						
Valchuk et al. [1979]	equatorward boundary of the diffuse aurora	diffuse aurora	equatorward boundary of the auroral oval	auroral oval	poleward boundary of the auroral oval	diffuse aurora poleward to the auroral oval	poleward boundary of the diffuse aurora	polar cap
Slater et al. [1980]	equatorward boundary of the diffuse aurora	diffuse auroral region						
Heelis et al. [1980]				region of relatively uniform electron precipitation from the CPS (sunward convection)		region with inverted V spectra from the BPS; gross convection reversal occurring within the BPS; high-latitude portion of the BPS is magnetically conjugate with boundary layer of the outer magnetosphere		
Gussenhoven et al. [1981]			the equatorial boundary of the diffuse aurora is the equatorward boundary of the oval	diffuse auroral electrons from the central plasma sheet (CPS)				
Tanskanen et al. [1981]				the region of the diffuse auroral precipitation from the central plasma sheet		the region of complex structured precipitation and the most poleward bend of soft electron precipitation from the boundary plasma sheet		
Lui et al. [1982]			equatorward boundary of the diffuse aurora	diffuse aurora equatorward of the discrete auroral region represents the optical "foot point" of the central plasma sheet				

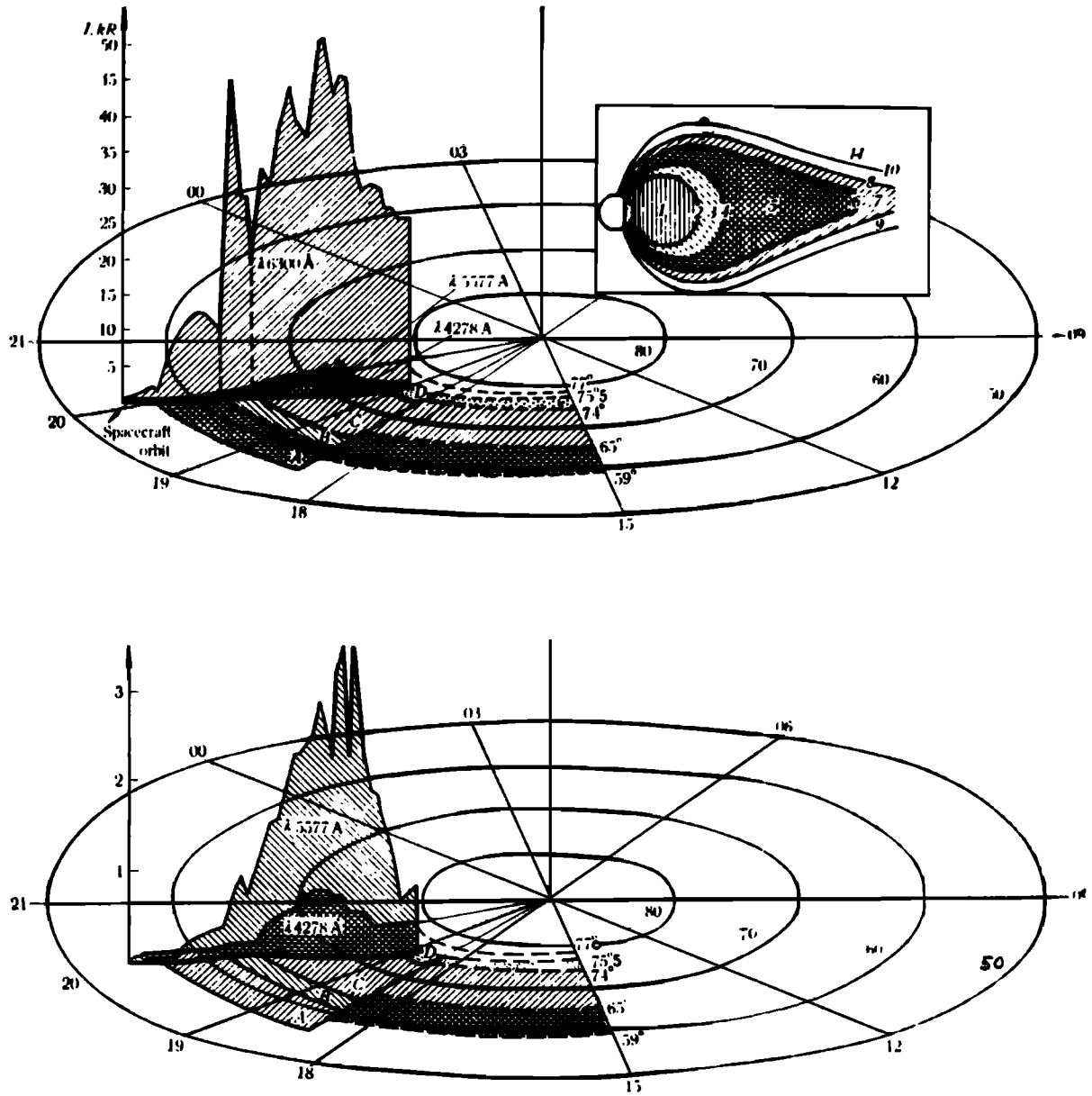

Fig. 23. The intensities of the 6300-, 5577-, and 4278-Å emissions in the dusk sector on April 4, 1979, inferred from the Intercosmos 19 data obtained in the southern hemisphere [*Gogoshev et al.*, 1981*a*]. See the text for an explanation of zones A, B, C, and D. The intensities of the 5577-Å and 4278-Å emissions are shown on a larger scale in the bottom part of the figure. Use is made of the invariant latitude (MLT) intensity (in rayleighs) cylindrical coordinate system. Shown in the inset of the top figure is the magnetospheric structure in the dusk sector during magnetically disturbed periods (see Figure 22).

increasing rapidly from $\varphi \sim 56°$ and reaches 12.7 kR at $\varphi \sim 61°$. In this region the intensities of the λ5577-Å and λ4278-Å emissions are low, which confirms a soft spectrum of the precipitating electrons (the A zone). Starting from $\varphi \sim 62°$, a growth of the λ5577-Å emission intensity begins, and starting from $\varphi \sim 64°$, the λ4278-Å emission also becomes more intense. This zone of structured luminescence is extended to $\varphi \sim 73°$. The maximum emission intensities were ~50 kR in λ6300 Å and ~3 kR in λ5577 Å. At higher latitudes the emission intensities decrease for all these emissions but still remain considerable for λ6300 Å. This is the near-pole region of soft precipitation (the D zone) with the abrupt poleward termination at $\varphi \sim 74.5°$ because the satellite left the earth's shadow. According to *Gogoshev et al.* [1981*a*, *b*] the luminescence zones A, C, and D, in their latitudinal localizations, are very close to the above described zones of soft precipitations, i.e., the remnant layer (3), the central (low latitude) plasma sheet (5), and the outer (high latitude) plasma sheet (7), respectively, during geomagnetic disturbances. These zones are shown schematically in the upper right corner of Figure 23. The difference between the patterns in Figures 21 and 23 has its signature in other geophysical phenomena.

Figure 20 shows the interpretative diagram according to *Frank and Ackerson* [1972]. This diagram was, and still is, widely used in the literature on the subject, and it is in agreement with the precipitation diagram shown in Figure 21 for the region $\varphi \geq 60°$. This diagram was partly modified by *Feldstein* [1973]. Figure 24 shows a new set of composite diagrams based on the notions of *Valchuk et al.* [1979] in the dusk sector and on the concepts of *Muliarchik et al.* [1982] in the day sector of the magnetosphere. Also used were the results from the papers by *Maezawa* [1976], *Kintner et al.* [1978],

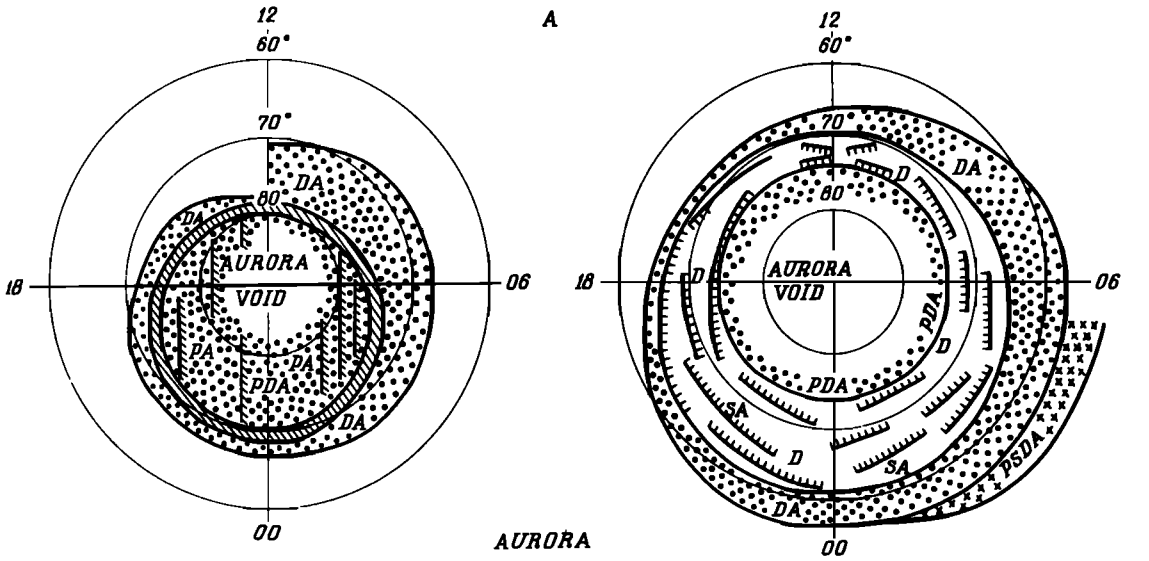

Fig. 24*a*

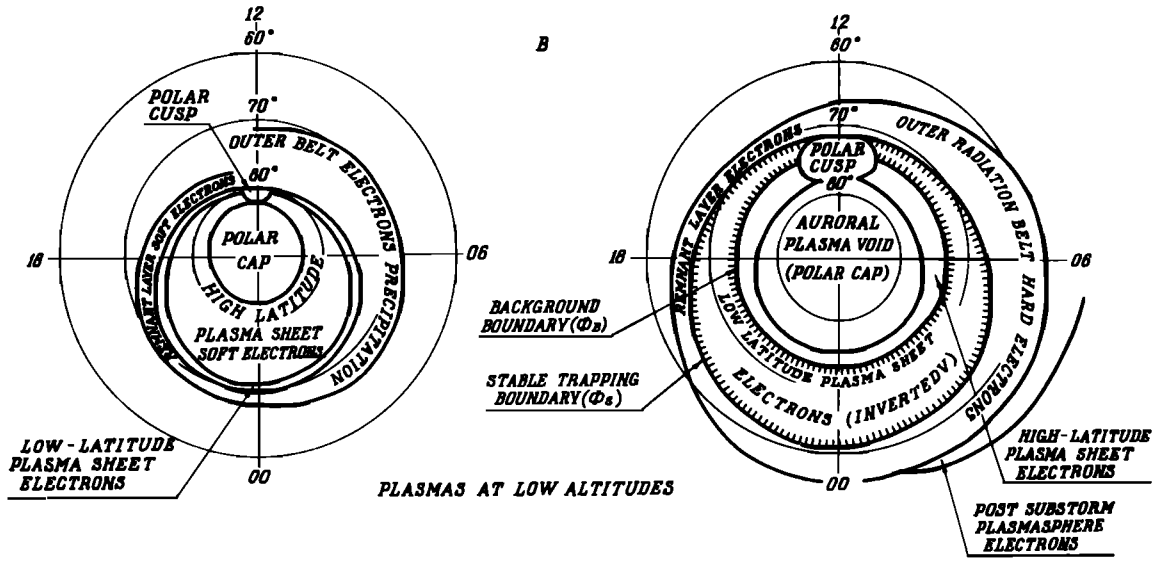

Fig. 24*b*

Fig. 24. Schemes illustrating high-latitude distributions of various geophysical events in magnetically quiet ($Kp = 0$) and magnetically disturbed ($Kp = 5$) periods. The coordinate grid is the corrected geomagnetic latitude, MLT. (*a*) The types of auroras: PA, sunward oriented polar cap arcs; PDA, polar diffuse auroras; SA, structured auroras in the auroral oval; D, diffuse auroras in the auroral oval; DA, diffuse auroras equatorward of the auroral oval; PSPA, postsubstorm plasmaspheric auroras. (*b*) Plasmas at low altitudes. (*c*) Plasma domains in the distant magnetosphere. (*d*) Convection in the magnetosphere. The scheme of the isolines of electrostatic potential during an equinox. The numerals at the focuses of the dusk and dawn vortices show the potential in kilovolts. The boundaries of the auroral oval are shaded. The scheme is smoothed and oversimplified; convection close to discrete forms is omitted. (*e*) Large-scale field-aligned currents above the ionosphere. The scheme is very approximate because the commonly adopted concepts concerning the relationships of the large-scale currents to the magnetospheric structure are lacking. (*f*) Geomagnetic field topology. (Figure 24 continues on the following two pages.)

McDiarmid et al. [1976, 1978, 1979, 1980], *Klumpar* [1979, 1980], *Winningham* [1979], *Heelis et al.* [1980], *Burke et al.* [1980], *Levitin et al.* [1982], *Robinson et al.* [1982], *Senior et al.* [1982], *Cowley* [1983], *Coley* [1983], and *Makita et al.* [1983] and the results referred to in the discussions above.

The distributions of various geophysical phenomena at $\varphi \geq 60°$ are separately presented for magnetically quiet ($Kp \sim 0$) and for magnetically disturbed ($Kp \sim 5$) periods. The large-scale convection and field-aligned currents ($j_{\parallel}$) are typical of the periods when the IMF has a component transverse to the plane of the ecliptic $B_Z = +4$ nT (quiet conditions) and $B_Z = -4$ nT (disturbed conditions) and the azimuthal component $B_Y = 0$ nT. The adopted values for solar wind velocity $v_{sw} \sim 500$ km s^{-1} and density $n \sim 4$ particles cm^{-3} are for moderate solar wind flow conditions.

Figure 24*a* presents the distribution of different types of auroral luminescence in the quiet (to the left) and disturbed (to

TABLE 3. Proposed Nomenclature and Abbreviations

	Abbreviation
Diffuse aurora boundary	DAB
Diffuse precipitation boundary	DPB
Diffuse aurora	DA
Structured (discrete) aurora	SA
Polar diffuse aurora	PDA
Polar arcs	PA

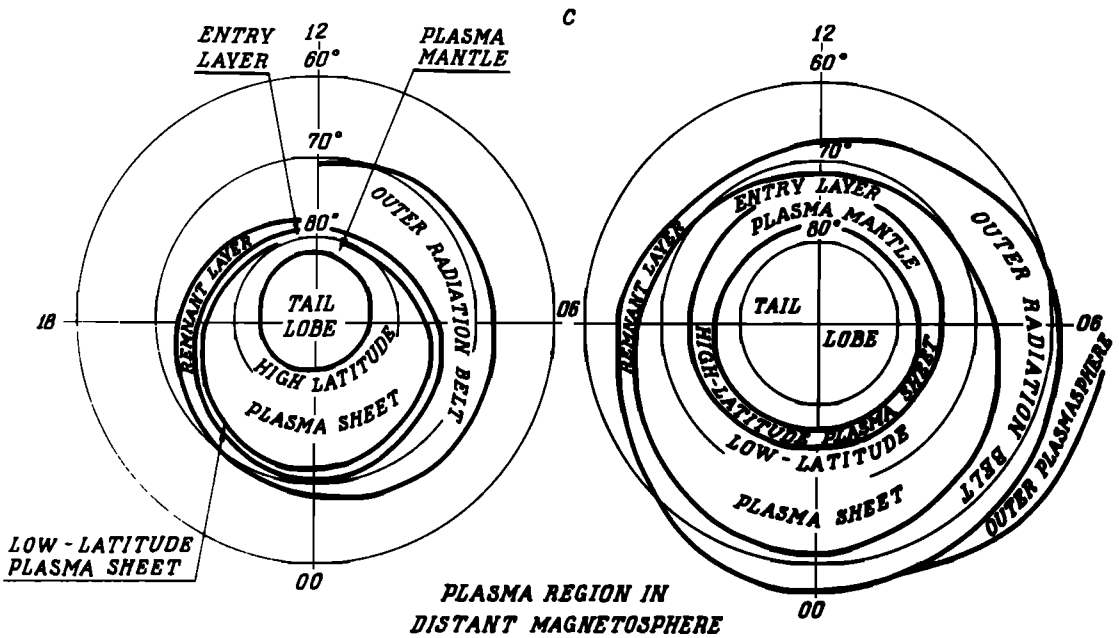

Fig. 24c

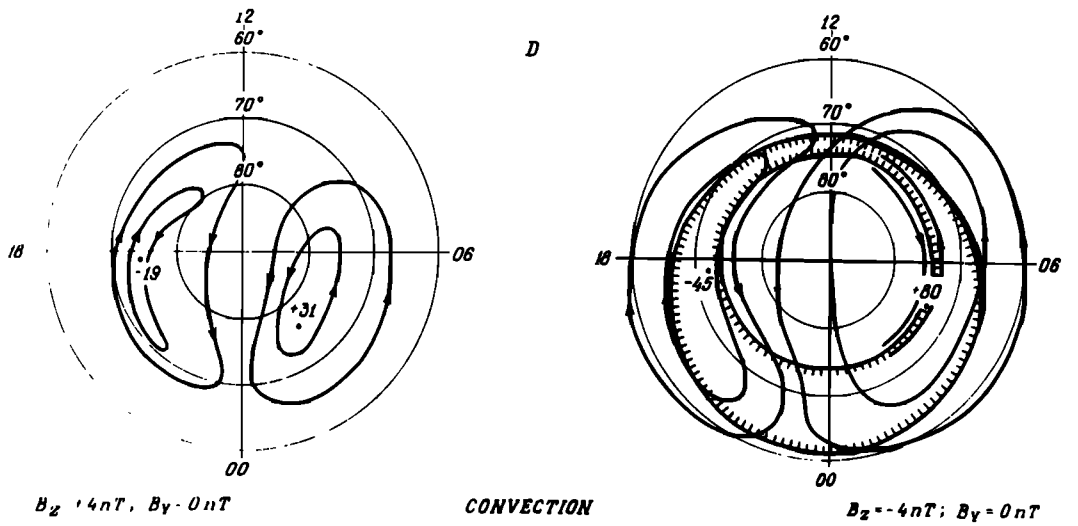

Fig. 24d

the right) periods. The exact locations of the equatorward boundary of the polar cap where significant auroral soft electron precipitations are absent, depending on the activity and for different MLT sectors, have not been studied sufficiently as yet; hence their description in Figure 24*a* should be considered to be but tentative. It is known that during quiet periods a considerable portion of the near-pole region at $\varphi \geq 80°$ is filled with the auroral luminescence, while during disturbances the diffuse luminescence poleward of the oval (PDA) is confined to within a narrow band. The diffuse auroral luminescence equatorward of the oval (DA) in the dusk sector is produced by the precipitation of soft electrons causing the λ6300-Å emission prevailing in the ionospheric F region. In the dawn sector the latitude range of this remnant layer, produced by previous injections of hot plasma, is considerably widened and intensified owing to enhanced precipitation of hard electrons trapped in the outer radiation belt. Therefore the DA in the dawn sector is concentrated at E region altitudes near the equatorward boundary (the λ5577-Å and 3914-Å emissions) and is observable also in the F region, especially at higher latitudes where soft electron fluxes increase. In the day sector during a magnetically quiet period, there occurs a latitude jump of the location of the equatorward boundary of DA due to an important intensity decrease toward the noon sector of precipitating high-energy outer zone electrons during their longitudinal drift.

Figure 24*b* shows the distribution of the parameters of precipitating electrons at low altitudes. The poleward and equatorward boundaries of the auroral oval during magnetically disturbed periods (to the right) are shown by dashes. They coincide with the background trapping boundary φ_b of the high-energy ($\geq$40 keV) electrons and with the stable trapping boundary φ_s, respectively. During magnetically quiet periods the high-latitude (outer) part of the plasma sheet is significantly expanded poleward, as a result of which the near-pole region proves to be nearly filled with auroral radiation. The

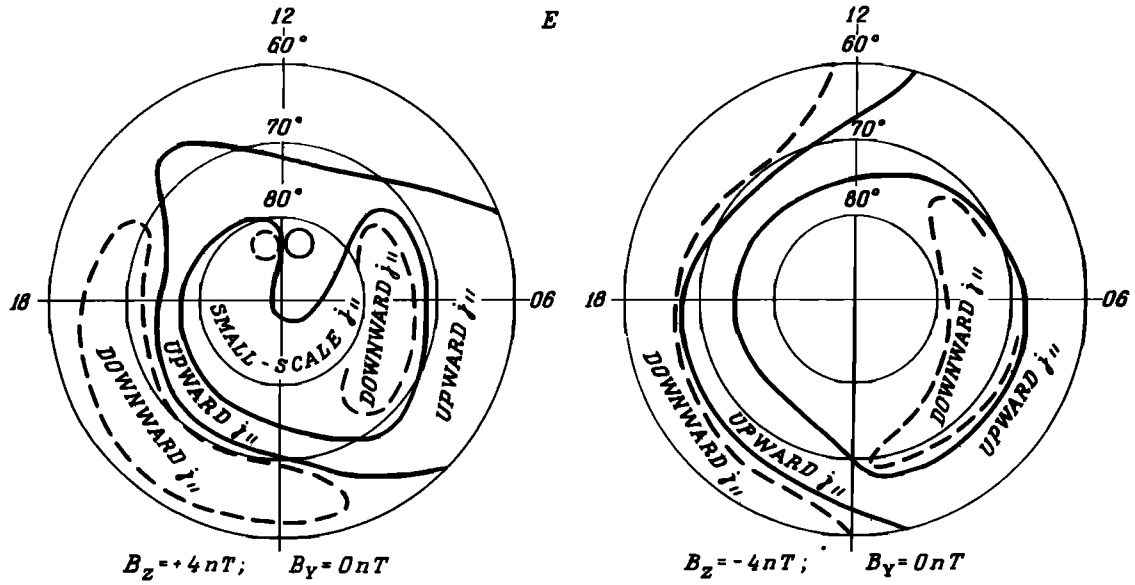

Fig. 24e

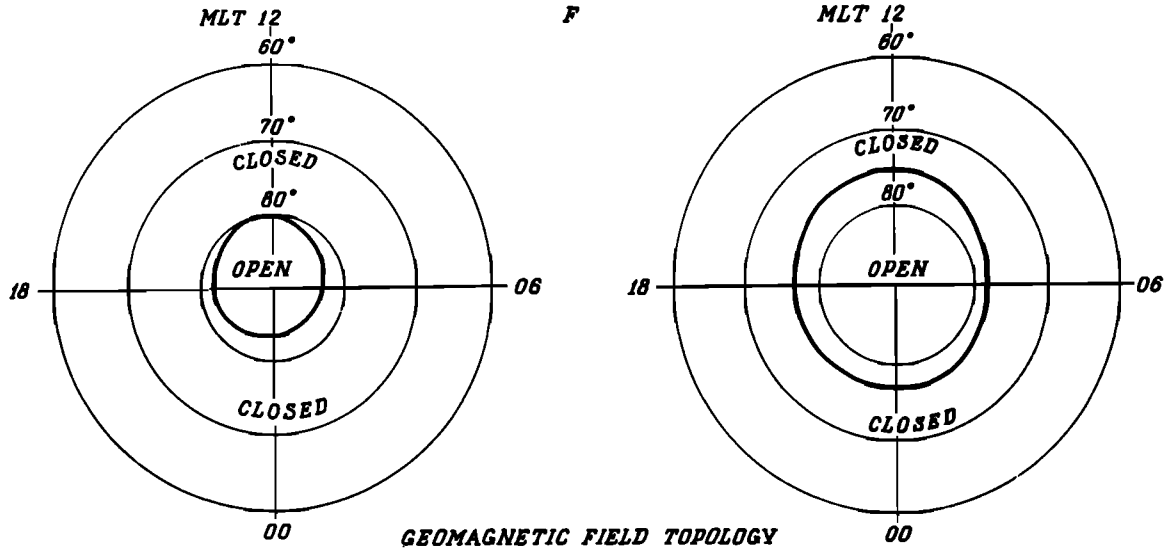

Fig. 24f

inverted V precipitations in the auroral oval are associated with the entry layer on the dayside and with the low-latitude (main, central) plasma sheet on the nightside. The magnetosheath plasma and the high-latitude plasma sheet are responsible for the diffuse luminescence poleward from the auroral oval. The magnetospheric plasma domains responsible for various types of auroral luminescence are presented in Figure 24*c*.

Figure 24*d* presents the diagrams of the large-scale electrostatic field equipotentials above the ionosphere for the two cases described above for the interplanetary medium. The equipotentials in MHD approximation coincide with the plasma drift trajectories of the large-scale plasma convection in the magnetosphere. The figures shown close to the foci of the dusk and dawn votices are peak values of the potential in kilovolts. The hatched lines correspond to the auroral oval boundaries. The high-latitude diffuse soft precipitation poleward of the oval is usually located in the region of antisunward convection. At oval latitudes the antisunward convection is located only on its poleward edge in the dusk sector (Figure 24*d*, to the right). In fact, the entire oval in the dawn sector and a considerable part of it in the dusk sector, together with the region equatorward of the oval, are located inside the region of the sunward convection characteristic of the inner parts of the outer magnetosphere.

In the two situations presented in Figure 24*d*, the convection in the near-pole region at $\varphi \geq 80°$ is antisunward. At $B_Z \geq 10$ nT the convection in the near-pole region becomes sunward. It is quite possible that θ auroras observed in the periods of positive B_Z are just located along the sunward convecting plasma [*Frank et al.*, 1983].

The large-scale field-aligned currents $j_\parallel$ (Figure 24*e*) in the dusk sector flow out from the ionosphere at the auroral oval latitudes and flow into the ionosphere in the diffuse luminescence region equatorward of the auroral oval. In the morning sector during magnetic disturbances at the auroral oval latitudes, the downward and upward currents $j_\parallel$ are observed. However, the upward field-aligned currents are generally

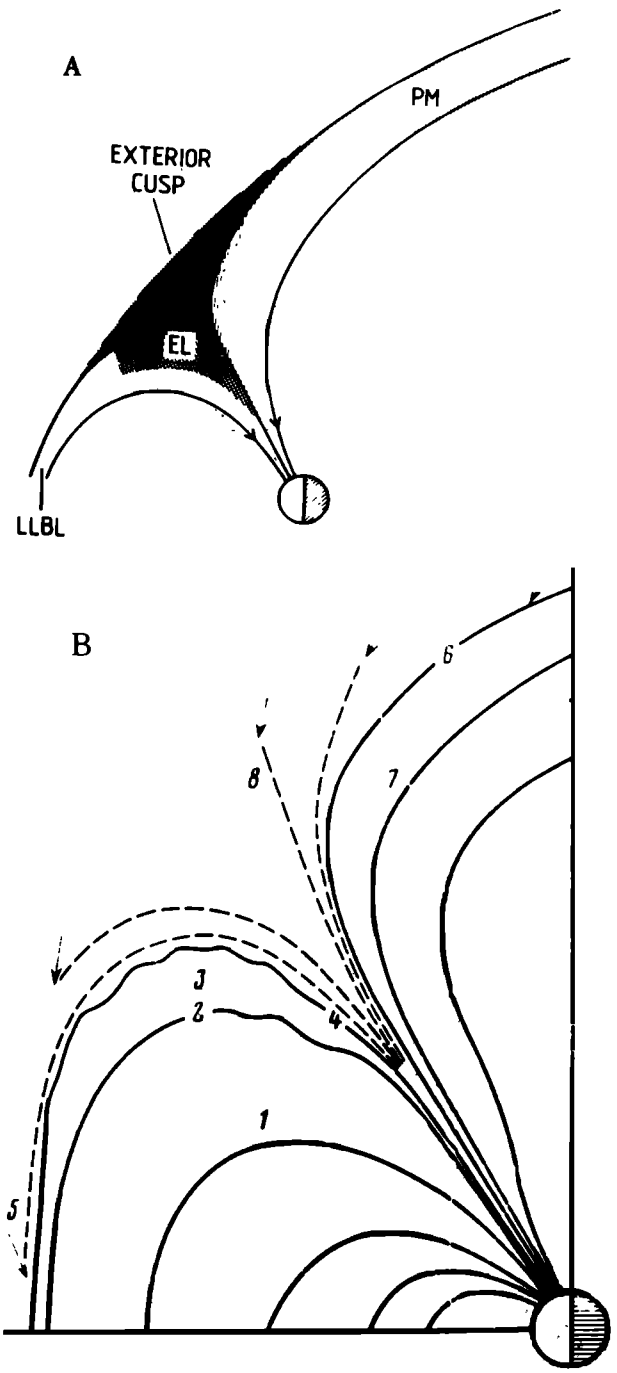

Fig. 25. (*a*) Schematic meridional cross section of the high-latitude dayside magnetosphere and magnetosheath [*Sckopke*, 1979]. LLBL is low-latitude boundary layer, EL is entry layer, and PM is plasma mantle. (*b*) Meridional magnetospheric profile through the 11-hour meridian [*Muliarchik et al.*, 1982]: 1, outer radiation belt; 2, stable trapping boundary φ_s, equatorward boundary of the discrete auroral oval; 3, entry layer mapped on the auroral oval; 4, closed field line region boundary φ_b located near the magnetopause in the dayside sector; 5, magnetopause; 6, nightside magnetopause; 7, plasma mantle mapped on diffuse auroras poleward of the auroral oval; 8, exterior cusp which constitutes, together with the entry layer and plasma mantle, the polar cusp.

spread over the diffuse luminescence equatorward of the auroral oval. During magnetically quiet conditions in the day sector, there appears a pair of field-aligned currents which are directly associated with the currents of the high-latitude magnetopause. The $j_{\parallel}$ diagrams presented do not include some of the important small-scale details associated with auroral arcs and other small-scale features. Moreover, the substorm effects are smoothed in the diagrams, and they should, therefore, be only considered to be much simplified. At present, the relationships of the large-scale field-aligned currents to the magnetosphere structure are being intensively studied on the basis of the data of the measurements of various types; so in the near future one may expect a refining of this simplistic pattern and the establishment of quantitative correlations to the parameters of the interplanetary medium, probably allowing for the neutral atmosphere circulation modified by substorms. With respect to geomagnetic field topology, the lines of force may be closed within the magnetosphere or reconnected with the IMF (open). In Figure 24*f* the magnetic field lines of the polar cap (loosely defined as the region of nearly absent auroral luminescence) and of the plasma mantle are treated as open. Over the remaining outer magnetosphere structural regions, including the entry layer, the geomagnetic field lines are closed. The location of the boundary separating the closed and open field lines should be treated as tentative. It is possible that the open field lines do not form a unified coherent bundle and appear locally and more or less sporadically on the magnetopause [*Cambou and Galperin*, 1974; *Russell and Elphic*, 1979].

Now we shall use the proposed composite patterns to examine the fundamental problem concerning the localization of the initial substorm-generating shell in the magnetosphere. In numerous and highly reliable measurements, the brightening of an equatorward auroral arc in the night sector [*Akasofu*, 1968] or the appearance, near (but somewhat poleward of) such an arc, of a new arc which then rapidly moves poleward [*Starkov and Feldstein*, 1971] is taken to be an auroral substorm onset. According to *Pellinen and Heikkila* [1978] this burst is preceded by a short-term weakening of the auroral arc brightness. This means that "the first sign of the auroral substorm occurs along the boundary of the quasi-circular diffuse and discrete auroral regions, namely, near the poleward boundary of the diffuse aurora and the equatorward boundary of the belt of discrete auroras" [*Akasofu*, 1974*b*]. In the diagrams proposed above, the equatorward arc is located in the night sector near the inner boundary of the plasma sheet. Therefore the process of initiating the expansion phase of an auroral substorm commences on closed magnetic field lines of the plasma sheet in the magnetospheric tail. Apparently, such a process must be considered as a signature of some internal magnetospheric processes originating from, or stimulated by, the conditions of the interplanetary medium, especially of the IMF. This conclusion is in good agreement with recent observations [*Lui and Burrows*, 1978; *Baumjohann et al.*, 1981]. It is of great importance that a substorm expansion phase commence near midnight on closed magnetic field lines. If it were directly driven by the solar wind, it would have commenced at the poleward edge (at the boundary between open and closed field lines) and then traveled inward, i.e., deeper into the magnetosphere, which is at variance with observational data. More detailed discussion of this problem may be found in the work of *Akasofu* [1977*b*, 1981*b*], *Rostoker et al.* [1980], *Rostoker* [1983], and *Pellinen and Heikkila* [1984].

Let us now discuss in more detail the relationships of the auroral luminescence and auroral electron precipitations to the plasma domains in the distant dayside magnetosphere. The structure of the plasma domains in the day sector of the high-latitude magnetosphere presented in Figure 25*a* was substantiated by *Paschmann* [1979], *Sckopke* [1979], and *Haerendel* [1980]. The low-latitude signatures of this structure were studied by *Reiff* [1979] and *Muliarchik et al.* [1982] using the data of low-orbiting satellites. In Figure 25*b* the mag-

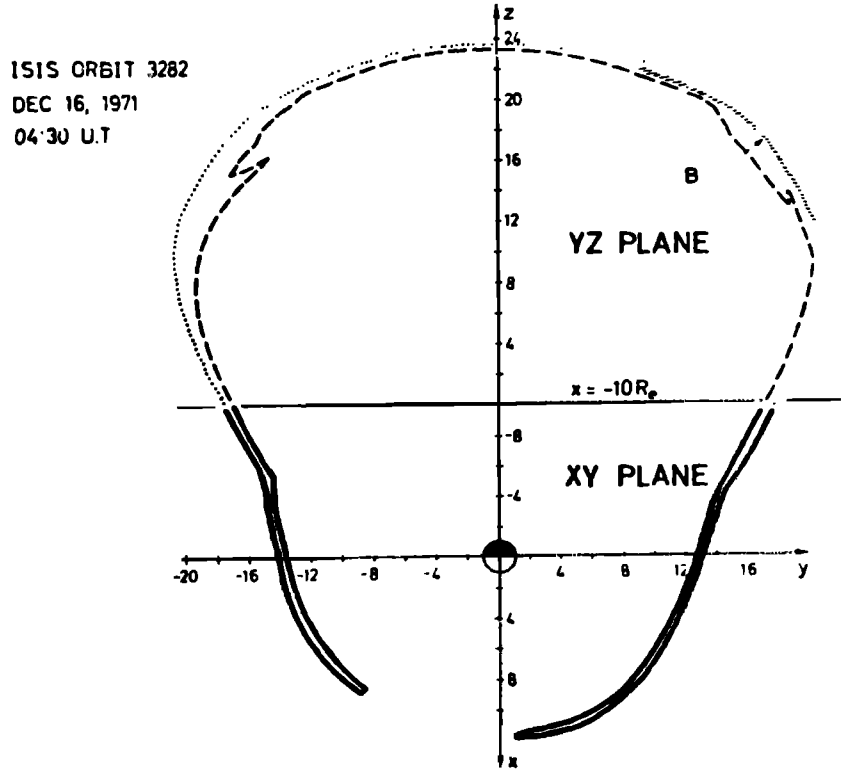

Fig. 26. The dayside cusp auroras mapped on the equatorial plane and on the magnetospheric tail cross section perpendicularly to the earth-sun line at $X = -10\ R_E$. The two cross sections are joined at $X = -10\ R_E$ [*Shepherd and Shepherd*, 1985].

netospheric cross section through the day sector is presented together with the geomagnetic field structure, plasma domains in the outer magnetosphere, and the associated auroral electron precipitation regions [*Muliarchik et al.*, 1982]. Numeral 1 denotes the region of high-energy electron precipitation from the outer radiation belt equatorward of φ_s. In this region the drift shell splitting occurs together with considerable temporal variation of the particle fluxes due to substorm effects. The low-latitude boundary of the entry layer 2 coincides with the stable trapping boundary φ_s, while the entry layer 3 proper is mapped on the day sector of the auroral oval. Thus the auroral oval is located in the day sector mainly at the latitudes where the field lines are closed. The exterior cusp (8) and the plasma mantle (7) are mapped on the spotlike "cusp" region of soft solar wind particle precipitation producing the diffuse luminescence and ion velocity dispersion effects due to convection poleward of the auroral oval.

The meridional cross section through the 1300 hour meridian is essentially the same as it is in Figure 25*b*; the only difference is that a band of auroral soft electron precipitations from the remnant layer appears in the outer radiation belt near φ_s.

Thus if the region of precipitating auroral electrons, whose spectrum is the same as the magnetosheath spectrum, is taken to be a criterion for finding an immediate projection of the polar cusp at the magnetopause onto low altitudes, the polar cusp projection will spread over the dayside oval sector and over the diffuse luminescence poleward of the auroral oval. *Akasofu* [1977*a*] has shown that a variety of geophysical phenomena at the cusp latitudes coincide with the dayside sector of the oval, whereas in the model of *Frank* [1971*b*] the region of soft electron precipitation poleward of the auroral oval is only related to the dayside cusp region. *Shepherd and Shepherd* [1985] used an empirical geomagnetic field model [*Fairfield and Mead*, 1975] to map the dayside region of the auroral 6300-Å luminescence into the magnetosphere. Figure 26 presents the magnetospheric cross section in the equatorial plane (XY) and across the earth-sun line (YZ plane) at a geocentric distance of $-10\ R_E$. The dotted line in the tail magnetosphere cross section and the solid line in the equatorial cross section show the dayside >0.5-kR luminescence boundary projections. The observations were carried out from ISIS 2 on December 16, 1971, at 0403 UT. The luminescence region is mapped on the regions near the magnetopause both in the plasma mantle (the YZ plane) and in the low-latitude boundary layer (the XY plane).

Gussenhoven et al. [1981] and *Fontaine and Blanc* [1983] have compared the location of DPB at various disturbance levels with the boundary between the closed and open equipotentials in the outer magnetosphere. Along the open equipotentials, thermal plasma is transferred from the magnetospheric tail toward the earth. The boundary between the two types of equipotentials corresponds to the Alfvén layer for thermal electrons. Figure 27*a* presents the location of the DPB according to *Gussenhoven et al.* [1981] for the various disturbance levels and boundaries of the Alfvén layer of thermal electrons at two values of the parameter γ. This parameter characterizes the inhomogeneity degree of the magnetospheric electric field (in the homogeneous field $\gamma = 1$). It is seen that the DPB coincides precisely with the boundary of convection of thermal plasma, which is transferred to the earth owing to the large-scale magnetospheric electric field, from the tail to the magnetospheric inside. In other words, the DPB coincides in practice with the plasmapause. The same conclusion was

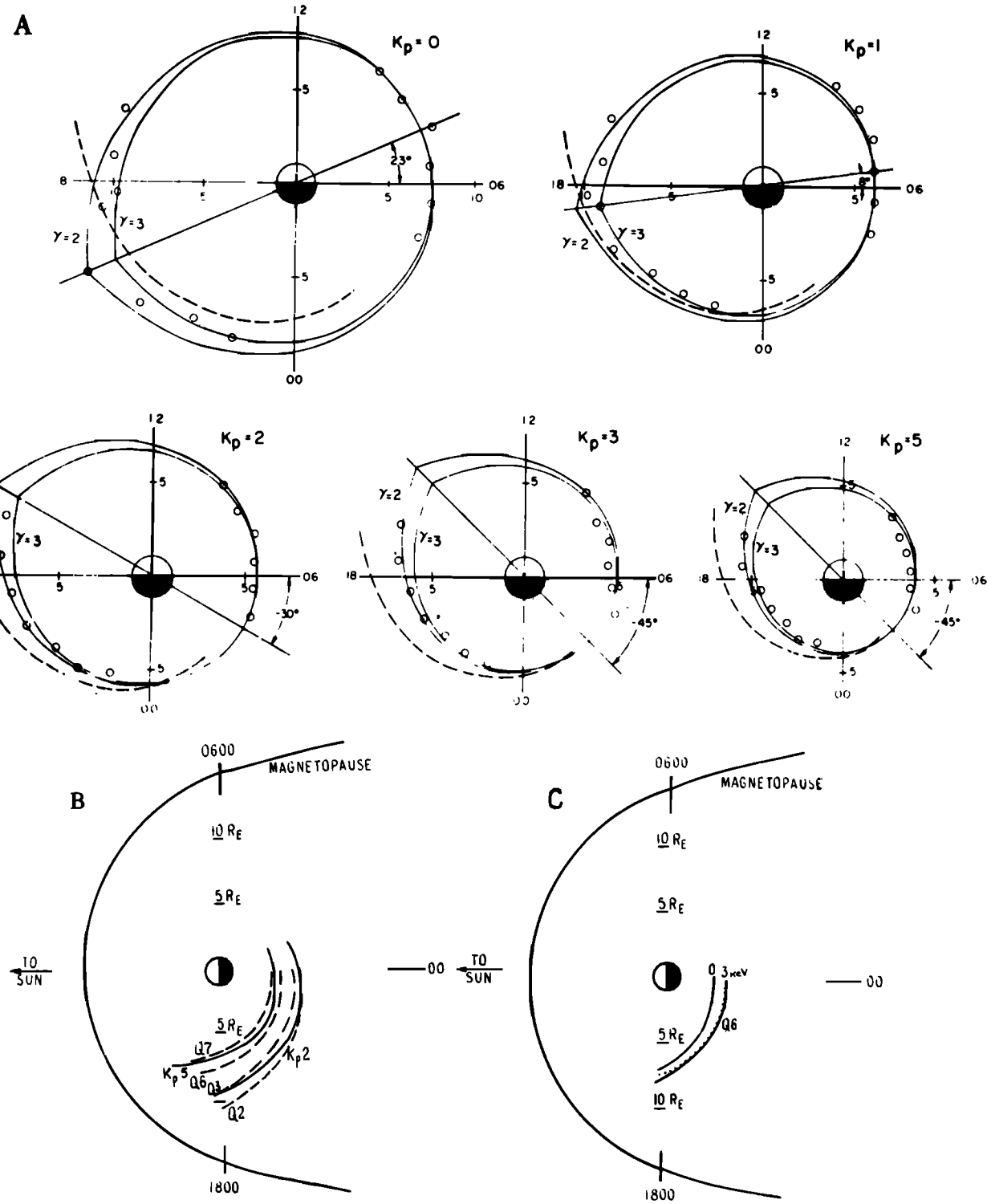

Fig. 27. (*a*) The comparison [*Gussenhoven et al.*, 1981] of the DPB position with the Alfvén layer of thermal electrons. The solid lines are the positions of the convection boundaries for various laws of the magnetospheric electrostatic potential variations with distance (the parameter γ). The circles show the DPB projection. (*b*) Comparison of the position of the equatorward boundary of the auroral oval in the dusk sector at various disturbance levels (Q) with the plasma injection boundary [*Mauk and McIlwain*, 1974] from the magnetospheric tail. (*c*) Comparison of the position of the equatorward boundary of the auroral oval in the dusk sector at $Q = 6$ with the boundary on $L = 6.6$ of the 0- and 3-keV electron convection from the magnetospheric tail. The convection boundaries are shown according to *Hultqvist et al.* [1982].

drawn by *Fontaine and Blanc* [1983] from a more rigorous theory of the Alfvén layer formation.

McIlwain [1974] and *Mauk and McIlwain* [1974] proposed the concept of an "injection boundary" as the region of the magnetospheric tail where hot plasma is originated (heated and/or accelerated) during a substorm. The particle measurements on board the geostationary satellite ATS 5 have shown that the local time of the observation of the boundary shifts

toward earlier local time (LT) with increasing Kp. If the observed dependence is presented analytically,

$$LT = 25.5 - 1.5\ Kp$$

then the geocentric location of the injection boundary L_b in earth radii is

$$L_b = \frac{122 - 10\ Kp}{LT - 7.3}$$

The data obtained simultaneously from three synchronously orbiting satellites were used by *Nagai* [1982] to obtain the relation $LT = 24.3 - 1.5\ Kp$ which is very close to the data of *Mauk and McIlwain* [1974].

Figure 27*b* presents the location of the injection boundary (the solid lines) in the equatorial plane of the magnetosphere in the dusk sector at $Kp = 2$ and $Kp = 5$ according to *Mauk and McIlwain* [1974]. During magnetically quiet periods ($Kp = 0$), the injection boundary is located outside the geostationary orbit, and therefore the above relation describes the L_b location inaccurately. Also shown are the equatorial boundaries of the auroral oval at a moderate (Q indices 2 and 3) and at a high (Q indices 6 and 7) magnetic disturbance (the thick dashed lines). From the figure it is seen that the injection boundary coincides, apparently, with the equatorward boundary of the auroral oval. Indeed, as the disturbance level gets higher, the two features shift to lower latitudes, i.e., the region of the origin approaches the earth in the equatorial cross section of the magnetosphere.

DPB is located near the convection boundary of zero-energy plasma particles (i.e., near the last closed equipotential which, in the steady state case, coincides with the plasmapause). The convection boundary increases its radial distance with increasing energy of the drifting particles [*Kivelson et al.*, 1979; *Hultqvist et al.*, 1982]. Therefore the boundary of the auroral oval in the night sector which, as was described above, is identified with the plasma sheet inner boundary projection onto the ionosphere altitudes, can be related to the convection boundary of the higher-energy plasma particles. Figure 27*c* shows the location of the convection boundary of the 0- to 3-keV electrons in the equatorial plane according to *Hultqvist et al.* [1982]. The electric field in the magnetospheric tail is assumed to be homogeneous; the stagnation point in the dusk sector is located at $L_0 = 7$ for electrons of zero energy. Also shown is the location of the auroral oval at $Q = 6$. It is seen how obediently the mean position of the oval boundary in the dusk sector follows the above described changes in the position of the kilovolt range electron convection boundary. The projection of the duskside diffuse luminescence region onto the magnetosphere is located in the equatorial plane (see Figure 27*c*) between the convection boundaries of electrons with energies of 0 and 3 keV. According to the diagram of Figure 21, it corresponds to the central plasma sheet location, but according to Figure 22 it corresponds to the remnant layer.

The inner boundary of the plasma sheet inferred from the 3-keV electron observations on board the geostationary satellite ATS 1 is mapped along magnetic field lines in the dusk sector onto the Harang discontinuity [*Zi-Min-Yun et al.*, 1982]. The location of the discontinuity was determined by measuring the ionospheric inhomogeneity drifts at the E layer altitudes with the STARE radar. Thus the Harang discontinuity in the dusk sector is aligned along the equatorward boundary of the auroral oval. The direct measurement data from GEOS 2 and DMSP have confirmed the earlier conclusion by *Galperin et al.* [1977] and *Jorjio et al.* [1978] that the plasmapause in the dusk and midnight sectors during disturbed periods is mapped onto the equatorward boundary of the diffuse auroral zone. Therefore the diffuse auroral luminescence is located between the projection of the plasma sheet inner boundary inferred from the ~3-keV electron measurements and the plasmapause projection onto ionospheric altitudes.

8. CONCLUSION

The planetary auroral pattern is the visual imprint of the complicated processes in hot and rarefied magnetospheric plasma.

Satellite measurements have yielded information about the large-scale pattern of high-energy particle precipitation from the plasma sheet to the ionosphere, about the associated luminosity of discrete and diffuse auroras, and about the large- and small-scale field-aligned currents related closely to the auroral events. The auroras and the field-aligned currents are characteristic of not only the earth's magnetosphere but also the magnetospheres of Jupiter, Saturn, and, probably, other giant planets. It was shown recently [*Gurevitch et al.*, 1983] that the field-aligned currents in pulsar magnetospheres also determined the magnetospheric form and that the associated electric fields determined the particle acceleration processes, thereby giving rise to peculiar "auroras."

Ever growing interest is being taken, therefore, in the study of the diverse signatures of particle acceleration processes in the earth's magnetosphere which give rise to the "auroral effects" observed in a broad band from X rays to radio waves but most clearly in the visible light band.

The latest studies of the precipitation of hot plasma particles from the outer magnetosphere to polar ionosphere have elucidated the spatial locations and the temporal dynamics of the main plasma domains in the circumterrestrial plasma. The present review is an attempt to systematize the auroral oval data bearing on (1) the energy of hot particle precipitation from the plasma sheet to the ionosphere and the integral brightness of auroras; (2) the relationship of the energy spectral shape of precipitating electrons to the types of auroras produced by such electrons, which makes it possible to obtain satellite determinations of the position of the boundary between diffuse precipitations and the discrete auroral oval; (3) the positions of the boundaries of typical particle precipitations and of relevant auroral luminosity depending on the geomagnetic activity indices and on the IMF vector; (4) the correspondence between typical auroras and the overlying plasma domains in the circumterrestrial space.

It has been concluded that the discrete auroral oval is the locus of projection of the most intensive field-aligned currents and relevant electric fields. The discrete auroral oval has also been shown to be the region of the highest mean energy flux supplied from the magnetosphere to the upper polar atmosphere in all its forms. The oval is located on the magnetic force tubes closed inside the magnetosphere and bordering, but positioned mainly outside, the stable trapping zone of the outer radiation belt high-energy particles. The force tubes of the oval are characterized by the absence of equipotentiality along them and by an anomalously low concentration of magnetospheric thermal plasma supplied from the polar ionosphere but somewhat lost in auroral acceleration processes. In quiet periods with the IMF B_Z component greater than 0, the

poleward boundaries of the diffuse precipitation zones recede far toward the poles, thereby limiting the polar caps to small areas and resulting in a comparatively small magnetic flux of "open" field lines (which extend far to the magnetospheric tail and are probably connected to the IMF). At higher activities, the oval extends to lower magnetic latitudes, so the polar cap inside the oval proves to be largely "open" and the multiple hot plasma injections from the plasma sheet fill the entire space up to the plasmapause, thereby leading to an intensification of the diffuse auroras whose time inertia is high.

The results described have been used to propose a set of generalized schemes of the earth's high-latitude regions which summarize the concepts concerning the spatial distribution of the auroras of various types, the relevant parameters of the high-energy particles precipitating into the atmosphere, the magnetospheric plasma domains as sources of such particles, and the large-scale hydrodynamic motions of the circumterrestrial plasma (convection) with the respective electric fields and currents penetrating the entire space near the earth. The set of the schemes may be considered as a certain proposed concept of magnetospheric structure during quiet and disturbed periods which is open to experimental verification.

Finally, a unified nomenclature of the appropriate regions and zones of high-energy particle precipitations, the types of auroras produced by them, the relevant magnetospheric plasma domains, and the boundaries between them is proposed with a view to describing the magnetospheric structure pattern (Table 3). The proposed nomenclature is aimed at ordering the description of experimental data, at facilitating their comparison in coordinated experiments (for example, when analyzing the IMS data base), and at assisting the theoretical and simulation, or model, studies in formalization of the circumterrestrial plasma parameters as measured by various research groups using different techniques. The authors would consider their task to be fufilled if the present review serves but one of these purposes.

Acknowledgments. The authors are indebted to L. M. Nikolaenko for her valuable assistance in processing and analyzing the AUREOL 1 and 2 data and to G. V. Gerasimova and L. I. Masyuk for their assistance in preparation of the manuscript. This review has been stimulated and written to a significant extent owing to G. Shepherd's kind attention.

REFERENCES

Ackerson, K. L., and L. A. Frank, Correlated satellite measurements of low-energy electron precipitation and ground-based observations of a visible auroral arc, *J. Geophys. Res., 77*, 1128–1136, 1972.

Afonina, R. G., B. A. Belov, V. Y. Gaidukov, N. I. Gershenson, A. E. Levitin, D. S. Faermark, and Y. I. Feldstein, Model of electric field at the meridian morning-evening in the north polar cap (in Russian), *Geomagn. Aeron., 22*, 519–522, 1982.

Ahn, B. H., R. M. Robinson, Y. Kamide, and S.-I. Akasofu, Electric conductivities, electric fields and auroral particle energy injection rate in the auroral ionosphere and their empirical relations to the horizontal magnetic disturbances, *Planet. Space Sci., 31*, 641–653, 1983*a*.

Ahn, B. H., S.-I. Akasofu, and Y. Kamide, Energy dissipation rates in the polar ionosphere, *J. Geophys. Res., 88*, 6275–6287, 1983*b*.

Akasofu, S.-I., The auroral oval, the auroral substorm, and their relations with the internal structure of the magnetosphere, *Planet. Space Sci., 14*, 587–595, 1966.

Akasofu, S.-I., *Polar and Magnetospheric Substorms*, D. Reidel, Hingham, Mass., 1968.

Akasofu, S.-I., Midday auroras and polar cap auroras, *Geofys. Publ., 29*, 73–85, 1972.

Akasofu, S.-I., A study of auroral displays photographed from the DMSP-2 satellite and from the Alaska meridian chain of stations, *Space Sci. Rev., 16*, 617–725, 1974*a*.

Akasofu, S.-I., Discrete, continuous and diffuse auroras, *Planet. Space Sci., 22*, 1723–1726, 1974*b*.

Akasofu, S.-I., Recent progress in studies of DMSP auroral photographs, *Space Sci. Rev., 19*, 169–215, 1976.

Akasofu, S.-I., *Physics of Magnetospheric Substorms*, D. Reidel, Hingham, Mass., 1977*a*.

Akasofu, S.-I., Magnetospheric substorms, *Q. J. R. Astron. Soc., 18*, 170–187, 1977*b*.

Akasofu, S.-I., Auroral arcs and auroral potential structure, in *Physics of Auroral Arc Formation, Geophys. Monogr. Ser.*, vol. 25, edited by S.-I. Akasofu and J. R. Kan, pp. 1–14, AGU, Washington, D. C., 1981*a*.

Akasofu, S.-I., Energy coupling between the solar wind and the magnetosphere, *Space Sci. Rev., 28*, 121–190, 1981*b*.

Akasofu, S.-I., and S. Chapman, *Solar-Terrestrial Physics*, Clarendon, Oxford, 1972.

Akasofu, S.-I., and J. R. Kan, Dayside and nightside auroral arc systems, *Geophys. Res. Lett., 7*, 753–756, 1980.

Akasofu, S.-I., and D. S. Kimball, Auroral morphology as shown by all-sky photographs: Arctic and Antarctic, *Ann. Int. Geophys. Year, 38*(1), 1965.

Akasofu, S.-I., and M. Roederer, Polar cap arcs and the open regions, *Planet. Space Sci., 31*, 193–196, 1983.

Akasofu, S.-I., D. S. Kimball, and C.-I. Meng, The auroral and polar magnetic substorms over Alaska, *Ann. Int. Geophys. Year, 45*(2), 1969.

Akasofu, S.-I., E. W. Hones, M. D. Montgomery, S. J. Bame, and S. Singer, Association of magnetotail phenomena with visible auroral features, *J. Geophys. Res., 76*, 5985–6003, 1971.

Akasofu, S.-I., D. N. Convey, and C.-I. Meng, Dependence of the geometry of the region of open field lines on the interplanetary magnetic field, *Planet. Space Sci., 29*, 803–807, 1981.

Alekseev, V. N., E. K. Zickratch, A. P. Mamrukov, L. D. Filippov, V. L. Khalipov, and I. V. Shalbaeva, Covariations of equatorial boundaries of F2S oblique ionospheric reflections and of diffuse emission of 6300 Å, in *Magnetospheric Substorm and Geophysical Events*, edited by V. P. Samsonov, pp. 23–31, Yakutsk Department, Academy of Sciences, Yakutsk, USSR, 1980.

Alekseeva, I. A., V. A. Sergeev, and A. G. Yakhnin, Characteristics of sporadic ionisation above the polar cap: Relationship with particle precipitations depending on IMF orientation, in *Geomagnetic Investigations*, no. 26, pp. 72–79, Sovietskoye Radio, Moscow, 1979.

Allen, J. H., C. C. Abston, and L. D. Morris, Auroral electrojet magnetic activity indices *AE*(11) for 1971, *Rep. UAG-39*, World Data Center A for Sol.-Terr. Phys., Boulder, Colo., 1975.

Anger, C. D., Photometric imaging of the aurora from the ISIS-2 satellite, in *Magnetospheric Study 1979*, pp. 1–5, Japanese International Magnetospheric Study Committee, Tokyo, 1979.

Anger, C. D., A. T. Y. Lui, and S.-I. Akasofu, Observations of the auroral oval and westward traveling surge from ISIS 2 satellite and Alaska meridian all-sky cameras, *J. Geophys. Res., 78*, 3020–3026, 1973.

Anger, C. D., M. C. Moshupi, D. D. Wallis, J. S. Murphree, L. H. Brace, and G. G. Shepherd, Detached auroral arcs in the trough region, *J. Geophys. Res., 83*, 2683–2689, 1978.

Anistratenko, A. A., and E. A. Ponomarev, Simulation of the formation conditions of particle precipitations and electric fields and currents in the nightside polar magnetosphere (in Russian), *Stud. Geomagn. Aeron. Sol. Phys. Moscow, 53*, 15–26, 1981.

Atkinson, G., Inverted V's and/or discrete arcs: A three-dimensional phenomenon at boundaries between magnetic flux tubes, *J. Geophys. Res., 87*, 1528–1534, 1982.

Atkinson, G., and D. Hutchison, Effect of the day-night ionospheric conductivity gradient on polar cap convective flow, *J. Geophys. Res., 83*, 725–729, 1978.

Aubry, M. P., M. G. Kivelson, R. L. McPherron, C. T. Russel, and D. S. Colburn, Outer magnetosphere near midnight at quiet and disturbed times, *J. Geophys. Res., 77*, 5487–5502, 1972.

Baumjohann, W., R. J. Pellinen, H. J. Opgenoorth, and E. Nielsen, Joint two-dimensional observations of ground magnetic and ionospheric electric fields associated with auroral zone currents: Current systems associated with local auroral break-ups, *Planet. Space Sci., 29*, 431–447, 1981.

Belousov, B. G., L. V. Lukina, and Y. I. Feldstein, Magnetic activity and aurora at Vostok station during the IQSY, *Sov. Antarct. Exped. Inf. Bull. Engl. Transl., 66*, 36–41, 1968.

Benkova, N. P., E. F. Kozlov, A. M. Mozhaev, N. K. Osipov, and N. I. Samorokin, The main ionospheric trough in the dayside sector by the data of vertical sounding (in Russian), *Geomagn. Aeron.*, *20*, 817–821, 1980.

Berkey, F. T., V. M. Driatsky, K. Henriksen, B. Hultqvist, D. H. Jelly, T. J. Shchuka, A. Theander, and J. Yliniemi, A synoptic investigation of particle precipitation dynamics for 60 substorms in IQSY (1964–1965) and IASY (1969), *Planet. Space Sci.*, *22*, 255–307, 1974.

Berkey, F. T., L. L. Cogger, and Y. Kamide, Evidence for a correlation between sun-aligned arcs and the interplanetary magnetic field direction, *Geophys. Res. Lett.*, *3*, 145–147, 1976.

Bond, F. R., and S.-I. Akasofu, Comparison of auroral oval from all-sky camera studies and from satellite photographs, *Planet. Space Sci.*, *27*, 541–549, 1979.

Bond, F. R., and I. L. Thomas, The southern auroral oval, *Aust. J. Phys.*, *24*, 97–102, 1971.

Buchau, J., G. J. Gassman, C. P. Pike, R. A. Wagner, and J. A. Whalen, Precipitation patterns in the arctic ionosphere determined from airborne observations, *Ann. Geophys.*, *28*, 443–455, 1972.

Burch, J. L., Precipitation of low-energy electrons at high latitudes: Effects of substorms, interplanetary magnetic field, and dipole tilt angle, *J. Geophys. Res.*, *77*, 6696–6705, 1972.

Burch, J. L., Effects of the interplanetary magnetic field on the auroral oval and plasmapause, *Space Sci. Rev.*, *23*, 449–464, 1979.

Burch, J. L., S. A. Fields, W. B. Hanson, K. A. Heelis, R. A. Hoffman, and R. W. Janetzke, Characteristics of auroral electron acceleration regions observed by Atmosphere Explorer C, *J. Geophys. Res.*, *81*, 2223–2230, 1976.

Burch, J. L., S. A. Fields, and R. A. Heelis, Polar cap electron acceleration regions, *J. Geophys. Res.*, *84*, 5863–5874, 1979.

Burke, W. J., Electric fields, Birkeland currents and electron precipitation in the vicinity of discrete auroral arcs, in *Physics of Auroral Arc Formation, Geophys. Monogr. Ser.*, vol. 25, edited by S.-I. Akasofu and J. R. Kan, pp. 164–172, AGU, Washington, D. C., 1981.

Burke, W. J., D. A. Hardy, F. J. Rich, M. C. Kelley, M. Smiddy, B. Shuman, R. C. Sagalyn, R. P. Vancour, P. J. L. Wildman, and S. T. Lai, Electrodynamic structure of the late evening sector of the auroral zone, *J. Geophys. Res.*, *85*, 1179–1193, 1980.

Burke, W. J., M. S. Gussenhoven, M. C. Kelley, D. A. Hardy, and F. J. Rich, Electric and magnetic field characteristics of discrete arcs in the polar cap, *J. Geophys. Res.*, *87*, 2431–2443, 1982.

Burrows, J. R., The plasma sheet in the evening sector, in *Magnetospheric Physics*, edited by B. M. McCormac, pp. 179–197, D. Reidel, Hingham, Mass., 1974.

Burrows, J. R., M. D. Wilson, and I. B. McDiarmid, Simultaneous field aligned current and charged particle measurements in the cleft, in *Magnetospheric Particles and Fields*, edited by B. M. McCormac, pp. 111–123, D. Reidel, Hingham, Mass., 1976.

Cambou, F., and Yu. I. Galperin, Resultats d'ensemble obtenus grace à l'experience ARCAD à bord du satellite AUREOLE, *Ann. Geophys.*, *30*, 9–19, 1974.

Cambou, F., and Yu. I. Galperin, Main results of the joint French-Soviet space project ARCAD-1 and ARCAD-2 for magnetospheric, auroral and ionospheric physics, *Ann. Geophys.*, *38*, 83–105, 1982.

Candidi, M., and C.-I. Meng, Nearly simultaneous observations of the conjugate polar cusp regions, *Planet. Space Sci.*, *32*, 41–46, 1984.

Candidi, M., H. W. Kroehl, and C.-I. Meng, Intensity distribution of dayside polar soft electron precipitation and the IMF, *Planet. Space Sci.*, *31*, 489–498, 1983.

Carpenter, D. L., C. G. Park, and T. P. Miller, A model of substorm electric fields in the plasmasphere based on whistler data, *J. Geophys. Res.*, *84*, 6559–6563, 1979.

Chernouss, S. A., Peculiarities of planetary distribution of pulsating auroras, in *Geomagnetic Research*, no. 21, edited by A. N. Zaitzev and V. O. Papitashvili, pp. 16–24, Sovietskoye Radio, Moscow, 1977.

Chiu, Y. T., and D. J. Gorney, Eddy intrusion of hot plasma into the polar cap and formation of polar cap arcs, *Geophys. Res. Lett.*, *10*, 463–466, 1983.

Chiu, Y. T., J. M. Cornwall, J. F. Fennell, D. J. Gorney, and P. F. Mizera, Auroral plasmas in the evening sector: Satellite observations and theoretical interpretations, *Space Sci. Rev.*, *35*, 211–257, 1983.

Cogger, L. L., Polar cap optical emissions observed from the ISIS2 satellite, in *Exploration of the Polar Upper Atmosphere*, edited by C. S. Deehr and J. A. Holtet, pp. 159–164, D. Reidel, Hingham, Mass., 1980.

Cogger, L. L., J. S. Murphree, S. Ismail, and C. D. Anger, Characteristics of dayside 5577 Å and 3914 Å aurora, *Geophys. Res. Lett.*, *4*, 413–416, 1977.

Coley, W. R., Spatial relationship of field-aligned currents, electron precipitation, and plasma convection in the auroral oval (abstract), *Eos Trans. AGU*, *64*, 439, 1983.

Cowley, S. W. H., Interpretation of observed relations between solar wind characteristics and effects at ionospheric altitudes, in *High Latitude Space Plasma Physics*, edited by B. Hultqvist and T. Hagfors, 225, Plenum, New York, 1983.

Craven, J. D., and L. A. Frank, Asymmetries in the instantaneous spatial distribution of auroral luminosities during substorms (abstract), *Eos Trans. AGU*, *18*, 300, 1983.

Craven, J. D., L. A. Frank, and K. L. Ackerson, Global observations of a SAR arc, *Geophys. Res. Lett.*, *9*, 961–964, 1982.

Cresswell, G. R., and T. N. Davis, Observations on pulsating auroras, *J. Geophys. Res.*, *71*, 3155–3163, 1966.

Creutzberg, F., Morphology and dynamics of the instantaneous auroral oval, in *Magnetospheric Particles and Fields*, edited by B. M. McCormac, pp. 235–246, D. Reidel, Hingham, Mass., 1976.

Creutzberg, F., and D. J. McEwen, Dynamics of the dayside aurora, *Adv. Space Res.*, *2*, 85–88, 1983.

Dandekar, B. S., Relationship between the IMF, the midday gap, and auroral substorm activity, *J. Geophys. Res.*, *84*, 4413–4421, 1979.

Danielsen, C., Auroral observations at Thule, 1961–1965, *Det. Dan. Meteorol. Inst.*, 6–9, 1969.

Danielsen, C., The dependence of auroral activity upon *Kp* as determined by the use of an extensive database, *Geofys. Medd. Dan. Meteorol. Inst.*, *60*, 1980.

Davis, T. N., The morphology of the polar aurora, *J. Geophys. Res.*, *65*, 3497–3502, 1960.

Davis, T. N., Negative correlation between polar cap visual aurora and magnetic activity, *J. Geophys. Res.*, *68*, 4447–4453, 1963.

Deehr, C. S., A. Egeland, K. Aarsnes, K. Amundsen, H. R. Lindalen, F. Soraas, R. Dalziel, P. A. Smith, G. R. Thomas, P. Stauning, H. Borg, G. Gustafsson, L. A. Holmgren, W. Riedler, J. Raitt, C. Skovli, T. Wedde, and R. Janetzke, Particle and auroral observations from the ESRO-1 auroral satellite, *J. Atmos. Terr. Phys.*, *35*, 1979–2011, 1973.

Deehr, C. S., J. D. Winningham, F. Yasuhara, and S.-I. Akasofu, Simultaneous observations of discrete and diffuse auroras by the ISIS 2 satellite and airborne instruments, *J. Geophys. Res.*, *81*, 5527–5535, 1976.

Deehr, C. S., G. G. Sivjee, A. Egeland, K. Henriksen, P. E. Sandholt, R. Smith, P. Sweeney, C. Duncan, and J. Gilmar, Ground-based observations of *F* region aurora associated with the magnetospheric cusp, *J. Geophys. Res.*, *85*, 2185–2192, 1980.

De Forest, S. E., and C. E. McIlwain, Plasma clouds in the magnetosphere, *J. Geophys. Res.*, *76*, 3587–3611, 1971.

Denholm, J. V., and F. R. Bond, Orientation of polar aurora, *Aust. J. Phys.*, *14*, 193–196, 1961.

Dolginov, Sh. Sh., Y. I. Feldstein, and L. V. Strunnikova, Effect of field-aligned currents in the polar cap at the recovery phase of a magnetic storm, *Planet. Space Sci.*, *29*, 1315–1318, 1981.

Dyachenko, V. A., V. J. Lazarev, M. V. Telzov, and V. M. Feigin, Structure of electron precipitations in polar regions (according to data of METEOR series of satellites), in *Upper Atmosphere Studies With the Aid of Space Vehicles*, edited by V. E. Tulinov, pp. 25–41, Hydrometeoizdat, Moscow, 1980.

Eather, R. H., Auroral proton precipitation and hydrogen emissions, *Rev. Geophys.*, *5*, 207–285, 1967.

Eather, R. H., Latitudinal distributions of auroral and airglow emissions: The "soft" auroral zone, *J. Geophys. Res.*, *74*, 153–158, 1969.

Eather, R. H., Advances in magnetospheric physics: Aurora, *Rev. Geophys.*, *13*, 925–943, 1975.

Eather, R. H., Auroral motions under the dayside cusp, paper presented at IAGA Assembly, Int. Assoc. of Geomagn. and Aeron., Edinburgh, 1981.

Eather, R. H., and S.-I. Akasofu, Characteristics of polar cap auroras, *J. Geophys. Res.*, *74*, 4794–4798, 1969.

Eather, R. H., and S. B. Mende, Airborne observations of auroral precipitation patterns, *J. Geophys. Res.*, *76*, 1746–1755, 1971.

Eather, R. H., and S. B. Mende, High latitude particle precipitation and source regions in the magnetosphere, in *Magnetosphere-Ionosphere Interactions*, edited by K. Folkestad, pp. 139–154, Universitetsforlaget, Oslo, 1972.

Eather, R. H., S. B. Mende, and R. J. K. Judge, Plasma injection at synchronous orbit and spatial and temporal auroral morphology, *J. Geophys. Res.*, *81*, 2805–2824, 1976.

Eather, R. H., S. B. Mende, and E. J. Weber, Dayside aurora and relevance to substorm current systems and dayside merging, *J. Geophys. Res.*, *84*, 3339–3359, 1979.

Egeland, A., K. Henriksen, P. E. Sandholt, C. S. Deehr, and G. G.

Sivjee, Dayside cusp aurora—characteristics and problems, paper presented at the Y-th ESA-PAC Symposium, European Space Agency, Bournemouth, United Kingdom, April 14–18, 1980.

Evans, D. S., Evidence for the low altitude acceleration of auroral particles, in *Physics of the Hot Plasma in the Magnetosphere*, edited by B. Hultqvist and L. Stenflo, pp. 319–340, Plenum, New York, 1976.

Evans, D. S., and T. E. Moore, Precipitating electrons associated with the diffuse aurora: Evidence for electrons of atmospheric origin in the plasma sheet, *J. Geophys. Res.*, *84*, 6451–6457, 1979.

Evlashin, L. S., On the relation between several types of auroras and absorption of radiowaves in the ionosphere, in *Geophysical Events in the Auroral Zone*, edited by B. E. Brunelli, pp. 74–84, Nauka, Leningrad, USSR, 1971.

Evlashin, L. S., and L. N. Evlashina, On the problem of space-time distribution of auroral luminescence, in *Aurora and Airglow*, no. 28, edited by S. I. Isaev, Y. A. Nadubovich, and L. S. Evlashin, pp. 24–27, Nauka, Moscow, 1981.

Fairfield, D. H., Magnetic field signatures of substorms on high-latitude field lines in the nighttime magnetosphere, *J. Geophys. Res.*, *78*, 1553–1562, 1973.

Fairfield, D. H., and G. D. Mead, Magnetospheric mapping with a quantitative geomagnetic field model, *J. Geophys. Res.*, *80*, 535–542, 1975.

Fairfield, D. H., and A. F. Vinas, The inner edge of the electron plasma sheet: Where and why, *Eos Trans. AGU*, *64*, 297, 1983.

Feldstein, Y. I., Geographical distribution of aurorae and azimuth of auroral arcs, in *Investigations of the Aurorae*, no. 4, edited by B. A. Bagarjatsky, pp. 61–78, Academy of Sciences of the USSR, Moscow, 1960.

Feldstein, Y. I., Aurorae and magnetic activity in the near-pole region (in Russian), *Geomagn. Aeron.*, *2*, 851–854, 1962.

Feldstein, Y. I., On morphology of aurorae and magnetic disturbances in high latitudes (in Russian), *Geomagn. Aeron.*, *3*, 227–239, 1963*a*.

Feldstein, Y. I., The morphology of aurorae and geomagnetism, in *Aurorae and Airglow*, no. 10, edited by B. A. Bagarjatsky and V. I. Krasovsky, pp. 121–125, Academy of Sciences of the USSR, Moscow, 1963*b*.

Feldstein, Y. I., Peculiarities in aurora and magnetic disturbances distribution in high latitudes caused by the asymmetrical form of the magnetosphere, *Planet. Space Sci.*, *14*, 121–130, 1966.

Feldstein, Y. I., Polar auroras, polar substorms, and their relations with the dynamics of the magnetosphere, *Rev. Geophys.*, *7*, 179–218, 1969.

Feldstein, Y. I., Auroras and associated phenomena, in *Solar-Terrestrial Physics/1970*, edited by E. R. Dyer, pp. 152–191, D. Reidel, Hingham, Mass., 1972.

Feldstein, Y. I., The auroral oval, *J. Geophys. Res.*, *78*, 1210–1213, 1973.

Feldstein, Y. I., Night-time aurora and its relation to the magnetosphere, *Ann. Geophys.*, *30*, 259–272, 1974.

Feldstein, Y. I., Auroral oval and magnetospheric cusps, in *Aurora and Airglow*, no. 22, edited by V. I. Krasovsky, pp. 77–99, Sovietskoye Radio, Moscow, 1975.

Feldstein, Y. I., Global features of aurorae, advances in science and technology, in *Geomagnetism and Upper Atmosphere*, no. 4, edited by N. P. Benkova and A. D. Driving, Nauka, Moscow, 1978.

Feldstein, Y. I., and E. K. Solomatina, Aurorae in the southern hemisphere (in Russian), *Geomagn. Aeron.*, *1*, 534–539, 1961.

Feldstein, Y. I., and G. V. Starkov, Dynamics of auroral belt and polar geomagnetic disturbances, *Planet. Space Sci.*, *15*, 209–229, 1967.

Feldstein, Y. I., and G. V. Starkov, Auroral oval in the IGY and IQSY period and a ring current in the magnetosphere, *Planet. Space Sci.*, *16*, 129–133, 1968.

Feldstein, Y. I., and G. V. Starkov, The auroral oval and the boundary of closed field lines of geomagnetic field, *Planet. Space Sci.*, *18*, 501–508, 1970.

Feldstein, Y. I., and G. V. Starkov, Auroral oval planetary energetics, *J. Atmos. Terr. Phys.*, *33*, 197–203, 1971.

Feldstein, Y. I., and N. G. Vorfolomeeva, Distribution of auroras and large-scale field-aligned currents in the magnetosphere for different orientations of IMF, in *Solar Wind and Magnetospheric Investigations*, edited by A. E. Levitin, pp. 110–115, Izmiran, Moscow, 1980.

Feldstein, Y. I., L. V. Lukina, and B. G. Belousov, Auroral arc motions in polar cap, *Sov. Antarct. Exped. Inf. Bull. Engl. Transl.*, *69*, 50–53, 1968.

Feldstein, Y. I., S. I. Isaev, and A. I. Lebedinsky, The phenomenology and morphology of aurorae, *Ann. IQSY*, *4*, 311–348, 1969.

Feldstein, Y. I., G. V. Starkov, and V. L. Zverev, Conjugacy of auroral oval, in *Proceedings of the Antarctic Review Meeting*, edited by T. Nagata, pp. 29–38, Tokyo, 1974.

Feldstein, Y. I., Yu. I. Galperin, L. M. Nikolaenko, T. E. Valchuk, J. Crasnier, and J. A. Sauvaud, Latitudinal structure of auroral emission and soft electron energy spectra above the auroral ionosphere in relation to the plasma sheet structure in the premidnight sector, in *Programme and Abstracts of the XVII General Assembly of the IUGG, Canberra, Australia*, p. 302, International Union of Geodesy and Geophysics, Paris, 1979.

Filippov, L. D., A. P. Mamrukov, I. V. Shalbaeva, A. M. Novikov, and V. F. Smirnov, Zones of inhomogeneous anomalous ionisation in high-latitude ionospheric *F*-region from a chain of vertical and oblique sounding stations, in *Magnetospheric Substorm and Geophysical Phenomena*, edited by V. P. Samsonov, pp. 32–42, Yakutsk Department, Academy of Sciences, Yakutsk, USSR, 1980.

Fjodorova, N. I., and R. Knuth, *Study of an Ionospheric Bay Disturbance in Correlation With High-Energy Electron Measurements on Satellite Cosmos-348*, edited by M. J. Rycroft and A. C. Stickland, Pergamon, New York, 1978.

Fontaine, D., and M. Blanc, A theoretical approach to the morphology and dynamics of diffuse auroral zones, *J. Geophys. Res.*, *88*, 7171–7184, 1983.

Foster, J. C., and J. R. Burrows, Electron fluxes over the polar cap, 1, Intense keV fluxes during poststorm quieting, *J. Geophys. Res.*, *81*, 6016–6036, 1976.

Foster, J. C., G. S. Stiles, and J. R. Doupnik, Radar observations of cleft dynamics, *J. Geophys. Res.*, *85*, 3453–3460, 1980.

Frank, L. A., On the extraterrestrial ring current during geomagnetic storms, *J. Geophys. Res.*, *72*, 3753–3767, 1967.

Frank, L. A., Relationship of the plasma sheet, ring current, trapping boundary, and plasmapause near the magnetic equator and local midnight, *J. Geophys. Res.*, *76*, 2265–2275, 1971*a*.

Frank, L. A., Comments on a proposed magnetospheric model, *J. Geophys. Res.*, *76*, 2512–2515, 1971*b*.

Frank, L. A., Magnetospheric and auroral plasmas: A short survey of progress, *Rev. Geophys.*, *13*, 974–989, 1975.

Frank, L. A., and K. L. Ackerson, Observations of charged particle precipitation into the auroral zone, *J. Geophys. Res.*, *76*, 3612–3643, 1971.

Frank, L. A., and K. L. Ackerson, Local-time survey of plasma at low altitudes over the auroral zones, *J. Geophys. Res.*, *77*, 4116–4127, 1972.

Frank, L. A., N. A. Saflekos, and K. L. Ackerson, Electron precipitation in the postmidnight sector of the auroral zones, *J. Geophys. Res.*, *81*, 155–167, 1976.

Frank, L. A., J. D. Craven, K. L. Ackerson, M. R. English, R. H. Eather, and R. L. Carovillano, Global auroral imaging instrumentation for the Dynamics Explorer mission, *Space Sci. Instrum.*, *5*, 369–393, 1981*a*.

Frank, L. A., R. L. McPherron, R. J. DeCoster, B. G. Burek, K. L. Ackerson, and C. T. Russell, Field-aligned currents in the earth's magnetotail, *J. Geophys. Res.*, *86*, 687–700, 1981*b*.

Frank, L. A., J. D. Craven, J. L. Burch, and J. D. Winningham, Polar views of the earth's aurora with Dynamics Explorer, *Geophys. Res. Lett.*, *9*, 1001–1004, 1982*a*.

Frank, L. A., J. D. Craven, and E. J. Smith, Dynamical properties of theta auroras and their relationship to the interplanetary magnetic field (abstract), *Eos Trans. AGU*, *63*, 1056, 1982*b*.

Frank, L. A., J. D. Craven, J. L. Burch, and J. D. Winningham, Properties of theta auroras and implications for magnetotail dynamics, in *XVIII General Assembly of the IUGG, Programme and Abstracts, IAGA Bull. 48*, p. 381, Hamburg, Federal Republic of Germany, 1983.

Frank, L. A., C. Y. Huang, and T. E. Eastman, Currents in the earth's magnetotail, in *Magnetospheric Currents, Geophys. Monogr. Ser.*, vol. 28, edited by T. A. Potemra, pp. 147–157, AGU, Washington, D. C., 1984.

Frederick, J. E., and P. B. Hays, Magnetic ordering of the polar airglow, *Planet. Space Sci.*, *26*, 339–345, 1978.

Fukunishi, H., Dynamic relationship between proton and electron auroral substorm, *J. Geophys. Res.*, *80*, 553–574, 1975.

Galperin, Y. I., and H. Reme, Soviet-French project ARCAD-3 for studies of magnetosphere-ionosphere processes, in *Program and Abstracts of the International Symposium on the Physics of the Earth's Ionosphere, Magnetosphere and the Solar Wind*, p. 36, USSR, 1983.

Galperin, Y. I., et al., Suprathermal plasma and energetic particle measurements aboard the AUREOL-3 satellite, *Ann. Geophys.*, *38*, 583–592, 1982*a*.

Galperin, Y. I., et al., The ARCAD-3 project, *Ann. Geophys., 38*, 543–552, 1982*b*.

Galperin, Yu. I., Proton bombardment in aurora, *Planet. Space Sci., 10*, 187–193, 1963.

Galperin, Yu. I., N. V. Jorjio, I. D. Ivanov, I. P. Karpinski, E. L. Lein, R. A. Kovrazhkin, T. N. Muliarchik, B. V. Polenov, V. V. Temni, N. I. Fedorova, B. I. Khazanov, A. V. Shifrin, and F. K. Shuiskaia, Studies of geoeffective corpuscules, and photoelectrons on the COSMOS-261 satellite (in Russian), *Cosmic Res., 8*, 108–119, 1970.

Galperin, Yu. I., J. Crasnier, Yu. V. Lissakov, L. M. Nikolaenko, V. M. Sinitsin, J. A. Sauvaud, and V. L. Khalipov, Diffuse auroral zone, 1, Model of the equatorial border of diffuse auroral electron precipitation zone in the evening and near midnight sectors (in Russian), *Cosmic Res., 15*, 421–432, 1977.

Galperin, Yu. I., V. N. Ponomarev, and A. G. Zosimova, Equatorial ionospheric anomaly and interplanetary magnetic field, *J. Geophys. Res., 83*, 4265–4272, 1978.

Galperin, Yu. I., A. G. Zosimova, T. N. Larina, A. M. Mozhaev, N. K. Osipov, and Yu. N. Ponomarev, Variations in the structure of polar ionospheric *F*-region related to the sign reversal of the *Y*-component of IMF: Svalgaard-Mansurov effect in ionosphere (in Russian), *Cosmic Res., 18*, 877–898, 1980.

Gault, W. A., R. A. Koehler, R. Link, and G. G. Shepherd, Observations of the optical spectrum of the dayside magnetospheric cleft aurora, *Planet. Space Sci., 29*, 321–333, 1981.

Ghielmetti, A. G., R. G. Johnson, R. D. Sharp, and E. G. Shelly, The latitudinal, diurnal, and altitudinal distributions of upward flowing energetic ions of ionospheric origin, *Geophys. Res. Lett., 5*, 59–62, 1978.

Gogoshev, M. M., N. P. Petkov, Ts. N. Gogosheva, I. K. Nedkov, B. P. Komitov, S. H. Spassov, and K. B. Serafimov, Fine structure of South Pole oval during strong geomagnetic storm, *C. R. Acad. Bulg. Sci. 34*, 347–349, 1981*a*.

Gogoshev, M. M., N. P. Petkov, K. B. Serafimov, St. I. Sargoichev, Ts. N. Gogosheva, and B. P. Komitov, Optical investigations of magnetospheric-ionospheric coupling by using data from the Intercosmos-19 satellite, *Adv. Space Res., 1*, 193–196, 1981*b*.

Gurevitch, A. V., V. S. Beskin, and Yu. N. Istomin, Electrodynamics of the pulsars' magnetosphere (in Russian), *J. Exp. Theor. Phys. USSR, 85*, 401–433, 1983.

Gussenhoven, M. S., Extremely high latitude auroras, *J. Geophys. Res., 87*, 2401–2412, 1982.

Gussenhoven, M. S., D. A. Hardy, and W. J. Burke, Comment on "Diurnal variation of the auroral oval size" by C.-I. Meng, *J. Geophys. Res., 85*, 2373–2374, 1980.

Gussenhoven, M. S., D. A. Hardy, and W. J. Burke, DMSP/F2 electron observations of equatorward auroral boundaries and their relationship to magnetospheric electric fields, *J. Geophys. Res., 86*, 768–778, 1981.

Gussenhoven, M. S., D. A. Hardy, and N. Heinemann, Systematics of the equatorward diffuse auroral boundary, *J. Geophys. Res., 88*, 5692–5708, 1983.

Haerendel, G., The distant magnetosphere: Reconnection in the boundary layers, cusps and tail lobes, in *Exploration of the Polar Upper Atmosphere*, edited by C. S. Deehr and J. A. Holtet, pp. 219–228, D. Reidel, Hingham, Mass., 1980.

Hardy, D. A., W. J. Burke, M. S. Gussenhoven, N. Heinemann, and E. Holeman, DMSP/F2 electron observations of equatorward auroral boundaries and their relationship to the solar wind velocity and the north-south component of the interplanetary magnetic field, *J. Geophys. Res., 86*, 9961–9974, 1981.

Hardy, D. A., W. J. Burke, and M. S. Gussenhoven, DMSP optical and electron measurements in the vicinity of polar cap arcs, *J. Geophys. Res., 87*, 2413–2430, 1982.

Harel, M., R. A. Wolf, R. W. Spiro, P. H. Reiff, C.-K. Chen, W. J. Burke, F. J. Rich, and M. Smiddy, Quantitative simulation of a magnetospheric substorm, 2, Comparison with observations, *J. Geophys. Res., 86*, 2242–2260, 1981.

Hartz, T. R., Particle precipitation patterns, in *The Radiating Atmosphere*, edited by B. M. McCormac, pp. 225–238, D. Reidel, Hingham, Mass., 1971.

Hartz, T. R., and N. M. Brice, The general pattern of auroral particle precipitation, *Planet. Space Sci., 15*, 301–311, 1967.

Heelis, R. A., W. B. Hanson, and J. L. Burch, Ion convection velocity reversals in the dayside cleft, *J. Geophys. Res., 81*, 3803–3809, 1976.

Heelis, R. A., J. D. Winningham, W. B. Hanson, and J. I. Burch, The relationships between high-latitude convection reversals and the energetic particle morphology observed by Atmospheric Explorer, *J. Geophys. Res., 85*, 3315–3324, 1980.

Hill, V. J., D. S. Evans, and W. M. Retallack, A near real-time computer display showing the geographic location and intensity of auroral precipitation using TIROS/NOAA satellite observations (abstract), *Eos Trans. AGU, 63*, 1052, 1982.

Hoffman, R. A., Properties of low energy particle impacts in the polar domain in the dawn and dayside hours, in *Magnetosphere-Ionosphere Interactions*, edited by K. Folkestad, pp. 117–138, Universitetsforlaget, Oslo, 1972.

Holzworth, R. H., and C.-I. Meng, Mathematical representation of the auroral oval, *Geophys. Res. Lett., 2*, 377–380, 1975.

Hones, E. W., Review and interpretation of particle measurements made by Vela satellites in the magnetotail, in *Physics of the Magnetosphere*, edited by R. L. Carovillano, J. F. McCley, and H. R. Radoski, pp. 392–408, D. Reidel, Hingham, Mass., 1968.

Hones, E. W., J. R. Asbridge, S. J. Bame, and S. Singer, Energy spectra and angular distributions of particles in the plasma sheet and their comparison with rocket measurements over the auroral zone, *J. Geophys. Res., 76*, 63–87, 1971.

Horwitz, J. L., W. K. Cobl, C. R. Baugher, C. R. Chappell, L. A. Frank, T. E. Eastman, R. R. Anderson, E. G. Shelley, and D. T. Young, On the relationship of the plasmapause to the equatorward boundary of the auroral oval and to the inner edge of the plasma sheet, *J. Geophys. Res., 87*, 9059–9069, 1982.

Horwitz, J. L., J. Turnley, M. O. Chandler, C. R. Chappell, T. Nagai, J. D. Craven, L. A. Frank, S. D. Shawhan, J. L. Burch, J. D. Winningham, and D. W. Slater, Comparison of observed plasma boundaries in the inner magnetosphere (abstract), *Eos Trans. AGU, 64*, 296, 1983.

Hultqvist, B., Rocket and satellite observations of energetic particle precipitation in relation to optical aurora, *Ann. Geophys., 30*, 223–257, 1974.

Hultqvist, B., The aurora, in *The Magnetospheres of the Earth and Jupiter*, edited by V. Formisano, pp. 77–111, D. Reidel, Hingham, Mass., 1975*a*.

Hultqvist, B., The aurora, *Space Sci. Rev., 17*, 787–821, 1975*b*.

Hultqvist, B., H. Borg, L. A. Holmgren, H. Reme, A. Bahnsen, M. Jespersen, and G. Kremser, Quiet-time convection electric field properties derived from keV electron measurements at the inner edge of the plasma sheet by means of GEOS-2, *Planet. Space Sci., 30*, 261–283, 1982.

Ievenko, I. B., and V. P. Samsonov, Preliminary observational results of poleward auroral surge dynamics as seen in particular emissions, in *Bulletin of Science-Technical Information, Geophysical Problems*, edited by G. V. Shafer, pp. 19–23, Yakutsk Department, Academy of Sciences, Yakutsk, USSR, 1982.

Iijima, T., and T. A. Potemra, Large-scale characteristics of field-aligned currents associated with substorms, *J. Geophys. Res., 83*, 599–615, 1978.

Isaev, S. I., and M. I. Pudovkin, *Auroras and the Earth's Magnetospheric Processes*, 244 pp., Nauka, Leningrad, USSR, 1972.

Ismail, S., and C.-I. Meng, A classification of polar cap auroral arcs, *Planet. Space Sci., 30*, 319–330, 1982.

Ismail, S., D. D. Wallis, and L. L. Cogger, Characteristics of polar cap sun-aligned arcs, *J. Geophys. Res., 82*, 4741–4749, 1977.

Jorjio, N. V., Electrophotometrical measurements in the auroral zone, in *Spectral, Electrophotometrical and Radar Research of Aurora and Airglow*, edited by V. I. Krassovsky, no. 1, pp. 30–40, Academy of Sciences, Moscow, 1959.

Jorjio, N. V., J. Crasnier, J. A. Sauvaud, and V. M. Sinitsin, Auroral diffuse zone, III (in Russian), *Cosmic Res., 16*, 1978–1985, 1978.

Kamide, Y., and G. Rostoker, The spatial relationship of field-aligned currents and auroral electrojets to the distributions of nightside auroras, *J. Geophys. Res., 82*, 5589–5608, 1977.

Kamide, Y., and J. D. Winningham, A statistical study of the "instantaneous" nightside auroral oval: The equatorward boundary of electron precipitation as observed by the ISIS 1 and ISIS 2 satellites, *J. Geophys. Res., 82*, 5573–5588, 1977.

Kaneda, E., Auroral TV observation by KYOKKO, in *Magnetospheric Study 1979*, pp. 15–19, Japanese International Magnetospheric Study Committee, Tokyo, 1979.

Khalipov, V. L., Yu. I. Galperin, J. Crasnier, Yu. V. Lissakov, L. M. Nikolaenko, V. M. Sinitsin, and J. A. Sauvaud, Auroral diffuse zone, II, Formation and dynamics of the polar cliff of the ionospheric subauroral main trough in the evening auroral zone (in Russian), *Cosmic Res., 15*, 708–717, 1977.

Khalipov, V. L., L. D. Sivtzeva, A. E. Stepanov, and L. M. Nikolaenko, Structure of ionospheric *F*-region at latitude of the main trough in the morning sector, in *Complex Studies of Auroral Ionosphere*, edited by L. D. Sivtzeva, pp. 3–14, Yakutsk Department, Academy of Sciences, Yakutsk, USSR, 1983.

Khorosheva, O. V., On the space-time distribution of aurorae in the

Arctic during the winter 1957–1958, in *Aurorae and Airglow*, edited by B. A. Bagarjatsky, no. 7, pp. 14–21, Academy of Sciences, Moscow, 1961*a*.

Khorosheva, O. V., About the connection of high-latitudinal geomagnetic disturbances with aurorae (in Russian), *Geomagn. Aeron.*, *1*, 695–701, 1961*b*.

Khorosheva, O. V., Diurnal drift of the auroral closed ring (in Russian), *Geomagn. Aeron.*, *2*, 839–850, 1962.

Khorosheva, O. V., On the isochasms of aurorae, in *Aurorae and Airglow*, edited by B. A. Bagarjatsky and V. I. Krassovsky, no. 10, pp. 126–132, Academy of Sciences, Moscow, 1963.

King, J. H., Interplanetary medium data book—appendix, Natl. Space Sci. Data Center, NASA Goddard Space Flight Center, Greenbelt, Md., 1977.

Kintner, P. M., K. L. Ackerson, D. A. Gurnett, and L. A. Frank, Correlated electric field and low-energy electron measurements in the low-altitude polar cusp, *J. Geophys. Res.*, *83* 163–168, 1978.

Kivelson, M. G., S. M. Kaye, and D. J. Southwood, The physics of plasma injection events, in *Dynamics of the Magnetosphere*, edited by S.-I. Akasofu, pp. 385–394, D. Reidel, Hingham, Mass., 1979.

Klumpar, D. M., Relationships between auroral particle distributions and magnetic field perturbations associated with field-aligned currents, *J. Geophys. Res.*, *84*, 6524–6532, 1979.

Klumpar, D. M., ISIS observations of auroral particles and large scale Birkeland currents, in *Exploration of the Polar Upper Atmosphere*, edited by C. S. Deehr and J. A. Holtet, pp. 329–336, D. Reidel, Hingham, Mass., 1980.

Kvifte, G. J., and H. Pettersen, Morphology of the pulsating aurora, *Planet. Space Sci.*, *17*, 1599–1607, 1969.

Lassen, K., Geographical distribution and temporal variations of polar aurorae, *Publ. Dan. Meteorol. Inst.*, *16*, 5–79, 1953.

Lassen, K., On the classification of high latitude auroras, *Geofys. Publ.*, *29*, 87–104, 1972.

Lassen, K., Relation of the plasma sheet to the nighttime auroral oval, *J. Geophys. Res.*, *79*, 3857–3858, 1974.

Lassen, K., The quiet-time pattern of auroral arcs as a consequence of magnetospheric convection, *Geophys. Res. Lett.*, *6*, 777–780, 1979.

Lassen, K., and C. Danielsen, Quiet time pattern of auroral arcs for different directions of the interplanetary magnetic field in the *Y-Z* plane, *J. Geophys. Res.*, *83*, 5277–5284, 1978.

Lassen, K., C. Danielsen, and V. Singh, Diffuse and discrete optical emissions at the poleward border of the morning auroral oval, *Geophys. Pap. R-66*, pp. 1–6, Dan. Meteorol. Inst., Copenhagen, 1981.

Levitin, A. E., R. G. Afonina, B. A. Belov, and Y. I. Feldstein, Geomagnetic variation and field-aligned currents at northern high-latitudes, and their relations to the solar wind parameters, *Philos. Trans. R. Soc. London, Ser. A*, *304*, 253–301, 1982.

Lin, C. S., and R. A. Hoffman, Characteristics of the inverted-V event, *J. Geophys. Res.*, *84*, 1514–1524, 1979.

Lui, A. T. Y., and C. D. Anger, A uniform belt of diffuse auroral emission seen by the ISIS 2 scanning photometer, *Planet. Space Sci.*, *21*, 799–809, 1973.

Lui, A. T. Y., and J. R. Burrows, On the location of auroral arcs near substorm onset, *J. Geophys. Res.*, *83*, 3342–3348, 1978.

Lui, A. T. Y., P. Perreault, S.-I., Akasofu, and C. D. Anger, The diffuse aurora, *Planet. Space Sci.*, *21*, 857–861, 1973.

Lui, A. T. Y., C. D. Anger, D. Venkatesan, W. Sawchuk, and S.-I. Akasofu, The topology of the auroral ovals seen by the ISIS 2 scanning auroral photometer, *J. Geophys. Res.*, *80*, 1795–1804, 1975*a*.

Lui, A. T. Y., C. D. Anger, and S.-I. Akasofu, The equatorial boundary of the diffuse aurora and auroral substorms as seen by the ISIS 2 auroral scanning photometer, *J. Geophys. Res.*, *80*, 3603–3614, 1975*b*.

Lui, A. T. Y., D. Venkatesan, C. D. Anger, S.-I. Akasofu, W. J. Heikkila, J. D. Winningham, and J. R. Burrows, Simultaneous observations of particle precipitations and auroral emissions by the ISIS 2 satellite, *J. Geophys. Res.*, *82*, 2210–2226, 1977.

Lui, A. T. Y., C.-I. Meng, and S. Ismail, Large-amplitude undulations of the equatorward boundary of the diffuse aurora, *J. Geophys. Res.*, *87*, 2385–2400, 1982.

Lyatsky, V. B., *The Current Systems of Magnetosphere-Ionosphere Disturbances*, Nauka, Leningrad, USSR, 1978.

Lyatsky, V. B., About the distribution of the aurorae (in Russian), *Geomagn. Aeron.*, *22*, 149–151, 1982.

Maehlum, B. N., Universal time control of the low-energy electron fluxes in the polar regions, *J. Geophys. Res.*, *73*, 3459–3468, 1968.

Maezawa, K., Magnetospheric convection induced by the positive and negative *Z* components in the interplanetary magnetic field: Quantitative analysis using polar cap magnetic records, *J. Geophys. Res.*, *81*, 2289–2303, 1976.

Makita, K., and C.-I. Meng, The average electron precipitation pattern during extremely quiet times and its dependence on the magnetospheric substorm (abstract), *Eos Trans. AGU*, *63*, 1066, 1982.

Makita, K., C.-I. Meng, and S.-I. Akasofu, Comparison of the auroral electron precipitations in the northern and southern conjugate regions by two DMSP satellites, in *Proceedings of the V Symposium on Coordination and Observation of the Ionosphere and Magnetosphere in the Polar Regions, Spec. Issue 26*, pp. 149–159, National Institute of Polar Research, Tokyo, 1983.

Mauk, B. H., and C. E. McIlwain, Correlation of *Kp* with the substorm-injected plasma boundary, *J. Geophys. Res.*, *79*, 3193–3196, 1974.

Mawson, D., Records of the aurora polaris, *Sci. Rep. Aust. Antarct. Exped.*, *2*, 1, 1925.

McDiarmid, I. B., and J. R. Burrows, Local time asymmetries in the high-latitude boundary of the outer radiation zone for the different electron energies, *Can. J. Phys.*, *46*, 49–57, 1968.

McDiarmid, I. B., J. R. Burrows, and E. E. Budzinsky, Average characteristics of magnetospheric electrons (150 eV to 200 keV) at 1400 km, *J. Geophys. Res.*, *80*, 73–79, 1975.

McDiarmid, I. B., J. R. Burrows, and E. E. Budzinsky, Particle properties in the dayside cleft, *J. Geophys. Res.*, *81*, 221–226, 1976.

McDiarmid, I. B., J. R. Burrows, and M. D. Wilson, Comparison of magnetic field perturbations at high latitudes with charged particle and IMF measurements, *J. Geophys. Res.*, *83*, 681–688, 1978.

McDiarmid, I. B., J. R. Burrows, and M. D. Wilson, Large-scale magnetic field perturbations and particle measurements at 1400 km on the dayside, *J. Geophys. Res.*, *84*, 1431–1441, 1979.

McDiarmid, I. B., J. R. Burrows, and M. D. Wilson, Comparison of magnetic field perturbations and solar electron profiles in the polar cap, *J. Geophys. Res.*, *85*, 1163–1170, 1980.

McIlwain, C. E., Substorm injection boundaries, in *Magnetospheric Physics*, edited by B. McCormac, pp. 143–154, D. Reidel, Hingham, Mass., 1974.

Mead, G. D., and D. N. Fairfield, A quantitative magnetospheric model derived from spacecraft magnetometer data, *J. Geophys. Res.*, *80*, 523–532, 1975.

Mende, S. B., and R. H. Eather, Monochromatic all-sky observations and auroral precipitation patterns, *J. Geophys. Res.*, *81*, 3771–3780, 1976.

Meng, C.-I., Electron precipitation and polar auroras, *Space Sci. Rev.*, *22*, 223–300, 1978.

Meng, C.-I., Polar cap variations and the interplanetary magnetic field, in *Dynamics of the Magnetosphere*, edited by S.-I. Akasofu, pp. 23–46, D. Reidel, Hingham, Mass., 1979*a*.

Meng, C.-I., Diurnal variation of the auroral oval size, *J. Geophys. Res.*, *84*, 5319–5324, 1979*b*.

Meng, C.-I., Reply, *J. Geophys. Res.*, *85*, 2375, 1980.

Meng, C.-I., Electron precipitation in the midday auroral oval, *J. Geophys. Res.*, *86*, 2149–2174, 1981*a*.

Meng, C.-I., The auroral electron precipitation during extremely quiet geomagnetic conditions, *J. Geophys. Res.*, *86*, 4607–4627, 1981*b*.

Meng, C.-I., Polar cap arcs and the plasma sheet, *Geophys. Res. Lett.*, *8*, 273–276, 1981*c*.

Meng, C.-I., and S.-I. Akasofu, The relation between the polar cap auroral arc and the auroral oval arc, *J. Geophys. Res.*, *81*, 4004–4006, 1976.

Meng, C.-I., and S.-I. Akasofu, Electron precipitation equatorward of the auroral oval and the mantle aurora in the midday sector, *Planet. Space Sci.*, *31*, 889–899, 1983.

Meng, C.-I., and H. W. Kroehl, Intense uniform precipitation of low-energy electrons over the polar cap, *J. Geophys. Res.*, *82*, 2305–2313, 1977.

Meng, C.-I., R. H. Holzworth, and S.-I. Akasofu, Auroral circle, delineating the poleward boundary of the quiet auroral belt, *J. Geophys. Res.*, *82*, 164–172, 1977.

Meng, C.-I., B. Mauk, and C. E. McIlwain, Electron precipitation of evening diffuse aurora and its conjugate electron fluxes near the magnetic-equator, *J. Geophys. Res.*, *84*, 2545–2558, 1979.

Mizera, P. F., and J. F. Fennell, Signatures of electric fields from high and low altitude particle distributions, *Geophys. Res. Lett.*, *4*, 311–314, 1977.

Möller, H. G., Backscatter results from Lindau, 11, The movements of curtains of intense irregularities in the polar *F*-layer, *J. Atmos. Terr. Phys.*, *36*, 1487–1501, 1974.

Montbriand, L. E., The proton aurora and auroral substorm, in *The Radiating Atmosphere*, edited by B. M. McCormac, pp. 366–373, D. Reidel, Hingham, Mass., 1971.

Moore, T. E., R. L. Arnoldy, J. Feynman, and D. A. Hardy, Propagating substorm injection fronts, *J. Geophys. Res.*, *86*, 6713–6726, 1981.

Moshupi, M. C., C. D. Anger, J. S. Murphree, D. D. Wallis, J. H. Whitteker, and L. H. Brace, Characteristics of trough region auroral patches and detached arcs observed by ISIS 2, *J. Geophys. Res.*, *84*, 1333–1346, 1979.

Mozer, F. S., C. A. Cattell, M. K. Hudson, R. L. Lysak, M. Temerin, and R. B. Torbert, Satellite measurements and theories of low altitude auroral particle acceleration, *Space Sci. Rev.*, *27*, 155–213, 1980.

Muliarchik, T. M., Yu. I. Galperin, V. A. Gladishev, L. M. Nikolaenko, J. A. Sauvaud, J. Crasnier, and Y. I. Feldstein, Diffuse auroral zone, VI, Precipitation of electrons and protons in the dayside sector (in Russian), *Cosmic Res.*, *20*, 244–263, 1982.

Murphree, J. S., and C. D. Anger, An observation of the instantaneous optical auroral distribution, *Can. J. Phys.*, *58*, 214–223, 1980.

Murphree, J. S., and L. L. Cogger, Observed connections between apparent polar cap features and the instantaneous diffuse auroral oval, *Planet. Space Sci.*, *29*, 1143–1149, 1981.

Murphree, J. S., L. L. Cogger, C. D. Anger, S. Ismail, and G. G. Shepherd, Large scale 6300 Å, 5577 Å, 3914 Å dayside auroral morphology, *Geophys. Res. Lett.*, *7*, 239–242, 1980.

Murphree, J. S., C. D. Anger, and L. L. Cogger, ISIS 2 observations of auroral arc systems, in *Physics of Auroral Arc Formations, Geophys. Monogr. Ser.*, vol. 25, edited by S.-I. Akasofu and J. R. Kan, pp. 15–23, AGU, Washington, D. C., 1981*a*.

Murphree, J. S., L. L. Cogger, and C. D. Anger, Characteristics of the instantaneous auroral oval in the 1200–1800 MLT sector, *J. Geophys. Res.*, *86*, 7657–7668, 1981*b*.

Murphree, J. S., C. D. Anger, and L. L. Cogger, The instantaneous relationship between polar cap and oval auroras at times of northward interplanetary magnetic field, *Can. J. Phys.*, *60*, 349–356, 1982.

Murphree, J. S., S. Ismail, L. L. Cogger, D. D. Wallis, G. G. Shepherd, R. Link, and D. M. Klumpar, Characteristics of optical emissions and particle precipitation in polar cap arcs, *Planet. Space Sci.*, *31*, 161–172, 1983.

Nagai, T., Local time dependence of electron flux changes during substorms derived from multisatellite observation at synchronous orbit, *J. Geophys. Res.*, *87*, 3456–3468, 1982.

Nagata, T., T. Hirasawa, and M. Agukawa, Discrete and diffuse auroral belts in Antarctica, *Rep. Ionos. Res. Space Res. Jpn.*, *29*, 149–156, 1975.

Nakai, H., and Y. Kamide, Response of nightside auroral oval boundaries to the interplanetary magnetic field, *J. Geophys. Res.*, *88*, 4005–4014, 1983.

Nikolaenko, L. M., Yu. I. Galperin, Y. I. Feldstein, J. A. Sauvaud, and J. Crasnier, Diffuse auroral zone, VII, Dynamics of equatorial boundary of diffuse auroral precipitation in response to geomagnetic activity and interplanetary medium parameters (in Russian), *Cosmic Res.*, *21*, 876–884, 1983.

Panasyuk, M. I., E. N. Sosnovetz, L. V. Tverskaja, and O. V. Khorosheva, About the origin of global fine structure formations in the magnetosphere during substorms (in Russian), *Geomagn. Aeron.*, *18*, 172–175, 1978.

Paschmann, G., Plasma structure of the magnetopause and boundary layer, in *Proceedings of the Magnetospheric Boundary Layers Conference, Spec. Publ. 148*, pp. 25–36, European Space Agency, Neuilly, France, 1979.

Pellinen, R. J., and W. J. Heikkila, Observations of auroral fading before breakup, *J. Geophys. Res.*, *83*, 4207–4217, 1978.

Pellinen, R. J., and W. J. Heikkila, Inductive electric fields in the magnetotail and their relation to auroral and substorm phenomena, *Space Sci. Rev.*, *37*, 1–61, 1984.

Peterson, R. N., R. A. Koehler, G. J. Gotschalks, J. F. Pieau, and G. G. Shepherd, Photometric observations of the dayside cleft emission from Cambridge Bay, December 1976, *Planet. Space Sci.*, *28*, 149–158, 1980.

Pike, C. P., and B. S. Dandekar, Evening sector auroral oval dynamics from DMSP photographs, *J. Geophys. Res.*, *84*, 3389–3402, 1979.

Pike, C. P., and J. A. Whalen, Satellite observations of auroral substorms, *J. Geophys. Res.*, *79*, 985–1000, 1974.

Pikelner, S. B., Theory of magnetic storms and auroras, *Izv. Krimean Astrophys. Observ.*, *16*, 104–121, 1956.

Ponomarev, E. A., Energy relationships for the magnetosphere, *Stud. Geomagn. Aeron. Sol. Phys. Moscow*, *53*, 27, 1981.

Pudovkin, M. I., V. P. Kozelov, L. L. Lazutin, O. A. Troshichev, and A. D. Chertkov, *The Physical Grounds of Magnetospheric Disturbance Predictions*, 312 pp., Nauka, Leningrad, USSR, 1977.

Rearwin, S., and E. W. Hones, Near-simultaneous measurement of low-energy electrons by sounding rocket and satellite, *J. Geophys. Res.*, *79*, 4322–4325, 1974.

Reid, G. C., and M. H. Rees, The systematic behaviour of hydrogen emissions in the aurora, *Planet. Space Sci.*, *5*, 99–105, 1961.

Reiff, P. H., Low-altitude signatures of the boundary layers, in *Proceedings of the Magnetospheric Boundary Layers Conference, Spec. Publ. 148*, pp. 167–173, European Space Agency, Neuilly, France, 1979.

Reiff, P. H., J. L. Burch, and R. A. Heelis, Dayside auroral arcs and convection, *Geophys. Res. Lett.*, *5*, 391–394, 1978.

Rezhenov, B. V., V. G. Vorobjev, and Y. I. Feldstein, The interplanetary magnetic field B_Z-component influence on the geomagnetic field variations and on the auroral dynamics, *Planet. Space Sci.*, *27*, 699–716, 1979.

Robinson, R. M., R. R. Vondrak, and T. A. Potemra, Electrodynamic properties of the evening sector ionosphere within the region 2 field-aligned current sheet, *J. Geophys. Res.*, *87*, 731–741. 1982.

Roldugin, V. K., and G. V. Starkov, About the zone of pulsating auroras (in Russian), *Geomagn. Aeron.*, *10*, 97–100, 1970.

Romick, G. J., and N. B. Brown, Midday auroral observations in the oval cusp region, and polar cap, *J. Geophys. Res.*, *76*, 8420–8424, 1971.

Rostoker, G., Triggering of expansive phase intensifications of magnetospheric substorms by northward turnings of the interplanetary magnetic field, *J. Geophys. Res.*, *88*, 6981–6993, 1983.

Rostoker, G., S.-I. Akasofu, J. Foster, R. A. Greenwald, Y. Kamide, K. Kawasaki, A. T. Y. Lui, R. L. McPherron, and C. T. Russell, Magnetospheric substorms: Definition and Signatures, *J. Geophys. Res.*, *85*, 1663–1668, 1980.

Royorvik, O., and T. N. Davis, Pulsating aurora: Local and global morphology, *J. Geophys. Res.*, *82*, 4720–4740, 1977.

Russell, C. T., and R. C. Elphic, ISEE observations of flux transfer events at the dayside magnetopause, *Geophys. Res. Lett.*, *6*, 33–36, 1979.

Saflekos, N. A., T. A. Potemra, and T. Iijima, Small-scale transverse disturbances in the polar regions observed by Triad, *J. Geophys. Res.*, *83*, 1493–1502, 1978.

Samsonov, V. P., and Y. A. Romaschenko, Geophysical phenomena as indicators of structure and dynamics of ionosphere and magnetosphere from data of a meridional chain of ground-based stations in 1976–1977, in *Studies of Ionosphere-Magnetosphere Coupling at Yakutia Meridian*, edited by A. V. Sobolev, pp. 3–24, Yakutsk Department, Academy of Sciences, Yakutsk, USSR, 1982.

Sandford, B. P., Aurora and airglow intensity variations with time and magnetic activity at southern high latitudes, *J. Atmos. Terr. Phys.*, *26*, 749–769, 1964.

Sandford, B. P., Variations of auroral emissions with time, magnetic activity and the solar cycle, *J. Atmos. Terr. Phys.*, *30*, 1921–1942, 1968.

Sandholt, P. E., K. Henriksen, C. S. Deehr, G. G. Sivjee, G. K. Romick, and A. Egeland, Dayside cusp auroral morphology related to nightside magnetic activity, *J. Geophys. Res.*, *85*, 4132–4138, 1980.

Sandholt, P. E., A. Egeland, K. Henriksen, R. Smith, and P. Sweeney, Optical measurements of a nightside poleward expanding aurora, *J. Atmos. Terr. Phys.*, *44*, 71–79, 1982.

Sauvaud, J. A., Yu. I. Galperin, V. A. Gladyshev, A. K. Kuzmin, T. M. Muliarchick, and J. Crasnier, Spatial inhomogeneity of magnetosheath proton precipitation along the dayside cusp from the ARCAD experiment, *J. Geophys. Res.*, *85*, 5105–5112, 1980.

Sauvaud, J. A., J. Crasnier, Yu. I. Galperin, Y. I. Feldstein, and L. M. Nikolaenko, Dynamics of the diffuse auroral zone low latitude boundary in the pre-midnight sector—A statistical study (abstract), *Eos Trans. AGU*, *63*, 1317, 1982.

Sauvaud, J. A., J. Crasnier, Yu. I. Galperin, and Y. I. Feldstein, A statistical study of the dynamics of the equatorial boundary of the diffuse aurora in the pre-midnight sector, *Geophys. Res. Lett.*, *10*, 749–752, 1983.

Schield, M. A., and L. A. Frank, Electron observations between the inner edge of the plasma sheet and the plasmasphere, *J. Geophys. Res.*, *75*, 5401–5414, 1970.

Sckopke, N., External plasma flow, in *Proceedings of the Magnetospheric Boundary Layers Conference, Spec. Publ. 148*, pp. 37–42, European Space Agency, Neuilly, France, 1979.

Sckopke, N., G. Paschmann, H. Rosenbauer, and D. H. Fairfield, Influence of the interplanetary magnetic field on the occurrence and thickness of the plasma mantle, *J. Geophys. Res.*, *81*, 2687–2691, 1976.

Sears, R. D., Characterization of the auroral ionosphere using optical

remote-sensing techniques, *AIAA J.*, *20*, 390–394, 1982.
Senior, C., R. M. Robinson, and T. A. Potemra, Relationship between field-aligned currents, diffuse auroral precipitation and the westward electrojet in the early morning sector, *J. Geophys. Res.*, *87*, 10,469–10,477, 1982.
Sergeev, V. A., and N. A. Tsyganenko, *The Earth's Magnetosphere*, Nauka, Moscow, 1980.
Sergeev, V. A., and A. G. Yakhnin, Motion of auroral arcs in polar caps (in Russian), *Geomagn. Aeron.*, *18*, 743–744, 1978.
Sergeev, V. A., and A. G. Yakhnin, A possible mechanism for the formation of sun-aligned aurora on polar cap field lines (in Russian), *Stud. Geomagn. Aeron. Sol. Phys. Moscow*, *47*, 49–57, 1979.
Sharber, J. R., The continuous (diffuse) aurora and auroral *E* ionization, in *Physics of Space Plasma*, edited by T. S. Chang, B. Coppi, and J. R. Jasperse, Scientific Publishers, Cambridge, England, 1981.
Sharp, R. D., and R. G. Johnson, Some average properties of auroral electron precipitation as determined from satellite observations, *J. Geophys. Res.*, *73*, 969–972, 1968.
Sharp, R. D., D. L. Carr, and R. G. Johnson, Satellite observations of the average properties of auroral particle precipitations: Latitudinal variations, *J. Geophys. Res.*, *74*, 4618–4630, 1969.
Sheehan, R. E., and R. L. Carovillano, Characteristics of the equatorward auroral boundary near midnight determined from DMSP images, *J. Geophys. Res.*, *83*, 4749–4754, 1978.
Shepherd, G. G., Dayside cleft aurora and its ionospheric effects, *Rev. Geophys.*, *17*, 2017–2033, 1979*a*.
Shepherd, G. G., ISIS auroral observations and their magnetospheric interpretation, in *Magnetospheric Study 1979*, pp. 6–10, Japanese International Magnetospheric Study Committee, Tokyo, 1979*b*.
Shepherd, G. G., Structure and dynamics of the red auroral oval in quiet and disturbed conditions, paper presented at the Symposium, on Magnetosphere-Ionosphere Processes and Airglow, Bulgarian Academy of Sciences, Stara Zagora, Oct. 1982.
Shepherd, G. G., and F. W. Thirkettle, Magnetospheric dayside cusp: A topside view of its 6300 Å atomic oxygen emission, *Science*, *180*, 737–739, 1973.
Shepherd, G. G., C. D. Anger, L. H. Brace, J. R. Burrows, W. J. Heikkila, J. Hoffman, E. Maier, and J. H. Whitteker, An observation of polar aurora and airglow from the ISIS 2 spacecraft, *Planet. Space Sci.*, *21*, 819–829, 1973.
Shepherd, G. G., F. W. Thirkettle, and C. D. Anger, Topside optical view of the dayside cleft aurora, *Planet. Space Sci.*, *24*, 937–944, 1976.
Shepherd, G. G., J. D. Winningham, F. E. Bunn, and F. W. Thirkettle, An empirical determination of the production efficiency for auroral 6300-Å emission by energetic electrons, *J. Geophys. Res.*, *85*, 715–721, 1980.
Shepherd, M. M., and G. G. Shepherd, Projection of auroral intensity contours into the magnetosphere, *Planet. Space Sci.*, *33*, 183–189, 1985.
Simons, S. L., P. H. Reiff, R. W. Spiro, D. A. Hardy, and H. W. Kroehl, A comparison of precipitating electron energy flux on March 22 1979 with the empirical model (abstract), *Eos Trans. AGU*, *64*, 293, 1983.
Siren, J. C., Pulsating aurora in high latitude satellite photographs, *Geophys. Res. Lett.*, *2*, 557–560, 1975.
Siren, J. C., Comment on "Pulsating aurora: Local and global morphology" by O. Royorvik and T. N. Davis, *J. Geophys. Res.*, *83*, 5325–5326, 1978.
Sivjee, G. G., Optical emissions from the midday aurora, *J. Atmos. Terr. Phys.*, *38*, 533–541, 1976.
Sivjee, G. G., Differences in near UV (~3400–4300 Å) optical emissions from midday cusp and nighttime auroras, *J. Geophys. Res.*, *88*, 435–441, 1983.
Sivjee, G. G., and C. S. Deehr, Difference in polar atmospheric optical emissions between mid-day and night-time auroras, in *Exploration of the Polar Upper Atmosphere*, edited by C. S. Deehr and J. Holtet, pp. 199–208, D. Reidel, Hingham, Mass., 1980.
Sivjee, G. G., and B. Hultqvist, Particle and optical measurements in the magnetic noon sector of the auroral oval, *Planet. Space Sci.*, *23*, 1597–1601, 1975.
Sivjee, G. G., G. J. Romick, and C. S. Deehr, Optical signatures of some magnetospheric processes on the dayside, *Geophys. Res. Lett.*, *9*, 676–679, 1982.
Sivtzeva, L. D., V. M. Filippov, V. L. Khalipov, Yu. I. Galperin, V. A. Ershova, L. M. Nikolaenko, Y. N. Ponomarev, and V. M. Sinitsin, Studies of the midlatitude ionospheric main trough with the aid of ground-based geophysical methods and synchronous measurements from satellites (in Russian), *Cosmic Res.*, *21*, 584–608, 1983.
Slater, D. W., L. L. Smith, and E. W. Kleckner, Correlated observations of the equatorward diffuse auroral boundary, *J. Geophys. Res.*, *85*, 531–542, 1980.
Snyder, A. L., and S.-I. Akasofu, Major auroral substorm features in the dark sector observed by a USAF DMSP satellite, *Planet. Space Sci.*, *22*, 1511–1517, 1974.
Snyder, A. L., and S.-I. Akasofu, Auroral oval photographs from the DMSP 8531 and 10533 satellites, *J. Geophys. Res.*, *81*, 1799–1802, 1976.
Snyder, A. L., J. Buchau, and S.-I. Akasofu, Formation of auroral patches in the midday sector during a substorm, *Planet. Space Sci.*, *20*, 1116–1119, 1972.
Snyder, A. L., S.-I. Akasofu, and T. N. Davis, Auroral substorms observed from above the north polar region by a satellite, *J. Geophys. Res.*, *79*, 1393–1402, 1974.
Spiro, R. W., P. H. Reiff, and L. J. Maher, Zone conductances: An empirical model, *J. Geophys. Res.*, *87*, 8215–8227, 1982.
Starkov, G. V., An analytical presentation of the equatorial boundary of the auroral oval (in Russian), *Geomagn. Aeron.*, *9*, 759–760, 1969.
Starkov, G. V., and Y. I. Feldstein, Variations of auroral oval zone boundaries (in Russian), *Geomagn. Aeron.*, *7*, 62–71, 1967.
Starkov, G. V., and Y. I. Feldstein, Auroral oval during magnetic disturbances, in *Aurora*, no. 17, edited by S. I. Isaev and Y. I. Feldstein, pp. 22–33, Nauka, Moscow, 1968.
Starkov, G. V., and Y. I. Feldstein, Auroral substorm (in Russian), *Geomagn. Aeron.*, *11*, 560–562, 1971.
Stenbaek-Nielsen, H. C., and T. J. Hallinan, Pulsating auroras: Evidence for noncollisional thermalization of precipitating electrons, *J. Geophys. Res.*, *84*, 3257–3271, 1979.
Swift, D. W., Mechanisms for the discrete aurora—A review, *Space Sci. Rev.*, *22*, 35–75, 1978.
Swift, D. W., Auroral mechanisms and morphology, *Rev. Geophys.*, *17*, 681–696, 1979.
Tanskanen, P. J., D. A. Hardy, and W. J. Burke, Spectral characteristics of precipitating electrons associated with visible aurora in the premidnight oval during periods of substorm activity, *J. Geophys. Res.*, *86*, 1379–1395, 1981.
Thomas, I. L., and F. R. Bond, An empirical equation for the austral auroral oval, *Geophys. Res. Lett.*, *4*, 411–412, 1977.
Thomas, I. L., and F. R. Bond, A spherical harmonic analysis of the austral oval, *Planet. Space Sci.*, *26*, 691–695, 1978.
Torbert, R. B., and F. S. Mozer, Electrostatic shocks as the source of discrete auroral arcs, *Geophys. Res. Lett.*, *5*, 135–138, 1978.
Tsurutani, B. T., E. J. Smith, R. M. Thorne, R. R. Anderson, D. A. Gurnett, G. K. Parks, C. S. Lin, and C. T. Russell, Wave-particle interaction at the magnetopause: Contributions to the dayside aurora, *Geophys. Res. Lett.*, *8*, 183–186, 1981.
Turunen, T., and L. Liszka, Comparison of simultaneous satellite measurements of auroral particle precipitation with bottomside ionosonde measurements of the electron density in the *F*-region, *J. Atmos. Terr. Phys.*, *34*, 365–372, 1972.
Tverskoy, B. A., On the field-aligned currents in the magnetosphere (in Russian), *Geomagn. Aeron.*, *22*, 991–995, 1982.
Valchuk, T. E., Yu. I. Galperin, J. Crasnier, L. M. Nikolaenko, J. A. Sauvaud, and Y. I. Feldstein, Auroral diffuse zone, IV, Latitudinal distribution of auroral optical emissions and particle precipitation and its relationship with the plasmasheet and magnetotail (in Russian), *Cosmic Res.*, *17*, 559–579, 1979.
Vasyliunas, V. M., A survey of low-energy electrons in the evening sector of the magnetosphere with OGO 1 and OGO 3, *J. Geophys. Res.*, *73*, 2839–2884, 1968.
Vasyliunas, V. M., Low energy particle fluxes in the geomagnetic tail, in *The Polar Ionosphere and Magnetospheric Processes*, edited by G. Skovli, pp. 25–47, Gordon and Breach, New York, 1970.
Vasyliunas, V. M., Magnetospheric plasma, in *Solar-Terrestrial Physics/1970*, edited by E. R. Dyer, vol. 3, pp. 192–211, D. Reidel, Hingham, Mass., 1972.
Vasyliunas, V. M., Magnetospheric cleft symposium, *Eos Trans. AGU*, *55*, 60–66, 1974.
Venkatarangan, P., J. R. Burrows, and I. B. McDiarmid, On the angular distributions of electrons in "inverted V" substructures, *J. Geophys. Res.*, *80*, 66–72, 1975.
Vorobjev, V. G., and V. L. Zverev, Effect of IMF component on the position of the auroral oval in the day sector, in *Aurora and Airglow*, no. 28, edited by S. I. Isaev, Y. A. Nadubovich, and L. S. Evlashin, pp. 21–24, Nauka, Moscow, 1981.

Vorobjev, V. G., G. Gustafsson, G. V. Starkov, Y. I. Feldstein, and N. F. Shevnina, Dynamics of day and night aurora during substorms, *Planet. Space Sci.*, *23*, 269–278, 1975.

Vorobjev, V. G., G. V. Starkov, and Y. I. Feldstein, The auroral oval during the substorm development, *Planet. Space Sci.*, *24*, 955–965, 1976.

Wallis, D. D., and E. E. Budzinski, Empirical models of height-integrated conductivities, *J. Geophys. Res.*, *86*, 125–137, 1981.

Wallis, D. D., C. D. Anger, and G. Rostoker, The spatial relationship of auroral electrojets and visible aurora in the evening sector, *J. Geophys. Res.*, *81*, 2857–2869, 1976.

Wallis, D. D., J. R. Burrows, M. C. Moshupi, C. D. Anger, and J. S. Murphree, Observations of particles precipitating into detached arcs and patches equatorward of the auroral oval, *J. Geophys. Res.*, *84*, 1347–1360, 1979.

Weber, E. J., and J. Buchau, Polar cap *F*-layer auroras, *Geophys. Res. Lett.*, *8*, 125–128, 1981.

Weill, G., M. Fafiotte, S. Huille, and J. Delannoy, La structure de la zone aurorale arctque en période de minimum d'activité solaire, *Ann. Geophys.*, *21*, 469–474, 1965.

Westerlund, L. H., The auroral electron energy spectrum extended to 45 eV, *J. Geophys. Res.*, *74*, 351–354, 1969.

Whalen, B. A., J. R. Miller, and I. B. McDiarmid, Sounding rocket observations of particle precipitation in a polar cap electron aurora, *J. Geophys. Res.*, *76*, 6847–6855, 1971.

Whalen, J. A., General characteristics of the auroral ionosphere, in *Physics of Space Plasma*, edited by T. S. Chang, B. Coppi, and J. R. Jasperse, Scientific Publishers, Cambridge, England, 1981.

Whalen, J. A., A quantitative description of the spatial distribution and dynamics of the energy flux in the continuous aurora, *J. Geophys. Res.*, *88*, 7155–7169, 1983.

Whalen, J. A., R. A. Wagner, and J. Buchau, A 12-hour case study of auroral phenomena in the midnight sector: Oval, polar cap, and continuous auroras, *J. Geophys. Res.*, *82*, 3529–3546, 1977.

Wiens, R. H., and A. Vallance Jones, Studies of auroral hydrogen emissions in west-central Canada, 3, Proton and electron auroral ovals, *Can. J. Phys.*, *47*, 1493–1517, 1969.

Winningham, J. D., Low altitude polar satellite results: An overview, in *Magnetospheric Study 1979*, pp. 58–61, Japanese International Magnetospheric Study Committee, Tokyo, 1979.

Winningham, J. D., and W. J. Heikkila, Polar cap auroral electron fluxes observed with ISIS 1, *J. Geophys. Res.*, *79*, 949–957, 1974.

Winningham, J. D., F. Yasuhara, S.-I. Akasofu, and W. J. Heikkila, The latitudinal morphology of 10-eV to 10-keV electron fluxes during magnetically quiet and disturbed times in the 2100–0300 MLT sector, *J. Geophys. Res.*, *80*, 3148–3171, 1975.

Winningham, J. D., C. D. Anger, G. G. Shepherd, E. J. Weber, and R. A. Wagner, A case study of the aurora, high-latitude ionosphere and particle precipitation during near-steady conditions, *J. Geophys. Res.*, *83*, 5717–5731, 1978.

Yakhnin, A. G., and V. A. Sergeev, Frequency of aurorae appearances in the polar cap and orientation of IMF (in Russian), *Geomagn. Aeron.*, *19*, 566–567, 1979.

Yakhnin, A. G., and V. A. Sergeev, Polar cap aurora: Dependence on IMF orientation and substorms, certain peculiarities of morphology, in *Aurora and Airglow*, no. 28, edited by S. I. Isaev, Y. A. Nadubovich, and L. S. Evlashin, pp. 27–35, Nauka, Moscow, 1981.

Zanetti, L. J., P. F. Bythrow, T. A. Potemra, K. Makita, and C.-I. Meng, Ground state of the earth's magnetosphere (abstract), *Eos Trans. AGU*, *63*, 1081, 1982.

Zi-Min-Yun, W. Lei, R. Gendrin, and B. Higel, The Harang discontinuity and the evening plasmapause boundary: A STARE-GEOS intercomparison, *J. Atmos. Terr. Phys.*, *44*, 671–679, 1982.

Zverev, V. L., G. V. Starkov, and Y. I. Feldstein, Structured and diffuse auroras in the morning sector, in *Auroras and Auroral Particles Precipitation*, edited by M. I. Pudovkin and S. I. Isaev, pp. 37–44, Nauka, Leningrad, USSR, 1976.

Zverev, V. L., G. V. Starkov, and Y. I. Feldstein, Influences of the interplanetary magnetic field on the auroral dynamics, *Planet. Space Sci.*, *27*, 665–667, 1979.

Y. I. Feldstein, Institute of Terrestrial Magnetism, Ionosphere, and Radio Wave Propagation, Academy of Sciences of the USSR, P.O. Akademgorodok, Moscow Region 142092, USSR.

Yu. I. Galperin, Institute of Space Research, Academy of Sciences of the USSR, Moscow 117810, USSR.

(Received March 13, 1984;
accepted April 3, 1985.)